

DESIGN OPTIMIZATION OF SPACE LAUNCH VEHICLES USING A GENETIC
ALGORITHM

Except where reference is made to the work of others, the work described in this dissertation is my own or was done in collaboration with my advisory committee.
This dissertation does not include proprietary or classified information.

Douglas James Bayley

Certificate of Approval:

John E. Cochran
Professor
Aerospace Engineering

Roy J. Hartfield, Chair
Associate Professor
Aerospace Engineering

John E. Burkhalter
Professor Emeritus
Aerospace Engineering

Christopher J. Roy
Assistant Professor
Aerospace Engineering

Joe F. Pittman
Interim Dean
Graduate School

DESIGN OPTIMIZATION OF SPACE LAUNCH VEHICLES USING A GENETIC
ALGORITHM

Douglas James Bayley

A Dissertation

Submitted to

the Graduate Faculty of

Auburn University

in Partial Fulfillment of the

Requirements for the

Degree of

Doctor of Philosophy

Auburn, Alabama
August 4, 2007

DESIGN OPTIMIZATION OF SPACE LAUNCH VEHICLES USING A GENETIC
ALGORITHM

Douglas James Bayley

Permission is granted to Auburn University to make copies of this dissertation at its discretion, upon the request of individuals or institutions and at their expense. The author reserves all publication rights.

Signature of Author

Date of Graduation

VITA

Douglas James Bayley, son of Howard J. Bayley Jr. and Marie (Caione) Bayley, was born on September 9, 1969 in New Britain, Connecticut. Douglas graduated from Xavier High School in Middletown, Connecticut in June 1987. He attended Florida Institute of Technology in the Fall of 1987. Douglas graduated magna cum laude with a Bachelor of Science Degree in Aerospace Engineering in June 1992. Douglas began graduate studies in the Fall of 1992 in the Department of Aerospace Engineering, Auburn University. He completed a Master of Science Degree in Aerospace Engineering in the Fall of 1994. In January 1995, Douglas began officer training and in May 1995, was commissioned a Second Lieutenant in the United States Air Force. After assignments in Montana, Colorado and California, Douglas returned to the Department of Aerospace Engineering, Auburn University in 2005 to complete his Doctor of Philosophy Degree in Aerospace Engineering. In 1998, Douglas married his beautiful bride Kelly (Draughon) Bayley. Douglas and Kelly have been blessed with four wonderful children: Thomas (8), Sarah (6), Anna (4) and Mary (1).

DISSERTATION ABSTRACT
DESIGN OPTIMIZATION OF SPACE LAUNCH VEHICLES USING A GENETIC
ALGORITHM

Douglas James Bayley

Doctor of Philosophy, August 4, 2007
(M.S., Auburn University, 1994)
(B.S., Florida Institute of Technology, 1992)

196 Typed Pages

Directed by Roy J. Hartfield

Disclaimer: The views expressed in this dissertation are those of the author and do not reflect the official policy or position of the United States Air Force, Department of Defense, or the U.S. Government.

The United States Air Force (USAF) continues to have a need for assured access to space. In addition to flexible and responsive spacelift, a reduction in the cost per launch of space launch vehicles is also desirable. For this purpose, an investigation of the design optimization of space launch vehicles has been conducted.

Using a suite of custom codes, the performance aspects of an entire space launch vehicle were analyzed. A genetic algorithm (GA) was employed to optimize the design of the space launch vehicle. A cost model was incorporated into the optimization process with the goal of minimizing the overall vehicle cost. The other goals of the design

optimization included obtaining the proper altitude and velocity to achieve a low-Earth orbit. Specific mission parameters that are particular to USAF space endeavors were specified at the start of the design optimization process. Solid propellant motors, liquid fueled rockets, and air-launched systems in various configurations provided the propulsion systems for two, three and four-stage launch vehicles. Mass properties models, an aerodynamics model, and a six-degree-of-freedom (6DOF) flight dynamics simulator were all used to model the system.

The results show the feasibility of this method in designing launch vehicles that meet mission requirements. Comparisons to existing real world systems provide the validation for the physical system models. However, the ability to obtain a truly minimized cost was elusive. The cost model uses an industry standard approach, however, validation of this portion of the model was challenging due to the proprietary nature of cost figures and due to the dependence of many existing systems on surplus hardware.

ACKNOWLEDGEMENTS

I would like to thank Dr. Roy J. Hartfield for his guidance and patience during this long and arduous process. This degree would not have been completed if not for Dr. Hartfield's steadfast support. He has been a true role model and mentor. I would also like to acknowledge the inspiration of Fr. Michael J. McGivney. Most importantly, I have to thank Kelly, Thomas, Sarah, Anna, and Mary for their love, support and sacrifices during this endeavor.

Style or journal used:

The American Institute of Aeronautics and Astronautics Journal

Computer software used:

Microsoft Word 2003, IMPROVE[®] 3.1 Genetic Algorithm, Compaq Visual FORTRAN

6.6, General Purpose 6-DOF Simulation, Tecplot 10, Microsoft Excel 2003

TABLE OF CONTENTS

LIST OF FIGURES	xii
LIST OF TABLES	xv
NOMENCLATURE	xviii
1.0 INTRODUCTION	1
2.0 CHRONOLOGY OF OPTIMIZATION TECHNIQUES.....	3
2.1 Introduction.....	3
2.2 Early Concepts	3
2.2.1 Newton and Calculus-Based Methods.....	4
2.2.2 Gradient Methods.....	4
2.3 Linear Programming.....	5
2.4 Pattern Search Optimization	5
2.5 Design of Experiments.....	7
2.6 Additional Methods	8
2.7 Genetic Algorithms.....	9
2.8 Recent Launch Vehicle Optimization Work.....	11
3.0 SYSTEM MODELING	16
3.1 Introduction.....	16
3.2 Objective Function Link to the Genetic Algorithm (GA).....	16
3.3 Genetic Algorithm (GA).....	19
3.4 Propulsion System Models	24
3.4.1 Solid Propellant Rocket Motors.....	26
3.4.2 Liquid Propellant Rocket Engines	27
3.5 Mass Properties Models.....	29
3.5.1 Mass Properties of Individual Components.....	32
3.5.1.1 Point Mass Example: Electronics	34
3.5.1.2 Cylinder Example: Motor Cases.....	34
3.5.1.3 Sphere Example: Compressed Gas Tank.....	35

3.5.1.4 Mass Table	36
3.5.2 Mass Properties of Entire Launch Vehicle	37
3.5.2.1 Entire Launch Vehicle Mass Properties Example: Phase I.....	37
3.6 Aerodynamics Model.....	38
3.7 Six-Degree-of-Freedom (6DOF) Flight Dynamics Simulator	41
3.8 Cost Model.....	42
3.8.1 Development Cost Submodel	44
3.8.2 Recurring Cost Submodel	46
3.8.3 Ground and Flight Operations Cost Submodel.....	47
3.8.4 Insurance Cost Submodel	48
3.8.5 Example Calculation.....	49
4.0 VALIDATION EFFORTS.....	51
4.1 Introduction.....	51
4.2 Validation Method	53
4.2.1 General Description	53
4.2.2 Specific Validation Process and Setup	54
4.2.3 Inert and Propellant Mass Fraction Calculations.....	56
4.3 Three-Stage Solid Propellant Vehicle vs. Minuteman III ICBM	57
4.4 Four-Stage Solid Propellant Vehicle vs. Minotaur I SLV	64
4.5 Two-Stage Liquid Propellant Vehicle vs. Titan II SLV	69
4.6 Air-Launched, Two-Stage Liquid Propellant Vehicle vs. QuickReach™	73
4.7 Mass Fractions for Three-Stage Solid/Liquid/Liquid Propellant Vehicle	76
4.8 Summary of Validation Efforts.....	79
4.8.1 Three-Stage Solid Propellant Launch Vehicle.....	80
4.8.2 Four-Stage Solid Propellant Launch Vehicle	80
4.8.3 Two-Stage Liquid Propellant Launch Vehicle	81
4.8.4 Air-Launched, Two-Stage Liquid Propellant Launch Vehicle	81
4.8.5 Three-Stage Solid/Liquid/Liquid Propellant Launch Vehicle	82
5.0 OPTIMIZATION RESULTS.....	83
5.1 Introduction.....	83
5.2 Initial Launch Vehicles	84
5.2.1 Case 1: Three-Stage Solid Propellant Launch Vehicle with Two Goals	85
5.2.2 Case 2: Three-Stage Solid Propellant Launch Vehicle with Three Goals	91
5.2.3 Conclusions: Initial Launch Vehicle Design Optimizations.....	94
5.3 Solid Propellant Vehicles.....	95
5.3.1 Case 3: Three-Stage Solid Propellant Launch Vehicle (VAFB)	98
5.3.2 Case 4: Three-Stage Solid Propellant Launch Vehicle (CCAFS)	108
5.3.3 Case 5: Four-Stage Solid Propellant Launch Vehicle (VAFB)	113

5.3.4 Case 6: Four-Stage Solid Propellant Launch Vehicle (CCAFS)	118
5.3.5 Conclusions: Solid Propellant Launch Vehicle Design Optimizations	122
5.4 Liquid Propellant Vehicles	122
5.4.1 Case 7: Three-Stage Liquid Propellant Launch Vehicle (VAFB)	124
5.4.2 Case 8: Three-Stage Liquid Propellant Launch Vehicle (CCAFS)	127
5.4.3 Case 9: Two-Stage Liquid Propellant Launch Vehicle (VAFB)	129
5.4.4 Case 10: Two-Stage Liquid Propellant Launch Vehicle (CCAFS)	133
5.4.5 Conclusions: Liquid Propellant Launch Vehicle Design Optimizations	135
5.5 Air-Launched Vehicles	136
5.5.1 Case 11: Air-Launched, Two-Stage Liquid Propellant Launch Vehicle (CCAFS)	137
5.5.2 Conclusions: Air-Launched Vehicle Design Optimization	143
5.6 Mixed Propellant Vehicles	144
5.6.1 Case 12: Three-Stage Solid/Liquid/Liquid Propellant Launch Vehicle (VAFB)	145
5.6.2 Case 13: Three-Stage Solid/Liquid/Liquid Propellant Launch Vehicle (CCAFS)	149
5.6.3 Conclusions: Mixed Propellant Vehicle Design Optimizations	152
5.7 Launch Vehicle Comparisons	153
5.7.1 Launch Vehicles Comparison of 1,000 lbm Payload Cases	153
5.7.2 Launch Vehicles Comparison of Propellant Mass Fractions	157
5.7.3 Launch Vehicles Comparison of Inert Mass Fractions	158
5.7.4 Launch Vehicles Comparison of Cost per Launch Values	158
6.0 CONCLUSIONS	160
6.1 Introduction	160
6.2 System Modeling and Validation	161
6.3 Design Optimizations	162
7.0 RECOMMENDED IMPROVEMENTS	165
7.1 Types of Solid and Liquid Propellants	165
7.2 Aerodynamics Model	166
7.3 Six-Degree-of-Freedom (6DOF) Flight Dynamics Simulator	166
7.4 Cost Model	167
7.5 Payload Masses and Orbits	167
REFERENCES	169
APPENDIX: Mass Table Example for Three-Stage Solid Propellant Launch Vehicle	176

LIST OF FIGURES

Figure 3-1. Objective Function Link to the GA.....	17
Figure 3-2. Tournament Selection.....	21
Figure 3-3. Solid Rocket Motor Schematic.....	26
Figure 3-4. Definition of Lengths.....	33
Figure 4-1. Three-Stage Solid Propellant Model vs. Minuteman III ICBM Schematic....	60
Figure 4-2. Minuteman III ICBM Ballistic Flight Profile.....	63
Figure 4-3. Validation Model Ballistic Flight Profile.....	64
Figure 4-4. Four-Stage Solid Propellant Model vs. Minotaur I SLV Schematic.....	66
Figure 4-5. Two-Stage Liquid Propellant Model vs. Titan II SLV Schematic.....	71
Figure 4-6. Air Launched, Two-Stage Liquid Propellant Model vs. QuickReach™ Launch Vehicle Schematic.....	74
Figure 4-7. Three-Stage Solid/Liquid/Liquid Propellant Launch Vehicles Schematic....	79
Figure 5-1. Progress of Best Performer to Meet Goal #1.....	87
Figure 5-2. Progress of Best Performer to Meet Goal #2.....	87
Figure 5-3. Three-Stage Solid Propellant Launch Vehicle Schematic.....	89
Figure 5-4. Altitude vs. Downrange Distance for Best Performer.....	89
Figure 5-5. Thrust vs. Time for Best Performer.....	90
Figure 5-6. Vehicle Mass vs. Time for Best Performer.....	90
Figure 5-7. Velocity vs. Time for Best Performer.....	91

Figure 5-8. Three-Stage Solid Propellant Launch Vehicle Schematic (Case 2/Run 1).....	94
Figure 5-9. Three-Stage Solid Propellant Launch Vehicle Schematic (Case 2/Run 2).....	94
Figure 5-10. Three-Stage Solid Propellant Launch Vehicle Schematic (VAFB).....	99
Figure 5-11. Velocity vs. Generation # for Three-Stage Solid Propellant Launch Vehicle.....	103
Figure 5-12. Altitude vs. Generation # for Three-Stage Solid Propellant Launch Vehicle.....	104
Figure 5-13. Total Vehicle Mass vs. Generation # for Three-Stage Solid Propellant Launch Vehicle.....	105
Figure 5-14. Final Velocity for Best, Worst, and Average Members of Generation #221.....	106
Figure 5-15. Final Altitude for Best, Worst, and Average Members of Generation #221.....	107
Figure 5-16. Total Vehicle Mass for Best, Worst, and Average Members of Generation #221.....	107
Figure 5-17. Three-Stage Solid Propellant Launch Vehicle Schematic (CCAFS).....	109
Figure 5-18. Mass Improvements for Three-Stage Solid Propellant Launch Vehicles...	112
Figure 5-19. Four-Stage Solid Propellant Launch Vehicles Schematic (VAFB).....	114
Figure 5-20. Four-Stage Solid Propellant Launch Vehicle Schematic (CCAFS).....	119
Figure 5-21. Three-Stage Liquid Propellant Launch Vehicle Schematic (VAFB).....	125
Figure 5-22. Three-Stage Liquid Propellant Launch Vehicle Schematic (CCAFS).....	128
Figure 5-23. Two-Stage Liquid Propellant Launch Vehicles Schematic (VAFB).....	130
Figure 5-24. Two-Stage Liquid Propellant Launch Vehicles Schematic (CCAFS).....	134
Figure 5-25. Air-Launched, Two-Stage Liquid Propellant Launch Vehicles Schematic (CCAFS).....	141
Figure 5-26. Three-Stage Solid/Liquid/Liquid Propellant Launch Vehicle Schematic (VAFB).....	146

Figure 5-27. Three-Stage Solid/Liquid/Liquid Propellant Launch Vehicle Schematic (CCAFS).....	150
Figure 5-28. Total Vehicle Mass Comparison.....	155
Figure 5-29. Cost per Launch Comparison.....	156
Figure 5-30. Propellant Mass Fraction (f_{prop}) Comparison.....	157
Figure 5-31. Inert Mass Fraction (f_{inert}) Comparison.....	158
Figure 5-32. Cost per Launch Comparison for All Launch Vehicles.....	159

LIST OF TABLES

Table 2-1: Design Variables for a Three-Stage Solid Propellant Launch Vehicle.....	15
Table 3-1: Example Design Parameters and Chromosome.....	19
Table 3-2: Liquid Propellant Fuels and Oxidizers.....	29
Table 3-3: Three-Stage Solid and Liquid Vehicle Components.....	32
Table 3-4: Mass Properties of Electronics.....	34
Table 3-5: Mass Properties of Stage 1 Motor Case.....	35
Table 3-6: Mass Properties of Stage 1 Compressed Gas Tank.....	36
Table 3-7: Inputs for Vehicle Cost Example Calculation.....	50
Table 3-8: Outputs for Vehicle Cost Example Calculation.....	50
Table 4-1: Typical Values of Real World Launch Vehicles.....	55
Table 4-2: Example Solid Rocket Motor Mass Fractions.....	56
Table 4-3: Three-Stage Solid Propellant Model vs. Minuteman III ICBM Comparison..	61
Table 4-4: Four-Stage Solid Propellant Model vs. Minotaur I SLV Comparison.....	66
Table 4-5: Four-Stage Solid Propellant Model Individual Stage Comparison.....	67
Table 4-6: Two-Stage Liquid Propellant Model vs. Titan II SLV Comparison.....	72
Table 4-7: Air Launched, Two-Stage Liquid Propellant Model vs. QuickReach™ Launch Vehicle Comparison.....	75
Table 4-8: Three-Stage Solid/Liquid/Liquid Propellant Vehicle Mass Fractions.....	77
Table 5-1: Space Launch Vehicle Design Optimization Cases.....	84
Table 5-2: Initial Launch Vehicles Mission Statistics.....	85

Table 5-3: Case 2 Runs Comparison/Three-Stage Solid Propellant Launch Vehicles.....	93
Table 5-4: Solid Propellant Launch Vehicles Mission Statistics.....	97
Table 5-5: Summary of Three-Stage Solid Propellant Launch Vehicle Characteristics (VAFB).....	102
Table 5-6: Summary of Three-Stage Solid Propellant Launch Vehicle Characteristics (CCAFS).....	111
Table 5-7: Four-Stage Solid Propellant Launch Vehicles Comparison.....	115
Table 5-8: Summary of Four-Stage Solid Propellant Launch Vehicle Characteristics (VAFB).....	117
Table 5-9: Summary of Four-Stage Solid Propellant Launch Vehicle Characteristics (CCAFS).....	121
Table 5-10: Liquid Propellant Launch Vehicles Mission Statistics.....	124
Table 5-11: Summary of Three-Stage Liquid Propellant Launch Vehicle Characteristics (VAFB).....	127
Table 5-12: Summary of Three-Stage Liquid Propellant Launch Vehicle Characteristics (CCAFS).....	129
Table 5-13: Summary of Two-Stage Liquid Propellant Launch Vehicle Runs (VAFB).....	130
Table 5-14: Summary of Two-Stage Liquid Propellant Launch Vehicle Characteristics (VAFB-Run #2).....	133
Table 5-15: Summary of Two-Stage Liquid Propellant Launch Vehicle Runs (CCAFS).....	134
Table 5-16: Summary of Two-Stage Liquid Propellant Launch Vehicle Characteristics (CCAFS-Run #2).....	135
Table 5-17: Air-Launched Vehicle Mission Statistics.....	137
Table 5-18: C-141 Transport Aircraft Characteristics.....	140
Table 5-19: Summary of Air-Launched, Two-Stage Liquid Propellant Launch Vehicle Characteristics (CCAFS).....	142

Table 5-20: Air-Launched, Two-Stage Liquid Propellant Launch Vehicles Comparison.....	143
Table 5-21: Mixed Propellant Launch Vehicles Mission Statistics.....	145
Table 5-22: Summary of Three-Stage Solid/Liquid/Liquid Propellant Launch Vehicle Characteristics (VAFB).....	148
Table 5-23: Summary of Three-Stage Solid/Liquid/Liquid Propellant Launch Vehicle Characteristics (CCAFS).....	152
Table 5-24: Optimized Cases for 1,000 lbm Payload Mass.....	154

NOMENCLATURE

a	System-Specific Constant Value
a^*	Speed of Sound at Nozzle Throat
A^*	Nozzle Throat Area
A_b	Solid Propellant Grain Burn Area
A_e	Nozzle Exit Area
A_{exposed}	Exposed Area
A_p	Solid Propellant Motor Port Area
alt_{orb}	Desired Orbital Altitude
alt_1	Final Altitude
A_{ref}	Reference Area
c^*	Characteristic Exhaust Velocity
CCAFS	Cape Canaveral Air Force Station
$C_{D\text{flatplate}}$	Coefficient of Drag for Flat Plate
$C_{\text{development}}$	Development Cost per Launch
$C_{\text{dev-total}}$	Total Vehicle Development Cost
$C_{\text{flight ops}}$	Flight Operations Cost per Launch
$C_{\text{insurance}}$	Insurance Cost per Launch
C_{launch}	Total Cost per Launch
$C_{\text{rec-total}}$	Total Vehicle Recurring Cost
C_T	Thrust Coefficient
C_{vehicle}	Recurring Cost per Launch
CER	Cost Estimating Relationship
CER_{solid}	Solid Rocket Motor Cost Estimating Relationship
CLV	Crew Launch Vehicle
ρ^*	Gas Density at Nozzle Throat
ρ_b	Solid Propellant Grain Density
$\Delta C_{D\text{corr}}$	Coefficient of Drag Correction Factor
Δv	Required Velocity Change (Delta-v)
DB	Double-Base Solid Propellant
DARPA	Defense Advanced Research Projects Agency
DC-X	Delta-Clipper X
D_{throat}	Nozzle Throat Diameter
EELV	Evolved Expendable Launch Vehicle
ε	Angular Fraction
f_{0d}	System Engineering and Integration Factor
f_{0p}	System Management, Vehicle Integration and Checkout Factor
f_1	Development Standard Factor
f_2	Technical Quality Factor

f_3	Team Experience Factor
f_4	Cost Reduction Factor for Series Production
f_6, f_7, f_8	Programmatic Cost Impact Factors
FALCON	Force Application and Launch from CONUS
F_{ES}	Recurring Cost of Solid Rocket Motor
f_{inert}	Inert Mass Fraction
f_{prop}	Propellant Mass Fraction
f_n	Fractional Nozzle Length
f_{var}	Fillet Radius
γ	Ratio of Specific Heats
g_o	Local Acceleration Due to Gravity
GA	Genetic Algorithm
GEM	Graphite Epoxy Solid Motor
h_e	Nozzle Exit Enthalpy
h_o	Combustion Chamber Total Enthalpy
H2O2-95%	Hydrogen Peroxide-95%
H_{ES}	Development Cost of Solid Rocket Motor
HMX	Cyclotetramethylene Tetranitramine
HTPB	Hydroxyl-Terminated Polybutadiene
ICBM	Intercontinental Ballistic Missile
inf	Inflation Rate
int	Interest Rate
IRFNA	Inhibited Red Fuming Nitric Acid
I_{sp}	Specific Impulse
ixx	X-axis Moment of Inertia
iyy	Y-axis Moment of Inertia
izz	Z-axis Moment of Inertia
l	String Bits Length
l_{grain}	Solid Propellant Grain Length
L_o	Launch Site Latitude
LEO	Low Earth Orbit
LF2	Liquid Fluorine
LH2	Liquid Hydrogen
LOX	Liquid Oxygen
l_{rate}	Launch Rate
\dot{m}	Mass Flow Rate
m_{inert}	Inert Mass
m_{prop}	Propellant Mass
max	Maximum Design Parameter Value
min	Minimum Design Parameter Value
MMH	Monomethyl Hydrazine
MYr	Man Year
N2O4	Nitrogen Tetroxide
n	Population Size
NAFCOM	NASA and Air Force Cost Model

NASA	National Aeronautics and Space Administration
NASP	National Aerospace Plane
nbits	Number of Bits in Chromosome String
npay	Number of Payments
nsp	Number of Star Points
nstg	Number of Stages
nunits	Number of Units
ORS	Operationally Responsive Space
p	Learning Factor
P_a	Atmospheric Pressure
P_c	Combustion Pressure
P_e	Exit Pressure
P_{avg}	Average Payment Value
$P_{constant}$	Constant Payment Value
PBAA	Polybutadiene-Acrylic Acid
PBAN	Polybutadiene-Acrylic Acid-Acrylonitrile Terpolymer
PS	Polysulfide
r	Solid Propellant Grain Burn Rate
R	Gas Constant
R_{annual}	Annual Reduction Factor
R_{bi}	Grain Outer Radius
R_i	Inner Star Radius
R_p	Outer Star Radius
RP-1	Rocket Propellant-1
R_{stg1}	Radius of Stage 1
R_{stg2}	Radius of Stage 2
6DOF	Six-Degree-of-Freedom
SLV	Space Launch Vehicle
SRB	Solid Rocket Booster
T	Thrust
T_c	Combustion Temperature
T_o	Combustion Chamber Total Temperature
UDMH	Unsymmetrical Dimethylhydrazine
USAF	United States Air Force
VAFB	Vandenberg Air Force Base
V^*	Gas Velocity at Nozzle Throat
V_e	Exit Velocity
x	System-Specific Cost-to-Mass Sensitivity Factor
xcg	Center of Gravity Location
y_{burn}	Solid Propellant Burn Direction

1.0 INTRODUCTION

From the early space launch attempts almost 50 years ago up until today, private companies, government agencies and entire countries have invested large amounts of capital attempting to lower the price of access to space. Concepts such as the National Aerospace Plane (NASP), the single-stage-to-orbit X-33 and the Delta Clipper-X (DC-X) have all been valiant attempts at achieving low cost, easy access to space.

Assured access to space and responsive spacelift are two very high priority topics in the United States Air Force (USAF) space community. As General Kevin P. Chilton, Commander, Air Force Space Command has put it: “The rockets we launch into space carry with them the communication, weather, surveillance, navigation, and other national assets which are integral to our national security as well as our economy.”¹ Thus, significant work will continue in order to guarantee that the United States has access to space and, if necessary, the capability to deny access to an adversary.

As a result, the USAF seeks assured and affordable access to space. The current USAF vision for achieving this capability is called Operationally Responsive Space (ORS). One broad outcome of ORS is to produce a launch vehicle with the following goals: launch a 1,000 lbm payload into low-Earth orbit at a cost of under \$5 million and launch the vehicle within 24 hrs of tasking.

In order to support ORS, the Defense Advanced Research Projects Agency (DARPA) and the USAF are “jointly sponsoring the Force Application and Launch from

CONUS (FALCON) program to develop technologies and demonstrate capabilities that will enable transformational changes in global, time critical strike missions.”² The goal of this program is to design a launch vehicle with a prompt global strike capability. The technologies needed for a prompt global strike capability are essentially the same as those needed to design a responsive and reliable space launch vehicle.

This dissertation describes an effort to optimize the design of an entire space launch vehicle that will carry a payload into low-Earth (circular) orbit. The launch vehicle consists of multiple stages and the design optimization uses a genetic algorithm (GA) with the goal of minimizing total vehicle weight and ultimately vehicle cost for a given mission from a given launch site. The entire launch vehicle system is analyzed using various multi-stage configurations to reach the desired low-Earth orbit. Three different types of conventional propulsion systems are considered: solid propellant motors, liquid-fueled rockets, and air-launched systems using an airborne platform as the first-stage. The vehicle performance modeling required that analysis from four separate disciplines be integrated into the design optimization process. Those disciplines are the propulsion characteristics, the mass properties, the aerodynamic characteristics and the six-degree-of-freedom (6DOF) flight dynamics characteristics.

2.0 CHRONOLOGY OF OPTIMIZATION TECHNIQUES

2.1 Introduction

The goal of design optimization is to find the optimum (from the Latin word *optimus*, meaning best) solution to the design problem. The theory of optimization has an enormous variety of real world applications that can benefit from an optimum solution. From traffic flow problems to space launch vehicle design, finding an optimum solution early in the problem solving process can pay huge dividends. Thus, it can be readily stated that the theory of optimization involves the use of mathematics to facilitate problem solving. Modern computers, with their incredibly fast computational capabilities, have turned optimization theory into a rapidly growing branch of applied mathematics. Numerous different optimization techniques exist from classical methods to modern evolutionary algorithms.

2.2 Early Concepts

According to Foulds,³ one of the first recorded uses of optimization theory dates back to ancient times. In 200 B.C., Archimedes correctly conjectured that the semicircle was the optimal geometric curve of given length, together with a straight line, that enclosed the largest possible area. More advanced techniques would not come about until the 17th century with Newton's development of calculus. Gauss developed the first formal optimization technique known as steepest descent.

2.2.1 Newton and Calculus-Based Methods

Newton formulated a straight forward method for determining the local maxima and minima of a function by using the first derivative of an equation. Setting the first derivative equal to zero and solving the equation provides the condition for a maximum or minimum. The sign (positive or negative) of the second derivative can be used as a test. However, according to Siddal,⁴ when multiple functions are used to describe the behavior of a system, this method can produce numerous nonlinear algebraic equations that must be solved simultaneously. Determining the actual maximum or minimum value from these equations can be difficult.

2.2.2 Gradient Methods

Gradient methods such as steepest ascent or steepest descent were developed in the 19th century. These methods attempt to “march” toward a local maximum (ascent) or local minimum (descent) by taking steps proportional to the gradient of the function at the current point. The marching can “stop” at the point where successive changes in the function become negligible indicating a maximum or minimum has been reached. This method can run into problems when there are numerous local maxima or minima. To avoid getting “stuck” in these local optima, gradient methods need a reasonable starting solution to begin the process. As a result, this restricts the possibility of finding a truly global maximum or minimum value of the function.

In addition, gradient methods are also dependent upon the nature of the function being analyzed. Since these methods operate on the first derivative of this “objective” function, the function must be differentiable in every independent variable. Otherwise, a

singularity will result and the ability to “march” toward a local maximum or local minimum value will be compromised.

2.3 Linear Programming

Gabasov and Kirillova⁵ state that “Linear programming problems were first formulated and studied by the Soviet mathematician L.V. Kantorovich in the 1930s. In the 1940s, the American mathematician G.B. Dantzig developed the simplex method of solution.” The general linear programming problem involves an objective function and constraints that are all linear. Additionally, the goal of the optimization is to simply maximize or minimize the objective function. The simplex algorithm was developed to analyze feasible solutions to the objective function until no improvement in the objective function could be made. The search space is modeled in a geometric form such as a polyhedron. The simplex algorithm simply marches along the outskirts of this shape in order to find a single optimal point. At this point, either the maximum or minimum value of the objective function has been found that satisfies the given constraints.

The advantages of linear programming are that this method is very efficient in practice and it is guaranteed to find a global optimum. The disadvantage is that this method cannot handle complex problems such as a multi-variable optimization because the objective function and constraints are required to be linear.

2.4 Pattern Search Optimization

When the problem is to maximize a real-valued function with no constraints, numerous methods exist to find a solution. Many methods look at the behavior of the function being analyzed and use this information to proceed to the solution. Direct methods and gradient methods fall into this category. The strategy often involves

selecting a point within the domain that is thought to be the most likely place where a maximum or minimum exists. If no information is available for choosing this point then one is chosen at random. From there, a particular method is used to generate more points that move closer and closer to the desired optimum solution.

As described by Foulds,³ pattern search optimization is a direct search method. Pattern search, the first direct search method to be examined, was developed by Hooke and Jeeves in 1961. Direct search methods differ from gradient methods in one important way. Given a function to be optimized, say $f(x)$, a direct search method requires that $f(x)$ be evaluated at each point in the optimization process. Gradient methods require the evaluation of the first derivatives of $f(x)$ at those same points.

The pattern search method is fairly straight forward. The function, $f(x)$, is evaluated at a chosen point. Then, exploration about this point is done in order to find the direction of improvement. Slight perturbations of each variable are performed and $f(x)$ is again evaluated at the chosen point. If an increase is observed (indicating improvement for a maximizing problem) then, the next variable is evaluated using the same perturbation. The process continues until all variables have been analyzed and the final best point has been established. Using the final best point and the original starting point, a step size is calculated as twice the Euclidean distance between these two points. Using this step size and the original starting point, the new evaluation point is determined and the process repeated. Thus, there is a general trend or improvement which Hooke and Jeeves called a pattern.

The method works well as long as each successful iteration produces a value closer to the maximum value of the function. The method does have a few short

comings. It requires an initial “guess” to get the process started. The nature of the function being investigated can also cause problems. If the function has any tightly curved ridges or sharp-cornered contours, the method may be unable to produce any improvements while still far from a local maximum. Also, the method only finds local maxima around the point initially chosen (i.e. the initial “guess”). Thus, it can not determine a global maximum independently. If numerous local maxima have been determined then comparison of these local maxima could yield a global maximum.

2.5 Design of Experiments

The concept known as the design of experiments was formulated in the 1920s when Sir Ronald Fisher wrote his book “Statistical Methods for Research Workers.” At the time, experimenters did not have any proven methods for interpreting the vast amount of data being generated in laboratories. Fisher went about inventing many of the techniques used today for conducting and analyzing experiments. Through statistical procedures, he wanted to remove criticism of the results of experiments where the interpretation of the results and the execution of the experiment were questioned. Fisher’s⁶ influential book “The Design of Experiments,” written in 1935, discussed the method known as the analysis of variance. This simple arithmetical procedure summarizes the experimental results and details the structure of the experiment. This allows for the proper testing (i.e. interpretation) of the experimental results.

According to Weber and Skillings,⁷ “a designed experiment is an experiment in which the experimenter plans the structure of the experiment.” The authors have developed specific steps that need to be followed when conducting an experiment. These steps are as follows: determining the goal of the experiment, defining the variables,

establishing the levels or ranges of the variables, designing the experiment, running the experiment and analyzing the results. A linear statistical model is then used to describe the structure of the data resulting from the experiment.

In addition to improving physical experiments themselves, the design of experiments method can be used as an optimization tool. In this application, analytical models can be used to predict the possible outcomes within a particular experimental region. The resulting optimal experimental point can then be determined. This process “designs” the experiment so that the optimum investigation can be performed.

2.6 Additional Methods

The response surface method is an optimization method that is computationally attractive and straight forward in application. Rodriquez⁸ explains that this method takes a complex and highly nonlinear function and replaces it with a simplified, multi-dimensional surface fit. This response surface fit results in a simple mathematical representation of the complex function. Both the values of the function and the gradient at other points can be determined with the response surface. Using a gradient-based optimizer, the optimal point in the response surface can be determined as well. The advantage of this method is that it is very efficient and effective at analyzing a complex function. The disadvantage of the response surface method is that the curve fit must be an accurate representation of the complex function or an optimal point will not be found.

Monte Carlo design optimization is another popular technique for solving complex physical and mathematical problems that possess many variables. The Monte Carlo method is considered to be stochastic in that it generates random numbers in order to evaluate the function. These values of the function are then averaged in order to

estimate the function's true value. In terms of optimization, the method will randomly "walk" throughout the design space and tend to move in a direction towards either a maximum or a minimum. A gradient method can be incorporated to help facilitate the determination of the optimum value. Monte Carlo methods have the advantage of searching a very large design space but at the same time are computationally expensive due to the large amount of random numbers required.

Finally, a method known as particle swarm optimization has been used successfully in the optimization of physical structures and artificial neural networks. The method is a population-based method similar to other evolutionary techniques. The members of the population follow (or swarm) towards the best performing member and each member knows its position and velocity compared to the optimum member. In subsequent generations, the position and velocity of each member are updated in order to get closer to the characteristics of the optimum member. The advantage of this method is that it can result in a computationally faster and cheaper method of finding an optimum solution.

2.7 Genetic Algorithms

Mitchell⁹ states that "Genetic algorithms (GAs) were invented by John Holland in the 1960s and were developed by Holland and his students and colleagues at the University of Michigan in the 1960s and 1970s." Holland wanted to take the evolutionary processes that are hypothesized to occur in nature (adaptation, survival-of-the-fittest, etc.) and incorporate them into a computer system. Holland's classic 1975 book "Adaptation in Natural and Artificial Systems" formulates evolutionary/population based algorithms that can be used to optimize a variety of real world systems.

According to Coley,¹⁰ GAs are numerical optimization algorithms built around natural selection and natural genetics. Sometimes GAs are referred to as evolutionary optimizers because they mimic some of the processes proposed in Darwinian evolution theory. Darwinian evolution theorizes that totally new species can be produced via mutation and random chance. However, unlike evolution, GAs operate more on the principal of improvement of an initial population of solutions to a design problem rather than pure optimization. Coley¹⁰ describes the make-up of a typical GA in a number of ways. First, a GA can be described as a number, or population, of guesses of the solution to the problem. Second, the GA employs a method of calculating how good or how bad the individual solutions within the population are. This method is called determining the fitness of the solution. Additionally, a method for mixing fragments of the better solutions to form new, on average even better solutions can be used. This method is called crossover. Finally, the GA is able to use a mutation operator to avoid permanent loss of diversity within the solutions.

One of the main benefits of using a GA is the fact that the algorithm can start without a single point, or guess, to get the optimization running. The previously described direct search and gradient methods all, except design of experiments, need an initial guess to the problem solution in order to “march” toward the desired optimized result; either a maximum or minimum value. The GA uses a population of guesses that are random and spread throughout the search space. Powerful operators such as selection, crossover and mutation help direct members of each population toward the desired goal(s) of the problem. A binary encoding system allows for a host of variables to be manipulated by the GA and then used in a suite of performance codes. These codes

analyze the performance of each member of the population and the GA ranks each one according to how well that member meets the desired goal(s). In GA terminology, the objective function is the function that determines the performance of a particular chromosome (i.e. member of the population).¹⁶ Thus, in this study, the suite of performance codes, grouped together as a whole, represent the objective function.

At the same time, the GA does have some disadvantages. In using the GA there is a greater likelihood that a global optimum solution will be found. However, finding this global optimum is not guaranteed. Even if the GA is in the neighborhood of the global optimum, there is a possibility through crossover and mutation that the global optimum may not be selected. Also, the GA does not address the robustness of the individual design solutions it creates. The GA simply attempts to meet the desired goals and will adjust the design parameters accordingly. Thus, it is up to the user to ensure the proper operation of the GA and to verify the results it generates. Finally, the satisfactory operation of the GA relies on the accuracy of the system models that make up the objective function. The GA used for this dissertation will be discussed in greater detail in Chapter 3.

2.8 Recent Launch Vehicle Optimization Work

In recent years, significant work has been done to advance the design and analysis of entire launch vehicle systems. Extensive research has gone into improving the design of solid rocket motors. In 1968, Billheimer¹¹ made one of the first attempts to perform an automated design of a solid rocket motor. The significance of this study emphasized the importance of automating the design process. Using a pattern search technique, in 1977, Woltosz¹² determined five critical design dimensions in order to find an optimum grain

geometry for a solid rocket motor. Foster and Sforzini¹³ then used the same pattern search technique to minimize the differences between desired and computed solid rocket motor ignition characteristics. Finally, in 1980, Sforzini¹⁴ performed an automated approach to analyzing the internal characteristics of a solid rocket motor and used the Space Shuttle solid rocket booster for comparison. Using the pattern search optimization technique, Sforzini¹⁴ was able to generate a head end pressure versus time profile that closely matched the Space Shuttle solid rocket motor.

In order to analyze the performance of an entire launch vehicle, a suite of analytical models is required. The aerodynamic characteristics of the vehicle must be determined over a wide-range of flight conditions for the portion of the flight during which the vehicle is in the atmosphere. It is fortunate that space launch vehicles spend only a short time in the Earth's atmosphere. Nonetheless, the aerodynamic characteristics play an important role and must be analyzed. In the past, gradient-based optimization techniques have been applied to optimize the aerodynamic characteristics of missiles. However, as stated previously, these methods have limited capability in finding globally optimized solutions. In 1990, Washington¹⁵ developed an aerodynamic prediction package, called AeroDesign, that can be used to determine the aerodynamic constants of different missiles. Additionally, based on the equations of motion described in Etkin's¹⁷ book, Anderson¹⁶ developed a six-degree-of-freedom (6DOF) flight dynamics simulator. This 6DOF flight dynamics simulator was used to fly the vehicle over a ballistic trajectory given an initial launch angle.

In 1998, Anderson¹⁶ assembled these performance codes and created an objective function that could analyze the performance of an entire, single-stage solid propellant

rocket vehicle. In addition, Anderson^{16,43} wrote a GA that was used to optimize the performance of these solid rockets given specific goals and using the suite of performance codes as the objective function.

In 2003 and 2006, Burkhalter et al.¹⁸ and Hartfield et al.¹⁹ took the design optimization of missile systems further. First, an additional model was created for the objective function in order to analyze the performance of liquid rocket engines. Second, the first attempt into multi-stage configurations was begun with the analysis of both a two-stage, solid propellant tactical missile and a solid propellant boosted ramjet system.

The foundation work necessary to use these system models, in the form of performance codes, and the GA to pursue the design optimization of space launch vehicles has been completed. In addition to analyzing the overall performance of each launch vehicle, a cost model has been developed in order to bring an economic factor into the optimization process.

The key to the current study is the GA and its ability to find a global optimum solution to a challenging design problem. Population-based, evolutionary algorithms, like the GA, are much more useful than pattern search methods or gradient methods when investigating a complex, multi-variable problem with non-differentiable objective functions. Typically, a number of discrete variables will be used by the GA and the objective function. Also, the functions describing the model can be complex, nonlinear, and not easily differentiable. This makes pattern search and gradient methods difficult, if not impossible, to use in solving the problem. In addition, because of the non-linearity of these functions, the number of local optima can be significant. Thus, since the pattern search method uses an initial “guess” to the solution, the odds of actually hitting the

global optimum with this guess are not especially likely. Finally, with the binary encoding system used by the GA, a large number of variables can be analyzed. Table 2-1 shows an example of the number and types of variables used to analyze a three-stage solid propellant launch vehicle. A total of 36 different design parameters were used to optimize the performance of this particular type of space launch vehicle.

Encoding these variables into a single string of bits of length (l) allows the GA to perform various operations on this single string. Then, the string of variables is decoded for analysis in the objective function. For the current study, typical string lengths are on the order of 200 bits. Using the length (l) for the string length, the number of possible solutions can be expressed as 2^l . By comparison, a problem that has a string length of 50 bits means that there are 2^{50} possible solutions to the problem (1.125 trillion). The GA is uniquely capable of efficiently analyzing such a large solution space in search of an optimum.

To summarize, evolutionary techniques have been used to solve a myriad of design optimization problems.²⁰⁻²⁴ Significant research has been performed in rocket-based vehicle design optimization using various evolutionary techniques.²⁵⁻³⁶ A recent study³⁷ attempted the design of a satellite launch vehicle using an evolutionary algorithm to minimize the gross lift-off weight of the vehicle. The vehicle model was based simply on delta-V requirements for the launch system. The delta-V for the model was determined by analyzing the performance capability of the Ariane 44L launch vehicle. Cost has also been considered in some additional studies;^{32, 38-40} however, this dissertation represents the first effort of its kind to minimize launch vehicle cost for Earth-to-orbit missions at the preliminary design level using a GA.

Table 2-1: Design Variables for a Three-Stage Solid Propellant Launch Vehicle

<u>Definition (units)</u>	<u>Maximum Value</u>	<u>Minimum Value</u>
<u>Stage 1</u>		
fuel type	9.0	1.0
propellant outer radius ratio	0.80	0.40
propellant inner radius ratio	0.99	0.01
number of star points	13.0	3.0
fillet radius ratio	0.20	0.01
epsilon star width	0.90	0.10
star point angle	40.0	1.0
fractional nozzle length ratio	0.99	0.60
throat diameter (inches)	35.0	5.0
total stage length (inches)	500.0	300.0
stage body diameter (inches)	90.0	70.0
<u>Stage 2</u>		
fuel type	9.0	1.0
propellant outer radius ratio	0.80	0.40
propellant inner radius ratio	0.99	0.01
number of star points	13.0	3.0
fillet radius ratio	0.20	0.01
epsilon star width	0.90	0.50
star point angle	40.0	1.0
fractional nozzle length ratio	0.99	0.60
throat diameter (inches)	35.0	5.0
total stage length (inches)	300.0	200.0
stage body diameter (inches)	70.0	60.0
<u>Stage 3</u>		
fuel type	9.0	1.0
propellant outer radius ratio	0.80	0.40
propellant inner radius ratio	0.99	0.01
number of star points	13.0	3.0
fillet radius ratio	0.20	0.01
epsilon star width	0.90	0.50
star point angle	40.0	1.0
fractional nozzle length ratio	0.99	0.60
throat diameter (inches)	35.0	5.0
total stage length (inches)	200.0	100.0
stage body diameter (inches)	60.0	50.0
<u>Miscellaneous</u>		
nose radius ratio	0.75	0.50
nose length (inches)	100.0	75.0
initial launch angle	89.99	70.0

3.0 SYSTEM MODELING

3.1 Introduction

The overall approach taken for modeling the launch vehicle systems considered in the design optimization process follows the method employed by Anderson,¹⁶ Burkhalter et al.,¹⁸ Hartfield et al.,¹⁹ and Metts.²⁰ Modeling of the launch vehicle consists of employing a suite of performance codes which are based on physical models for the propulsion system, the mass properties, the aerodynamics, and the vehicle flight dynamics. All critical vehicle performance parameters are calculated using these individual system models. The results are used to determine how well the particular launch vehicle meets the desired goals of the design optimization.

In addition to vehicle performance, a cost model, based on the work of Koelle⁴¹ and Wertz,^{38,42} has been incorporated into the objective function. The *TRANSCost 7.1* cost model created by Koelle⁴¹ is a mass-based model that provides cost estimates for a variety of launch vehicle types. As a result, the information generated in the mass properties models is utilized in the cost model.

3.2 Objective Function Link to the Genetic Algorithm (GA)

In general, the design optimization process can be broken into two distinct operations that are linked together. The objective function determines the performance of individual members of the population while the GA provides a continuous set of parameters to be analyzed based on probabilistic selection.

Figure 3-1 shows the program flow with the objective function, how it is linked to the GA, and the different GA operators.

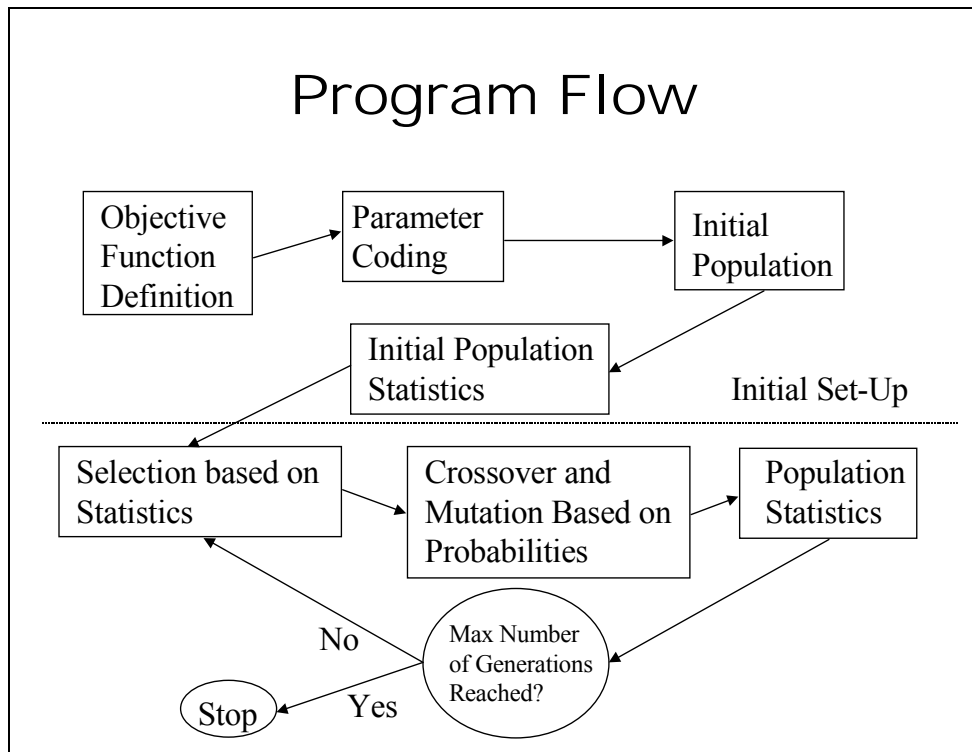


Figure 3-1. Objective Function Link to the GA

The objective function contains all of the performance codes required to determine the performance of a particular launch vehicle. In order to analyze different launch vehicles, some design parameters (e.g. propellant types, nozzle geometry, etc.), whose values can be altered, are chosen for analysis. Given the design parameters, the objective function can assemble and model the performance for any of a wide variety of launch vehicles.

In addition to determining the performance of each launch vehicle, the objective function uses performance criteria to analyze how well a particular launch vehicle meets the desired goals of the optimization. A quantitative measure is established by the user so that the objective function can determine which launch vehicles perform “better” than

others. For example, prior to starting the design optimization process, a desired orbital altitude ($altorb$) is chosen by the user. Next, the design optimization process is started and the GA creates a population of candidate launch vehicles. Each candidate launch vehicle is run through the objective function and attains a final altitude ($alt1$). Since one of the goals is to reach the desired orbit, the objective function must compare the two altitudes. This comparison is done in the following equation:

$$answer = \frac{|altorb - alt1|}{altorb} \quad (3.1)$$

In order to reach the desired orbit, the goal must be to minimize the answer to Equation (3.1). The launch vehicle with the smallest value of Equation (3.1) is considered to be the best performer for that generation. It is the highest ranked member of the population and its characteristics are carried on to the next generation where the process repeats itself.

Typically, a design optimization problem has one or more desired goals. If the goal is to find the launch vehicle that maximizes the thrust of a solid rocket motor, then the objective function must be run numerous times to find the rocket with the desired characteristics. This can be a tedious and inefficient process which will require trial and error in order to find the optimum launch vehicle that meets the desired goal. As Anderson¹⁶ wrote: “The goal of this research is to remove the human designer from the tedious task of searching for the optimal parameter set.” The GA can be used in place of the human designer for the function of evaluating the objective function and deciding on proposed areas of the design space to explore.

3.3 Genetic Algorithm (GA)

The GA for this study was developed by Anderson⁴³ and uses the biological concept of generational adaptation to solve a design optimization problem that may contain numerous local optima. The GA is considered to be an adaptive optimizer. The process is one in which the GA encodes potential solutions to the design problem into a numerical string (usually called a chromosome). Some corresponding design parameters and an example chromosome that might make up a potential solid rocket design solution are shown in Table 3-1. This chromosome string illustrates the binary encoding method used by the GA and described below.

Table 3-1: Example Design Parameters and Chromosome

Parameter	Real Value	Binary Form
Number of Star Points	10	1010
Total Stage Length	120 inches	1111000
Stage Diameter	50 inches	110010
Chromosome String	1010111000110010	

The chromosome string can then be manipulated via different genetic-type operations such as reproduction, crossover, and mutation. In addition, a selection process is employed which allows various solutions to compete against one another. The “better” or more fit solutions are passed on to subsequent generations while the characteristics of “lesser” solutions “die off.” The goal is to create increasingly better solutions as time successive generations are developed.

Rather than define the first generation of designs from an initial “guess” provided by the user, the user specifies a range (maximum, minimum, and resolution) for each design parameter, and the GA randomly generates a population of candidate solutions

from parameters within the prescribed design space. After each candidate is analyzed by the performance codes that make up the objective function, the GA ranks the candidates (members) in order of fitness, or how closely they match the objective function.

The process by which possible solutions are converted to a form that can be manipulated by the GA is known as parameter encoding. The most popular type of encoding for a GA is binary encoding. Here the design parameters are converted into 1s and 0s to form the chromosome string that represents a possible solution. Using the maximum, minimum and resolution values, each design parameter can be converted into a number of bits using the equation:

$$nbits = \frac{\ln\left(\frac{\max - \min}{\text{resolution}}\right)}{\ln(2)} + 1 \quad (3.2)$$

Each design parameter is converted in this way and then all the parameters are strung together to form one member among a population of possible solutions. The GA can manipulate each string (or chromosome) and thus produce all the members that make up one generation. Each individual string can be decoded into real numbers prior to its use in the objective function.

For this study, a tournament-based GA is used to control the design process. Specifically, the IMPROVE[©] 3.1 GA, developed by Anderson,⁴³ has been implemented. The tournament selection process involves an essentially three step process shown in Figure 3-2. First, two members of the current population are chosen at random and compete against each other. The member that performs better survives to an intermediate population. The “losing” member returns to the current population. Next, two more members from the current population are chosen at random (the “losing” member could

actually be chosen again) and compete. Again, the member that performs better survives to the intermediate population. Finally, crossover and mutation operations are performed on the two “winning” members in order to create two new members that replace the members lost in the tournament process. This process continues until the new population has been filled with the required number of new members.

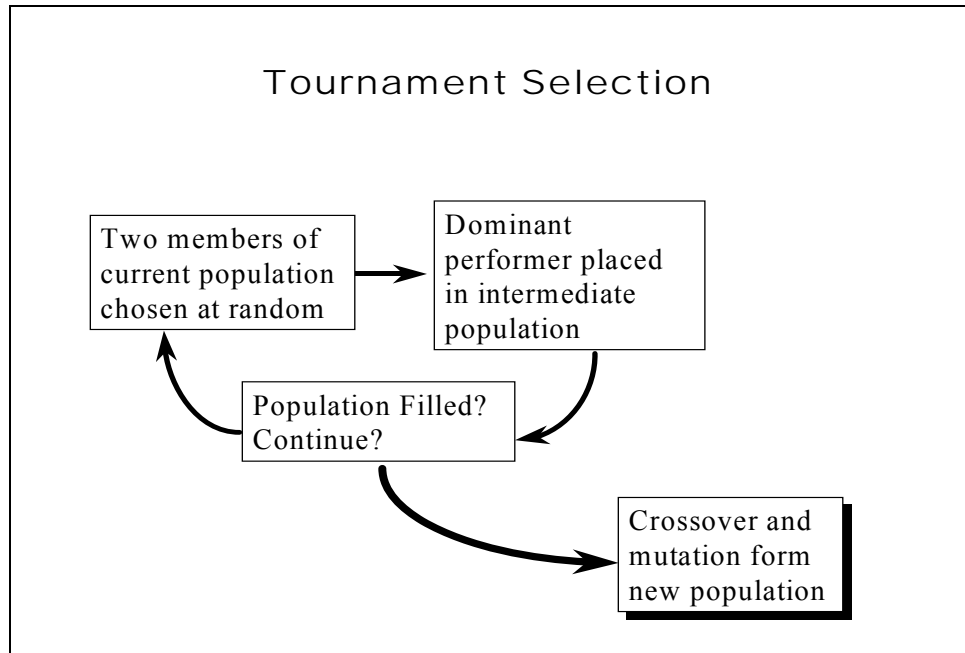


Figure 3-2. Tournament Selection

The tournament selection method is thus used to create the next generation of members, which will possess characteristics of the previous population but in different combinations which may result in better overall fitness. When properly configured, the GA will find solution types that increasingly approach the target fitness over the course of many generations.

The IMPROVE[®] 3.1 GA employs two powerful tools for ensuring that diverse populations of potential solutions are maintained throughout the design optimization.

First, crossover is the process where two “parent” solutions exchange portions of their

genetic code thus producing two “offspring.” The goal here is to take advantage of good genes by promulgating and mixing them with future generations. This helps the IMPROVE[®] 3.1 GA to improve beyond the initial population or any local optima. The second tool, mutation, allows for the random altering of individual bits/genes that make up a chromosome. This provides robustness as 1s are randomly switched to 0s and vice versa. Like crossover, mutation gives the IMPROVE[®] 3.1 GA the ability to jump beyond any local optima that may have been encountered.

The performance codes that make up the objective function analyze each member generated by the IMPROVE[®] 3.1 GA to determine the overall performance of the vehicle. This allows the IMPROVE[®] 3.1 GA to find solution types that not only meet the target fitness but which are also realistic (i.e. valid). Does one design/solution stand out among all the others? In reality, one design/solution might produce highly desirable results that meet the goals exactly. However, other designs might not meet the goals exactly but still produce results that are “close” to the desired system. In this study, the answer to finding the optimum design is the IMPROVE[®] 3.1 GA. But the GA by itself does not indicate that a model is valid. In fact, the GA makes no statement at all as to the validity of the underlying system models. The IMPROVE[®] 3.1 GA simply chooses the optimum design that meets the desired system goals. It is up to the user to take the information generated by the IMPROVE[®] 3.1 GA and make the important decisions as to which design/solution is the best.

The number of members present in a single population, known as population sizing, is typically determined prior to the start of the optimization process. The determination of the number of members required for success of the IMPROVE[®] 3.1 GA

is not easy. As Anderson¹⁶ wrote: “Proper population sizing is a seriously debated issue when using genetic algorithms.” In general, for a complicated design problem with a large search space, a large population size is required. The population size (n) can be calculated by knowing the total number of genes required for each member of the population. In the binary encoding process, the number of genes is represented by the number of bits making up the chromosome string. Using Equation (3.2), the number of bits ($nbits$) is calculated and then used in Equation (3.3).

$$n = (3.0)nbits \quad (3.3)$$

This issue of determining the ideal number of generations for a particular design problem is also not explicitly defined. If the number of generations is high, the optimization is more likely to produce an optimum solution. However, a large number of generations combined with a large number of members in each generation results in significant computer run times. As the computing speed of modern computers increases, the ability to run a large amount of generations will improve. At the same time, using a large number of generations does not necessarily ensure the optimum design will be found. Other factors such as crossover and mutation also affect genetic diversity and robustness of the optimization. It is possible that a smaller number of generations could still produce the optimum solution. Currently, the ideal number of generations to use is a matter to be decided by the user.

Finally, the IMPROVE[®] 3.1 GA uses an additional tool in the design optimization process. Elitism is the process of preserving the “elite” member of each population and to allow that member to survive intact into the next generation. There are both benefits and drawbacks to elitism. The benefit is that elitism can keep an unfortunate crossover or

mutation from wreaking havoc in a particular generation. It allows at least one “good” member to be preserved, passed on to the next generation and hopefully improved upon. The drawback is that elitism can focus the optimization on the current best performer while at the same time ignoring an even better performer. The use of elitism is again a decision to be made by the user.

3.4 Propulsion System Models

After the GA has generated values for the set of design parameters, the propulsion system models are the first performance codes to be analyzed in the objective function. These models analyze the basic thrust characteristics of solid and liquid propulsion stages. Fuel and oxidizer properties are pre-loaded and used to calculate thrust, burn time, fuel/oxidizer mass, combustion pressure, etc. For example, the grain geometry of a solid propellant motor can be specified by the GA using the design parameters. From these values, the entire sea-level thrust profile of the motor is determined in the solid rocket propulsion model. Similar analyses can be done for the liquid propellant rocket engines.

For a multi-stage vehicle, the number of times each particular propulsion system model is evaluated corresponds to the number of stages in the vehicle. The propulsion characteristics of each stage are determined separately and in sequence.

It is useful to discuss some of the basic equations associated with rocket propulsion that are used in the propulsion system models. First, a steady flow assumption through a choked nozzle is assumed. This allows the mass flow discharged through the nozzle to be calculated as:

$$\dot{m}_{disch} = \rho * A * V * \tag{3.4}$$

Assuming isentropic flow in the nozzle and knowing that $V^*=a^*$, the following equation can be written:

$$\dot{m}_{disch} = A^* P_c \sqrt{\frac{\gamma}{RT_c}} \left(\frac{2}{\gamma+1} \right)^{\frac{\gamma+1}{2(\gamma-1)}} \quad (3.5)$$

The characteristic velocity of the rocket, c^* , can be written as:

$$c^* = \sqrt{\frac{RT_c}{\gamma}} \left(\frac{\gamma+1}{2} \right)^{\frac{\gamma+1}{2(\gamma-1)}} \quad (3.6)$$

Substituting Equation (3.6) into Equation (3.5) results in another equation for the rate of mass discharged through the nozzle:

$$\dot{m}_{disch} = \frac{P_c A^*}{c^*} \quad (3.7)$$

Additional equations are used to calculate the thrust of the rocket, the thrust coefficient, and the exit velocity. From the uniform, steady, one-dimensional momentum equation, the thrust, T , is determined to be:

$$T = \dot{m}V_e + (P_e - P_a)A_e \quad (3.8)$$

The thrust coefficient, C_T , is defined as:

$$C_T = \frac{T}{P_c A^*} \quad (3.9)$$

Substituting the thrust equation (Equation (3.8)) and the equation for the mass flow rate discharged through the nozzle (Equation (3.7)) into Equation (3.9) yields:

$$C_T = \frac{V_e}{c^*} + \left(\frac{P_e}{P_c} - \frac{P_a}{P_c} \right) \frac{A_e}{A^*} \quad (3.10)$$

The uniform, steady, one-dimensional energy equation can be used to determine the exit velocity of the nozzle assuming an adiabatic flow.

$$h_e + \frac{V_e^2}{2} = h_0 \quad (3.11)$$

Assuming an isentropic expansion through the nozzle and using some thermodynamic substitutions, the exit velocity can be written as:

$$V_e = \sqrt{\frac{2\gamma RT_0}{\gamma-1} \left(1 - \left(\frac{P_e}{P_c} \right)^{\frac{\gamma-1}{\gamma}} \right)} \quad (3.12)$$

3.4.1 Solid Propellant Rocket Motors

The solid propellant rocket propulsion model used in this analysis was developed by Burkhalter,⁴⁴ Sforzini⁴⁵ and, with modifications, Hartfield et al.¹⁹ Figure 3-3 provides a schematic showing the basic geometry of a solid rocket motor.

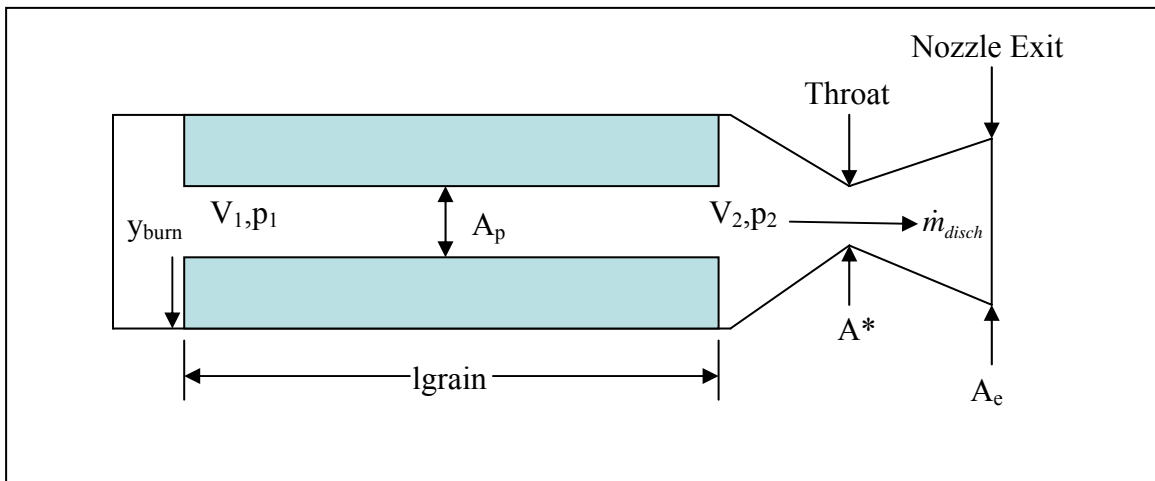


Figure 3-3. Solid Rocket Motor Schematic

Anderson,¹⁶ who used the model extensively, explained that some fundamental assumptions were made in the formulation of the software used to analyze solid rocket motors. One assumption is that the combustion of the solid propellant is stable (i.e. steady). Thus, the rate of mass produced by the burn must equal the rate of the mass

discharged through the throat of the nozzle. If the propellant grain burn area is A_b and the burn rate is r , the mass flow rate generated can be written as:

$$\dot{m}_{gen} = \rho_b A_b r \quad (3.13)$$

Setting Equation (3.13) equal to Equation (3.7), the mass flow rate generated can be written as:

$$\dot{m}_{gen} = \rho_b A_b r = \frac{P_c A^*}{c^*} = \dot{m}_{disch} \quad (3.14)$$

Equation (3.14) is the basic performance relationship used to determine chamber pressure and, in turn, sea-level thrust for the solid rocket motor. In this model, the chamber conditions are considered to be uniform and are “lumped” into a single variable. For that reason, this approach to modeling solid rocket motor performance is known as “lumped parameter” modeling.

3.4.2 Liquid Propellant Rocket Engines

The liquid propellant rocket propulsion model used in this analysis was created by Hartfield et al.¹⁹ with additional modifications by Riddle.²¹ The oxidizer and fuel are stored in separate tanks. An inert compressed gas is used to provide pressurization for both the fuel and oxidizer tanks. The pressure in the fuel and oxidizer tanks is kept relatively low; around 100 psia. Like the solid propellant motors, the temperature and pressure in the combustion chamber are assumed to be constant. Also, the thrust goes to zero at burnout for each stage and there is no delay between burnout of one stage and ignition of the next stage. The model is also based on the assumption that the turbopumps are used to pressurize the fuel and oxidizer prior to injection into the combustion chamber.

With some minor changes, Equations (3.4) thru (3.12) are used to determine the thrust, the thrust coefficient, the mass flow rate, and the exit velocity of the nozzle. The value of specific impulse, I_{sp} , for the propellants is used in the calculation of the thrust coefficient.

$$I_{sp} = \frac{V_e}{g_e} \quad (3.15)$$

Solving for V_e and substituting into Equation (3.8), allows the thrust coefficient to be written as:

$$C_T = \frac{I_{sp} g_e}{c^*} + \left(\frac{P_e}{P_c} - \frac{P_a}{P_c} \right) \frac{A_e}{A^*} \quad (3.16)$$

From the coefficient of thrust, the thrust, T , of the rocket can be determined from Equation (3.8):

$$T = P_c A^* C_T$$

The mass flow rate can then be determined using the thrust:

$$\dot{m} = \frac{g_e T}{c^*} \quad (3.17)$$

A wide variety of liquid propellant combinations are available for analysis in this study. The choice of propellants is a design variable for the GA. Riddle²¹ writes that propellant properties such as stoichiometric mixture ratio, combustor total temperature, molecular weight, characteristic exhaust velocity, sea-level specific impulse, and the ratio of specific heats are included in the list with their corresponding fuel/oxidizer combination. A few examples of different liquid propellant fuels and oxidizers available for use in the design optimization process are shown in Table 3-2.

Table 3-2: Liquid Propellant Fuels and Oxidizers

Oxidizer	Fuel
IRFNA	RP-1
H2O2-95%	Hydrazine
N2O4	MMH
ClF3	UDMH
LOX	LH2
LF2	Ammonia

Riddle²¹ has also incorporated a method for determining a variable specific impulse in order to further enhance the liquid propellant rocket propulsion model. Rather than use a constant I_{sp} , the model uses an equivalence ratio, (ϕ), chosen by the GA to determine the I_{sp} for that particular propellant combination. Using the thermochemical data of a propellant combination and the equivalence ratio, the I_{sp} values can be approximated using a 5th-order curve fit. For the current study, this method was not employed. However, future work should implement this procedure for use in the optimization of liquid propellant space launch vehicles.

3.5 Mass Properties Models

Upon completion of the propulsion system models, the objective function next determines the mass properties of the vehicle using the mass properties models. The mass properties of the vehicle are critical to accurate modeling of the vehicle during its flight to orbit. The mass of the vehicle is not constant as it burns and ejects propellant during flight. Thus, the mass properties change with time and the mass properties models used in this analysis reflect this change.

The physical model of the launch vehicle involves a basic setup where almost all of the individual components are stacked vertically adjacent to each other. Starting at the nosecone and working toward the aft end of the vehicle, the mass properties of each

component are analyzed individually and in sequence. There is no space between each component and the lengths of each component are added together to determine the total stage length. The total vehicle length is determined by summing the stage lengths, the electronics length and the nosecone length. Also, all components are oriented about the centerline of the vehicle thus making the entire vehicle axi-symmetric.

Some components are not considered to be stacked components. For example, the motor casing is modeled as a hollowed-out cylinder that contains a few of the internal solid rocket components. The length of the motor case is equal to the length of the propellant grain. Like the other components, the motor case cylinder is also oriented along the vehicle center line in order to ensure mass symmetry.

The process of determining the mass properties of the vehicle involves two sequential steps. First, the mass properties model determines the mass properties of the individual components of the launch vehicle. These components include the nosecone, the payload, an electronics section, rocket body casing, propellant tanks and feed lines, tail fins, and nozzles. Next, using the mass properties of the individual components, the overall mass properties of the entire vehicle are determined. These values are then summarized to create a mass properties data file that is used in the six-degree-of-freedom (6DOF) flight dynamics simulator model.

The calculations involving the solid and liquid propellants are unique because of their time-dependent nature. Except for the propellants, the mass properties of all the components of the launch vehicle are constant during the entire flight. Since the propellants are being burned and ejected thru the nozzle, their mass properties are changing which, in turn, changes the mass properties of the entire vehicle. These

changes must be accounted for. The previously mentioned mass properties data file is the tool used to keep track of the changing mass properties. At the start of the analysis, the mass properties of all the propellants are determined and are incorporated into the total vehicle mass properties. This constitutes the total mass of the vehicle at lift-off. The table of mass properties is developed starting with the vehicle fully fueled and ready for launch. Prior to the mass properties model, the burn time and propellant mass history were determined in the propulsion system models. The time-step and change in propellant mass from these models are now used in the mass properties model. The total mass of the vehicle is decreased based on the amount of propellant that has been ejected by the first stage of the vehicle. After this change, the mass properties of the entire vehicle are then recalculated. This process continues until all the propellant for the first stage has been expelled. The same analysis is performed for subsequent stages until the final burnout time has been reached. At this point in the flight, the thrust is zero, the propellant mass is zero and the remaining components fly a ballistic trajectory to orbital altitude.

There are five properties that the mass properties models calculate. Those five properties are:

1. Mass of the individual component and the entire launch vehicle system
2. Center of gravity relative to the nose of the rocket (x_{cg}) of the individual component and the entire launch vehicle system
3. X-axis moment of inertia (i_{xx}) of the individual component and the entire launch vehicle system

4. Y-axis moment of inertia (i_{yy}) of the individual component and the entire launch vehicle system

5. Z-axis moment of inertia (i_{zz}) of the individual component and the entire launch vehicle system

It should be noted that products of inertia (i_{xy} , i_{yz} , i_{zx}) reduce to zero because of the physical nature of the vehicle. The axi-symmetric configuration of all vehicle components causes the products of inertia to be zero.

3.5.1 Mass Properties of Individual Components

Table 3-3 lists the different components that make up a three-stage solid propellant launch vehicle and a three-stage liquid propellant launch vehicle. All five mass properties (mass, i_{xx} , i_{yy} , i_{zz} , and x_{cg}) are calculated for each of the individual components listed in the table below.

Table 3-3: Three-Stage Solid and Liquid Vehicle Components

Three-Stage Solid	Three-Stage Liquid
Blunt Nose	Blunt Nose
Ogive Section	Ogive Section
Payload	Payload
Electronics	Electronics
Stages 1-3	Stages 1-3
Curved Bulkhead	Compressed Gas
Ignitor	Compressed Gas Tank
Pressure Vessel/Motor Case	Fuel
Liner	Fuel Tank
Insulation	Oxidizer
Nozzle	Oxidizer Tank
Propellant Grain	Cylindrical Case
	Insulation
	Engine Assembly
	Nozzle

The equations for center of gravity and the moments of inertia use a local coordinate system for the individual component being calculated. However, each stage does not use the same local coordinate system (Stage 1 is farther from the nose than Stage 3). Thus, the lengths of each stage need to be reflected in the calculations so that the mass properties are relative to a consistent starting point. The consistent starting point used in this analysis is the nose of the vehicle.

Since there are numerous components of each stage, the “shape” of each component varies and the corresponding equations are used to describe their mass properties. For the most part, in a typical space launch vehicle, the more common shapes used are modeled as point masses (payload and electronics), cylinders (motor cases) or spheres (propellant tanks). Figure 3-4 defines the lengths that describe the orientation of a generic three-stage vehicle.

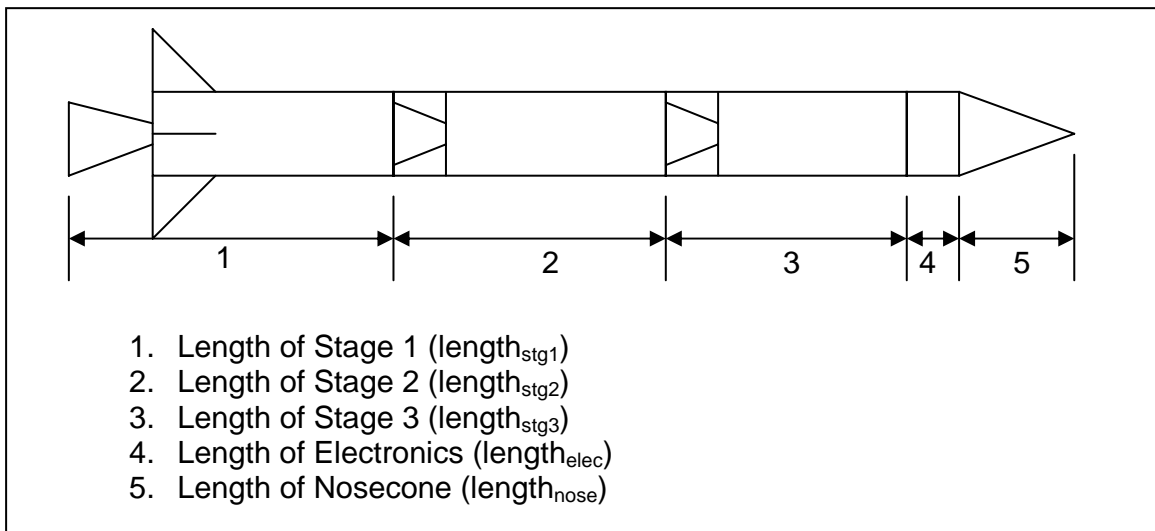


Figure 3-4. Definition of Lengths

3.5.1.1 Point Mass Example: Electronics

The mass properties of a point mass are described in this section. The electronics package is modeled as a point mass located directly behind the payload at the front end of the vehicle. The mass of the electronics ($mass_{elec}$) is a pre-defined variable determined by the user. The center of gravity ($x_{cg_{elec}}$) and the moments of inertia (ixx_{elec} , iyy_{elec} , and izz_{elec}) are calculated using standard dynamics equations for a point mass. In addition, Figure 3-4 defines the lengths used in the calculations. Table 3-4 summarizes the equations that determine the mass properties of the electronics.

Table 3-4: Mass Properties of Electronics

Property	Calculation
Mass	$mass_{elec}$
Center of Gravity	$x_{cg_{elec}} = length_{nose} + length_{elec} / 2$
X-axis Moment of Inertia	$ixx_{elec} = 0.0$
Y-axis Moment of Inertia	$iyy_{elec} = (mass_{elec})(radius_{elec}^2)$
Z-axis Moment of Inertia	$izz_{elec} = iyy_{elec}$

3.5.1.2 Cylinder Example: Motor Cases

The dominant shape of the bodies of nearly all launch vehicles is that of a cylinder. Cylinders are preferred for atmospheric flight because of their low coefficient of drag characteristics. In space, spheres are preferred because atmospheric drag is no longer a concern. A cylinder also provides excellent volumetric storage space. For a solid propellant vehicle, the propellant grain is housed in the center of a cylindrical motor case. Thus, the motor case can be described as a cylinder with the center core hollowed out. The distance to the local coordinate system is determined from the lengths defined in Figure 3-4. In this case, the distance to the beginning of the 1st-stage is called

length_{ph2}, because it encompasses the components that correspond to the second phase of flight, and is written as:

$$\text{length}_{\text{ph2}} = \text{length}_{\text{nose}} + \text{length}_{\text{elec}} + \text{length}_{\text{stg3}} + \text{length}_{\text{stg2}} \quad (3.18)$$

When calculating the mass properties of the 2nd-stage components, the distance is called length_{ph3} and uses the following lengths defined in Figure 3-4:

$$\text{length}_{\text{ph3}} = \text{length}_{\text{nose}} + \text{length}_{\text{elec}} + \text{length}_{\text{stg3}} \quad (3.19)$$

For the 3rd-stage components, the length_{nose} and length_{elec} terms are taken into account in the appropriate equations.

Additionally, the volume of the motor case is needed for the mass calculation. Knowing the length of the case (length_{case}), the radius of the cylinder (radius_{case}) and the thickness of the case wall (thick_{case}), the volume of the case can be written as:

$$V_{\text{case}} = 2.0 \pi (\text{radius}_{\text{case}})(\text{length}_{\text{case}})(\text{thick}_{\text{case}}) \quad (3.20)$$

Using these values for length_{ph2} and volume, Table 3-5 summarizes the equations involved for determining the mass properties of the 1st-stage motor case. The density of the tank material (ρ_{case}) is a pre-determined value chosen by the user.

Table 3-5: Mass Properties of Stage 1 Motor Case

Property	Calculation
Mass	$\text{mass}_{\text{case}} = (\rho_{\text{case}})(V_{\text{case}})$
Center of Gravity	$\text{xcg}_{\text{case}} = \text{length}_{\text{ph2}} + \text{length}_{\text{case}}/2$
X-axis Moment of Inertia	$\text{ixx}_{\text{case}} = (\text{mass}_{\text{case}})(\text{radius}_{\text{case}}^2)$
Y-axis Moment of Inertia	$\text{iyy}_{\text{case}} = (\text{mass}_{\text{case}}) \left(\frac{1}{2} r^2 + \frac{1}{3} L^2 \right)$
Z-axis Moment of Inertia	$\text{izz}_{\text{case}} = \text{iyy}_{\text{case}}$

3.5.1.3 Sphere Example: Compressed Gas Tank

Propellant tanks used in liquid propellant rockets are usually either spherical or cylindrical in shape. In order to keep both the fuel and oxidizer tanks properly

pressurized, an inert compressed gas, like nitrogen or helium, is fed into the propellant tanks. Knowing the radius of the gas tank ($radius_{tank}$), the volume of the sphere for the compressed gas tank can be determined by:

$$V_{tank} = \left(\frac{4\pi}{3}\right)(radius_{tank})^3 \quad (3.21)$$

Also, using Eqn. (3.15) and knowing that the length of the tank is $length_{tank}$, Table 3-6 summarizes the equations involved for calculating the mass properties of the 1st-stage compressed gas tank. The value of the density of the tank material (ρ_{tank}) is a predetermined value established at the start of the modeling process.

Table 3-6: Mass Properties of Stage 1 Compressed Gas Tank

Property	Calculation
Mass	$mass_{tank} = (\rho_{tank})(V_{tank})$
Center of Gravity	$xcg_{tank} = length_{ph2} + length_{tank}/2$
X-axis Moment of Inertia	$ixx_{tank} = (mass_{tank})\left(\frac{2}{3}radius_{tank}^3\right)$
Y-axis Moment of Inertia	$iyy_{tank} = (mass_{tank})\left(\frac{2}{3}xcg_{tank}^2\right)$
Z-axis Moment of Inertia	$izz_{tank} = iyy_{tank}$

3.5.1.4 Mass Table

A mass table is created that summarizes the five mass properties of all the individual components of the launch vehicle. This table provides a quick visual “sanity check” to ensure the calculated values are reasonable and realistic. Errors in the calculations can easily be determined by closely examining the results listed in the mass table. An example of a mass table for a three-stage solid propellant launch vehicle is shown in the Appendix.

3.5.2 Mass Properties of Entire Launch Vehicle

After the mass properties of the individual components have been determined, the next step is to determine the mass properties of the entire launch vehicle. This involves more than just summing the mass properties of all the individual components together. As previously described, during powered flight, the mass of the vehicle changes with time and as a result the mass properties of the vehicle must change accordingly.

In order to properly capture the time-dependent mass properties, the calculations for the entire launch vehicle are done systematically in four different phases for a three-stage launch vehicle. As each stage operates and loses mass as propellant burns, the mass properties are recalculated to take into account the slight changes in center of gravity and moments of inertia. Each phase corresponds to the time when an individual stage is firing and producing thrust. Thus, an entire profile from initial launch to 3rd-stage burnout is generated. A brief description of each phase is presented here:

1. Phase I: time = 0.0s, Stage 1 firing
2. Phase II: Stage 1 burnout, Stage 1 drops off, Stage 2 firing
3. Phase III: Stage 2 burnout, Stage 2 drops off, Stage 3 firing
4. Phase IV: Stage 3 burnout, ballistic flight, only payload and electronics remain

3.5.2.1 Entire Launch Vehicle Mass Properties Example: Phase I

The calculations for the mass properties of the entire launch vehicle are broken into two main steps with a few smaller sub-steps. Each of the two main steps is performed in each phase of flight with the corresponding components for that stage being considered in the five mass properties. An example for Phase I of a three-stage solid propellant vehicle is described.

The first main step involves two calculations that establish the initial mass properties of the entire launch vehicle. The five mass properties of all the individual components, except the propellant grain, are added together. Since the mass of the propellant grain will be changing, the mass properties of the propellant grain are added in separately to create the time-dependent variables. These time-dependent variables of the mass properties will be continuously updated in the second main step of this process. Here again, the initial center of gravity of the propellant grain uses the variable, $length_{ph2}$, to account for the distance from the nose to the 1st-stage propellant grain. At the conclusion of this step, the five mass properties of the entire launch vehicle sitting on the pad ready for launch (time = 0.0s) have been determined. These properties are written to a data file and saved for future use in the 6DOF flight dynamics simulator.

The second main step is to calculate the time-dependent mass properties as the vehicle's mass changes during flight. In the solid propellant propulsion model, the thrust profile of the 1st-stage is determined. In addition to the thrust calculations, the changes in the mass of the propellant are calculated. This information is used in a continuous loop that recalculates the mass properties during each time step during which a small amount of mass leaves the vehicle. The mass flow is assumed to be constant and steady. Again, this time-dependent information is saved in the data file for future use.

3.6 Aerodynamics Model

In recent years, evolutionary techniques have been applied to aerodynamic design. Gage and Kroo⁴⁶ focused their research on the topological design of non-planar wings and used a genetic algorithm to minimize induced drag given a fixed lift. Others have also attempted design optimizations of various aerodynamic shapes using a genetic

algorithm. In 1990, Washington¹⁵ developed an aerodynamic prediction package, called AeroDesign, which is capable of determining the aerodynamic constants of axisymmetric missiles of circular cross-section with cruciform wings or fins. AeroDesign has been chosen for use in the current study.

The AeroDesign model is equipped to handle a wide variety of flow field conditions. Initial conditions and physical parameters of the vehicle are inputted to the model. Next, empirical curve fits of wind tunnel data are performed and the aerodynamic constants are determined across a range of flow field conditions. Vehicle geometry and other necessary parameters are used to generate an aerodynamic database. AeroDesign assumes that there are no boundary layers and that no separation occurs.

AeroDesign can analyze either a cone or ogive shape for the nosecone and assumes a cylindrical body shape. The Mach number regime of the code is from subsonic to high supersonic/low hypersonic (\approx Mach 4.0) flow. For this study, the general shape that has been used is the ogive nosecone and cylindrical body. Four fins in a “+” shape configuration are located at the aft end of the 1st stage for some of the launch vehicles analyzed. No other stages have any fins or wings. The body diameter is constant for all vehicle stages with a few exceptions. AeroDesign has been modified for the three and four-stage solid propellant vehicle cases along with the air-launched two-stage case. For these cases, the body diameter is allowed to vary for each stage. The diameter of the 1st stage is equal to or greater than the diameter of the 2nd stage. In AeroDesign, a modification to the calculation of the drag coefficient has been made to account for differences in the 1st and 2nd stage diameters as well as the 2nd and 3rd stage

diameters. The drag coefficient for a flat plate ($C_{Dflatplate}$) is used as the baseline coefficient and is normal to the flow. The correction factor is determined as follows:

$$\Delta C_{Dcorr} = C_{Dflatplate} * \frac{A_{exposed}}{A_{ref}} \quad (3.22)$$

where

$$A_{exposed} = \pi(R_{stg1}^2 - R_{stg2}^2) \quad (3.23)$$

and

$$A_{ref} = \pi R_{stg1}^2 \quad (3.24)$$

A similar correction factor has been performed for the difference in the 2nd and 3rd stage diameters where the 2nd stage diameter is equal to or greater than the 3rd stage diameter. Additional modifications to AeroDesign would be required for a launch vehicle where the 2nd stage diameter is equal to or greater than the 1st stage diameter.

Using the AeroDesign package along with the known geometric parameters of the vehicle, the important aerodynamic coefficients are generated. Essential aerodynamic coefficients are determined for a range of flight Mach numbers and angles of attack. Like the mass properties, the aerodynamic data generated is saved and used in the 6DOF flight dynamics simulator.

The aerodynamics model is organized to determine the aerodynamic properties of the vehicle at each stage of flight. The model is run initially for the entire vehicle with all stages stacked together. In the 6DOF flight dynamics simulator, the aerodynamics model is called again after Stage 1 burnout. The aerodynamic properties are calculated again; this time with the first stage of the vehicle gone and the corresponding velocity and

pressure conditions being used. This procedure continues as subsequent vehicle stages burn out and the vehicle's geometry changes.

The 6DOF flight dynamics simulator keeps track of variables such as Mach number, atmospheric pressure, atmospheric density etc. This information in conjunction with the aerodynamic characteristics and the mass properties of the vehicle is used in calculating all of the aerodynamic forces on the vehicle in flight.

3.7 Six-Degree-of-Freedom (6DOF) Flight Dynamics Simulator

The culmination of the vehicle performance analysis occurs in the six-degree-of-freedom (6DOF) flight dynamics simulator. This system model is probably the most important part of the objective function since the information it provides is used to judge vehicle performance. A 7th/8th order Runge-Kutta numerical method is used to integrate the equations of motion. Position, velocity and orientation of the vehicle are determined at small time intervals throughout the flight. The vehicle flies a ballistic trajectory with the goal of reaching a low-Earth orbit.

This model begins by reading in mass properties, propulsion data and all initial conditions for vehicle flight. The equations of motion are then integrated and values such as altitude, velocity and orientation are saved for post-processing. The integration process continues until the vehicle has reached the apogee of the ballistic flight trajectory. Ideally, this would correspond to the orbital insertion point for a low-Earth, circular orbit. Two of the goals of the design optimization process are to attain the desired orbital altitude and orbital velocity for a pre-determined low-Earth orbit.

These final velocity and altitude values along with cost/total vehicle mass values are then sent to the goal determination algorithm. The desired orbital values are pre-

selected prior to the start of the optimization process and stored in the goal determination algorithm. These desired orbital values are compared to the values calculated in the 6DOF flight dynamics simulator. The goals of the optimization process are to minimize the differences between the values produced by the 6DOF flight dynamics simulator and the desired orbital values.

Finally, it is possible that a final short burn would be required for orbit insertion. However, this consideration was not explored for the current study. Future work should incorporate the use of an orbit insertion burn into the operation of the 6DOF flight dynamics simulator.

3.8 Cost Model

The cost model used in this analysis was derived by Dr. Dietrich E. Koelle and published in his book *Handbook of Cost Engineering for Space Transportation Systems, Revision 1, with TRANSCost 7.1*.⁴¹ The philosophy behind this cost model is different from cost models of past decades. In the early days of spaceflight, vehicles were designed without much consideration for cost (the Saturn V moon rocket for example). After the Apollo program ended, engineers started designing vehicles to fit a specific cost budget; called Design-to-Cost. The idea here was to maximize performance within a pre-determined budget. For current launch vehicles, Dr. Koelle has proposed a new concept known as “Cost Engineering.” “In the case of ‘Cost-Engineering’, its goal is the minimum vehicle design concept. This means that costs have to be taken into account as a criterion for each technical decision.”⁴¹

Another promising cost model currently in use today is the NASA and Air Force Cost Model (NAFCOM).⁶³ This model is a parametric based cost model developed in

1990 and updated in order to estimate the cost of both satellite and launch vehicle space systems. The use of the NAFCOM was not incorporated into the current study.

However, future design optimization work should include comparisons between the cost results generated by the *TRANSCost 7.1* cost model and the NAFCOM.

The *TRANSCost 7.1* cost model fits in well with the current effort of design optimization of space launch vehicles. In the current study, the designs being optimized reflect optimum solutions at the preliminary design stage. The *TRANSCost 7.1* cost model provides a powerful tool to aid in the minimization of vehicle launch costs at this stage of the design process. An additional economic model developed by Wertz⁴² is used in order to refine the *TRANSCost 7.1* cost model so that a cost per launch value can be calculated.

The *TRANSCost 7.1* cost model is broken into three submodels. These submodels are: the Development Cost Submodel, the Recurring Cost Submodel, and the Ground and Flight Operations Submodel. For this study, the cost of launch insurance is also included in the calculations to provide additional realism to the cost per flight determination.

Thus, the cost per launch is determined by using the following equation:

$$C_{\text{launch}} = C_{\text{development}} + C_{\text{vehicle}} + C_{\text{flightops}} + C_{\text{insurance}} \quad (3.25)$$

The various submodels employ system-level Cost Estimation Relationships (CERs) to predict cost. These CERs are the backbone of the model and provide the cost of a system in a generic unit called the “Man-Year (MYr).” The reason for using the MYr as the costing unit is that this unit provides firm cost data which is valid internationally and free from annual changes due to inflation and other factors. “For each of the technical

systems, a specific CER has been derived which is mostly mass-related with the basic form of:

$$CER = aM^x \quad (3.26)$$

where: CER = cost (MYr)

a = system-specific constant value

M = mass (kg)

x = system-specific cost-to-mass sensitivity factor⁴¹

The values of “a” and “x” in Equation (3.26) are determined for specific types of launch vehicle systems using a data fit of the cost-to-mass relationships of a group of similar systems.

3.8.1 Development Cost Submodel

Using historical data of previously built and flown solid propellant rocket motors, the basic CER for the Development Cost Submodel can be written as:

$$CER_{solid} = (19.2)M^{0.53} \quad (3.27)$$

Similar CERs have been established for liquid propellant rockets along with turbofan and turbojet engines.

Additionally, the CER alone does not provide the entire cost picture for a particular submodel. Various cost factors have been introduced to make the cost calculation more realistic. Some examples of these cost factors are the Development Standard Factor (f_1) and the Team Experience Factor (f_3). These factors can either increase or decrease the system cost. For example, a more experienced team that is designing a launch vehicle should be able to keep costs down since they can take advantage of prior knowledge. Thus, a more experienced team will have a numerically lower Team Experience Factor (f_3).

For the solid propellant rocket motor, the complete CER for the Development Cost Submodel (H_{ES}) of a single-stage vehicle is:

$$H_{ES} = (19.2)(M^{0.53})f_1f_3 \quad (3.28)$$

Finally, the total development cost ($C_{dev-total}$) of an entire multi-stage vehicle can be determined by summing up the CERs for each individual stage and employing additional cost factors such as the system engineering/integration factor (f_0) and programmatic cost impact factors (f_6, f_7, f_8).

$$C_{dev-total} = f_0(\sum H_{ES})f_6f_7f_8 \quad (3.29)$$

Thus, one equation has been derived for the total development cost (Development Cost Submodel) of a multi-stage solid propellant launch vehicle. For different types of propulsion systems, the corresponding CER can be used in Equation (3.29) to reflect the development cost of the entire vehicle.

The total value for the development cost calculated in Equation (3.29) is typically not used in the cost per launch determination ($C_{development}$). Wertz⁴² presented a method where this total value is spread out over a pre-determined period of time (usually the number of years of the contract) to produce a yearly development cost. This method takes into account inflation along with interest rate. Using $C_{dev-total}$ from Equation (3.29), amortization assumes a constant payment ($P_{constant}$) over time in real (then-year) dollars of:

$$P_{constant} = \frac{C_{dev-total} * \text{int}}{(1 - (1 + \text{int})^{-n_{pay}})} \quad (3.30)$$

where “int” is the interest rate and “npay” is the number of payments. For a given constant inflation rate, “inf”, the annual reduction, R_{annual} , in the value of money can be written as:

$$R_{annual} = \frac{1}{(1 + inf)} \quad (3.31)$$

Thus, the average payment, P_{avg} , will be reduced to:

$$P_{avg} = P_{constant} \left(\frac{R_{annual}}{npay} \right) \left(\frac{(1 - R_{annual}^{npay})}{(1 - R_{annual})} \right) \quad (3.32)$$

To determine the cost per launch of launch vehicle development, the yearly development cost, P_{avg} , is divided by the launch rate per year, $lrate$, which produces the value of $C_{development}$ used in Equation (3.24).

$$C_{development} = \frac{P_{avg}}{lrate} \quad (3.33)$$

The launch rate per year, $lrate$, multiplied by the number of years of the contract, $npay$, results in the number of units, $nunits$, to be built. This value for the number of units will be used in the Recurring Cost Submodel calculations.

3.8.2 Recurring Cost Submodel

The Recurring Cost Submodel is developed in a similar way to the Development Cost Submodel. The basic recurring cost CER is used with some different cost factors. The Learning Factor (p) is introduced and is used to determine the Cost Reduction Factor for Series Production (f_4). The Learning Factor takes into account the reduction of effort required after the initial vehicle rolls off the production line and experience is gained in producing more and more identical units. Typically, the value of the Learning Factor (p)

ranges between 0.70 and 0.95. Knowing this value and the number of units, “nunits”, to be produced, the value of f_4 is determined by:

$$f_4 = \frac{1}{nunits} \sum_1^{nunits} nunits \frac{\ln p}{\ln 2} \quad (3.34)$$

Using the solid propellant rocket motor as an example again, the CER for the Recurring Cost Submodel can be written as:

$$F_{ES} = (2.42)(nunits)(M^{0.395})f_4 \quad (3.35)$$

where “nunits” is the number of units being built.

In order to calculate the total recurring cost ($C_{rec-total}$), the system management, vehicle integration and checkout factor (f_0) is used to get:

$$C_{rec-total} = f_0 F_{ES} \quad (3.36)$$

The value used in the cost per launch calculation ($C_{vehicle}$) is obtained by taking the result of Equation (3.36) and dividing it by the number of units being built.

$$C_{vehicle} = \frac{C_{rec-total}}{nunits} \quad (3.37)$$

3.8.3 Ground and Flight Operations Cost Submodel

As stated by Koelle,⁴¹ “assessment and modeling of launch vehicles’ operations cost is the most difficult task compared to development cost and recurring cost modeling.” It is not an easy task to accurately estimate the costs associated with preparing a launch vehicle for flight.

Based on the work done by Wertz,⁴² for expendable launch vehicles, the flight operations cost is typically \$0.5 million to \$1.0 million per mission. The amount of \$1.0 million (in 2003 dollars) is used for $C_{flightops}$ in the Ground and Flight Operations Cost

Submodel and in Equation (3.24). This value will be constant throughout the design optimization process for all launch vehicle types.

3.8.4 Insurance Cost Submodel

The Insurance Cost Submodel ($C_{\text{insurance}}$) is modeled as a percentage of the launch vehicle recurring cost (C_{vehicle}). This insurance covers only the launch itself and does not include the cost of replacing the payload in the event of launch failure. Also, this model typically represents the upper limit of insurance cost. Most likely, insurance cost will drop as launch vehicle reliability is established with successful initial flights. Since this study focuses on the preliminary design, using the upper limit insurance cost is a prudent choice.

According to Wertz,⁴² a typical insurance cost is on the order of 15% of the launch vehicle recurring cost. Thus, in the cost model being used for this study, $C_{\text{insurance}}$ for the cost per launch determination is calculated by multiplying C_{vehicle} by 15%. Thus, the cost of production of an individual launch vehicle drives the cost to insure it. This makes sense when considering that it is much more expensive to insure a luxury car as opposed to an economy car, for example.

The inclusion of the insurance cost is more for realism since the overall cost model is mass-based. Due to the mass-based nature of the CERs, minimizing the mass of the vehicle should minimize the cost of the vehicle (C_{vehicle}) as well. Since the insurance is simply a percentage of C_{vehicle} , the results are not affected by the insurance cost. However, the goal here is to present as realistic a value as possible for this preliminary design study.

3.8.5 Example Calculation

An example cost calculation for a three-stage, solid propellant rocket is presented here. The vehicle is designed to carry a 1,000 lbm payload into a low-Earth orbit. The launch takes place from Cape Canaveral AFS, FL. The MYr unit has been converted to a dollar value representing currency in 2003. The values for the masses of each stage (m_{stg1} , m_{stg2} , m_{stg3}) are determined in the mass properties models and converted to kilograms in the cost model.

Assumptions have been made for the input values of the Launch Rate (l_{rate}), Number of Payments (n_{pay}), Development Standard Factor (f_1), Team Experience Factor (f_3) and the Learning Factor (p). A common sense, realistic approach has been used for these values. Since the USAF is attempting to field a responsive launch vehicle that can launch quickly and rapidly, an annual launch rate of 15 is a reasonable value. The number of payments reflects a 15 year contract. The Development Standard Factor (f_1) and the Team Experience Factor (f_3) can have a range from 0.4 to 1.4. Choosing values of 0.90 for both factors represents a standard project and a company/team with some related experience. For this study, investigating a state-of-the-art design with a brand new company is not the goal. Thus, the more “middle of the road” value of 0.90 makes sense. According to Koelle,⁴¹ the Learning Factor (p) for space systems ranges between 0.80 and 1.0. Here again, choosing a value of 0.85 for the Learning Factor (p) is reasonable.

Table 3-7 summarizes the inputs that are used to calculate the cost per launch for the three-stage solid propellant launch vehicle described above. Table 3-8 describes the results of the cost determination process. The Total Launch Vehicle Cost per Launch is

determined from Equation (3.24). From the results in Table 3-8, it can be seen that this particular launch vehicle is moderately priced (\$50.41 million) for an expendable, solid propellant launch vehicle.

Table 3-7: Inputs for Vehicle Cost Example Calculation

Mass of Stage 1 (mstg1)	22,186 kg
Mass of Stage 2 (mstg2)	13,390 kg
Mass of Stage 3 (mstg3)	5,470 kg
Launch Rate (lrate)	15
Number of Payments (npay)	15
Number of Units (nunits)	225
Development Standard Factor (f_1)	0.90
Team Experience Factor (f_3)	0.90
Learning Factor (p)	0.85

Table 3-8: Outputs for Vehicle Cost Example Calculation

Total Development Cost (C_{dev})	\$18.60 million
Cost Reduction Factor for Series Production (f_4)	0.364
Total Recurring Cost (C_{veh})	\$26.78 million
Total Flight Operations Cost (C_{ops})	\$1.0 million
Total Insurance Cost (C_{ins})	\$4.02 million
Total Launch Vehicle Cost per Launch (C_{lnch})	\$50.41 million

4.0 VALIDATION EFFORTS

4.1 Introduction

The employment of system modeling in a preliminary design process can provide a variety of results that represent different solutions to the stated design problem. Some results may produce a seemingly more desirable solution than other results. Simply taking these particular results as the optimum solution may lead to an unrealistic design that cannot to be reproduced in the real world. Basically, results that have not been validated could lead to designs that are not physically attainable. Thus, it is very important to validate the results that have been generated so that the degree of confidence in the accuracy of the modeling effort can be ascertained. In addition, these validation efforts are important because the outcome of the design optimization process is highly dependent on the accuracy of the system modeling. It should be noted that, for preliminary design purposes, validating the accuracy of the system modeling is always necessary regardless of whether or not design optimization is being performed. To that end, Cosner et al.⁴⁷ provide the definition of validation:

“The process of determining the degree to which a model is an accurate representation of the real world from the perspective of the intended uses of the model.”

Roy⁴⁸ adds that validation deals with the physics of the process that the system model is attempting to simulate.

Models form a crucial element of engineering design since they are the link between the design parameters being employed and the actual system performance. Of course, models are not perfect representations of real world systems. Uncertainty, both mathematical and physical, is introduced when computations are performed and assumptions are made. Additionally, predictive models can often produce a number of possible designs that meet the specified goals of the system using different combinations of the design parameters. This can either be a benefit or it can complicate the search for the desired design solution. Finally, statistical variations in the performance of physical systems must be taken into consideration when performing model validation. The importance of the validity of system models takes on greater significance in highly complex systems, including space launch vehicles, where the models must incorporate numerous design disciplines such as propulsion, aerodynamics and flight dynamics.

The various models used in the current study have been validated independently in previous work performed by their respective aerospace engineering researchers. The following sentences describe the work performed by these researchers. The solid propellant propulsion model was developed and validated by Burkhalter,⁴⁴ Sforzini⁴⁵ and, with modifications, Hartfield et al.¹⁹ This model was then used by Anderson¹⁶ and Metts²⁰ in the investigation and reverse engineering of small to medium-sized solid propellant tactical missiles. Jenkins¹⁸ developed the liquid propellant propulsion model and then used an existing real world system, the SCUD-B short range ballistic missile, to successfully validate the model. The aerodynamics model developed by Washington,¹⁵ known as AeroDesign, has been an industry standard since 1990. The six-degree-of-freedom (6DOF) flight dynamics simulator has been used extensively in the previous

work. Finally, Koelle⁴¹ has used a large supply of real world data to develop the Cost Estimate Relationships (CERs) used in his *TRANSCost 7.1* cost model. The use of this historical data has resulted in a successful validation of his cost model.

The goal for this study is to incorporate all these system models into one comprehensive model that represents an entire multi-stage space launch vehicle. With confidence in the validity of the individual system models, validation of the different stages as well as the entire launch vehicle can be undertaken. However, simply stating that “since the individual system models are valid then the entire launch vehicle must be valid as well” is not sufficient. A comprehensive validation of the entire launch vehicle, that is as detailed as possible, has been performed as follows.

4.2 Validation Method

4.2.1 General Description

The method used in this study for model validation follows the method used by Jenkins¹⁸ and Riddle⁴⁹ for the validation of a single-stage liquid propellant rocket model. The present method begins by researching and choosing a launch vehicle that is similar to the system being modeled by the various physical models included in the objective function. In the case of the work performed by Jenkins¹⁸ and Riddle,⁴⁹ a liquid propellant rocket was being reverse engineered. As a result, the liquid fueled SCUD-B was chosen as the real world system. Next, as much information on the chosen vehicle is determined and appropriately hard-coded into the appropriate input locations for the objective function. This information includes physical size, thrust values and/or propellant types. The objective function, along with other design parameters, is then manipulated in an attempt to reproduce the characteristics of the real world example. Also, in order to

attempt to match the real world example more closely, a design optimization can be run using the genetic algorithm (GA). The purpose of this optimization is not to maximize or minimize any particular vehicle performance characteristics but rather to allow the GA to “fine tune” the model by choosing the remaining unknown parameters so that the resulting vehicle matches, as closely as possible, the real world example. If the objective function can produce a launch vehicle that is strikingly similar to the real world example, given the real world example’s known and GA-determined parameters, then the validity of the model is substantially strengthened.

4.2.2 Specific Validation Process and Setup

For the current study, four specific system model validations have been performed. The availability of information on real world launch vehicles drove the selection of the types of system models to validate. The system models that have been validated are: the three and four-stage solid propellant launch vehicles, the two-stage liquid propellant launch vehicle and the air-launched, two-stage liquid propellant launch vehicle. An additional comparison involving a three-stage solid/liquid/liquid launch vehicle has also been performed.

The same validation method was used for each of the four system models with slight variations in the setup depending on the known parameters of the real world example launch vehicle. Given the known parameters, the system model was manipulated in an attempt to match the physical properties and the performance characteristics of the real world example. The known parameters of the real world example were:

- payload mass to orbit
- desired altitude and velocity
- individual stage geometry (diameter and length)
- individual stage propellants
- individual stage burn time (used for liquid propellant vehicles)

In order to more closely model United States Air Force (USAF) space launch vehicle systems, the objective function was configured to include the latitude and longitude coordinates of the two primary USAF launch sites: Vandenberg AFB, CA (VAFB) and Cape Canaveral AFS, FL (CCAFS). Also, typical payload, final altitude and final velocity values for the four real world examples were chosen as direct inputs to the objective function. These values are summarized in Table 4-1.

Table 4-1: Typical Values of Real World Launch Vehicles

<u>Model</u>	<u>Real World Example</u>	<u>Payload</u>	<u>Altitude</u>	<u>Velocity</u>	<u>Launch Site</u>
Three-Stage Solid	Minuteman III ICBM	2,540 lbm	750,000 ft	22,000 ft/s	VAFB
Four-Stage Solid	Minotaur I SLV	738 lbm	2,430,000 ft	25,004 ft/s	VAFB
Two-Stage Liquid	Titan II SLV	7,000 lbm	607,000 ft	25,600 ft/s	CCAFS
Air-Launched, Two-Stage Liquid	QuickReach™ Launch Vehicle	1,000 lbm	700,000 ft	25,532 ft/s	CCAFS

One important check on model validity for launch vehicles involves the calculation of propellant and inert mass fractions. These calculations can be performed using the resulting mass properties for the launch vehicle generated in the previously described validation method. These computed mass fractions are then compared to typical mass fractions for previously built and flown launch vehicles. The historical data

for these real world launch vehicles provides a record of successfully designed launch vehicle systems. For example, from Humble et al.,⁵⁰ the propellant mass fraction (f_{prop}) of solid rocket motors typically ranges from 0.80 to 0.95. Table 4-2 shows some example propellant mass fractions for existing solid rocket motors.

Table 4-2: Example Solid Rocket Motor Mass Fractions⁵⁰

Motor Designation	f_{prop}
Shuttle Advanced Solid Rocket Motor (ASRM)	0.895
Titan IV Solid Rocket Booster (SRB)	0.815
ORBUS 21	0.936
Star 48B	0.939
Pegasus 1 st Stage Orion 50	0.898
Pegasus 3 rd Stage Orion 38	0.859

4.2.3 Inert and Propellant Mass Fraction Calculations

Various mathematical tools can be used to determine the size of a particular launch vehicle. The inert mass fraction and the propellant mass fraction are two of those tools. Humble et al.⁵⁰ write the equations for inert mass fraction (f_{inert}) and propellant mass fraction (f_{prop}) as shown below in Equations 4.1 and 4.2:

$$f_{inert} = \frac{m_{inert}}{m_{prop} + m_{inert}} \quad (4.1)$$

$$f_{prop} = \frac{m_{prop}}{m_{prop} + m_{inert}} \quad (4.2)$$

where m_{prop} is the mass of the propellant and m_{inert} is the mass of the vehicle or stage minus the mass of the propellant and the mass of the payload (i.e. the dry mass). In addition, manipulating Equations 4.1 and 4.2 yields the relationship between these two types of mass fractions as written in Equation 4.3.

$$f_{prop} = 1 - f_{inert} \quad (4.3)$$

In their discussion of real world launch vehicles, Humble et al.⁵⁰ provide some historical data for both solid and liquid propellant launch vehicles. The data summarizes the typical values of propellant mass fraction for solid propellant motors as shown in Table 4-2. The inert mass fraction is chosen to describe the mass properties of liquid propellant rockets.

4.3 Three-Stage Solid Propellant Vehicle vs. Minuteman III ICBM

For solid propellant launch vehicles, much of the historical data is in the form of the propellant mass fraction. The historical data shows that the propellant mass fraction for solid propellant motors ideally should be around 0.90 based on the typical value of specific impulse (I_{sp}) for solid motors. There are essentially two explanations for why this value for the propellant mass fraction is used. First, for a given launch vehicle, with a known inert mass, the portion of the total vehicle mass not used for inert mass components must be divided between the payload mass and the propellant mass. The goal would be to minimize the propellant mass (hence minimize the propellant mass fraction) in order for the vehicle to be able to carry more payload mass to orbit. Equation 4.2 provides one way to determine the propellant mass fraction but the values from this equation range from 0 to 1. The propellant mass fraction must be somewhere between these two values. The propellant mass (m_{prop}) can be determined using a version of the ideal rocket equation given by Humble et al.⁵⁰ and written in Equation 4.4.

$$m_{prop} = \frac{m_{pay} \left(e^{\left(\frac{\Delta v}{I_{sp} g_o} \right)} - 1 \right) (1 - f_{inert})}{1 - f_{inert} e^{\left(\frac{\Delta v}{I_{sp} g_o} \right)}} \quad (4.4)$$

where m_{pay} is the payload mass, I_{sp} is the specific impulse, g_o is the local acceleration of gravity, Δv is the required change in velocity and f_{inert} is the inert mass fraction.

Knowing that the maximum vacuum I_{sp} for a solid propellant rocket motor is about 290s, using Equation 4.4 and knowing the inert mass of the vehicle, the minimum propellant mass fraction will be approximately 0.90 for Earth-to-orbit missions. In addition, many actual solid rocket motors use steel as the casing material which adds to the inert mass and leaves even less mass available for payload and other useful components. The historical data has shown that the value of 0.90 provides enough propellant to achieve orbit while leaving a large enough portion of the vehicle's mass for payload.

For the three-stage solid propellant vehicle model, the objective function has been manipulated and the resulting best performer has been compared to a real world example. The real world example launch vehicle chosen for the objective function to match is the Minuteman III intercontinental ballistic missile (ICBM), a three-stage solid propellant strategic weapon. The Minuteman III ICBM is launched from Vandenberg AFB, CA for testing purposes. Thus, the two vehicles being compared for this validation process are analyzed using Vandenberg AFB, CA as the launch site. The propellant mass fractions for the Minuteman III ICBM were determined from published values of the rocket's specifications.

Currently, there are no land-based, three-stage solid propellant launch vehicles used by any space-faring nation to put satellites into orbit. The Pegasus launch vehicle, operated by Orbital Sciences Corporation, is a three-stage solid propellant launch vehicle but it is air-launched from a modified L-1011 aircraft. Even though the Minuteman III ICBM is not designed to attain orbital velocity, it is comparable to a space launch vehicle; attaining a burn-out altitude of 750,000 feet and a burn-out velocity of 22,000 feet per second. According to the United States Air Force LGM-30G Minuteman III Fact Sheet⁵¹ “The Minuteman III is a strategic weapon system using a ballistic missile of intercontinental range.”

A schematic comparing the launch vehicle generated by the model and the Minuteman III ICBM is shown in Figure 4-1. The Minuteman III ICBM has a significantly more conical nose than the nose generated by the model. Also, the Minuteman III ICBM uses an inter-stage skirt between the between the first and second stages due to the diameter differences. This skirt was not used in the model thus showing the slightly larger diameter first stage more dramatically. Finally, the first-stage of the Minuteman III uses four nozzles whereas the first-stage of the model is designed to use a single nozzle. Generally, the schematic shows a very good match between the two launch vehicles.

Table 4-3 summarizes the physical and performance characteristics generated by the three-stage solid propellant launch vehicle model compared to the Minuteman III ICBM. The **bold*** values were direct inputs into the objective function based on the published characteristics of the Minuteman III ICBM. All other values for the model were calculated using the various system models that make up the objective function.

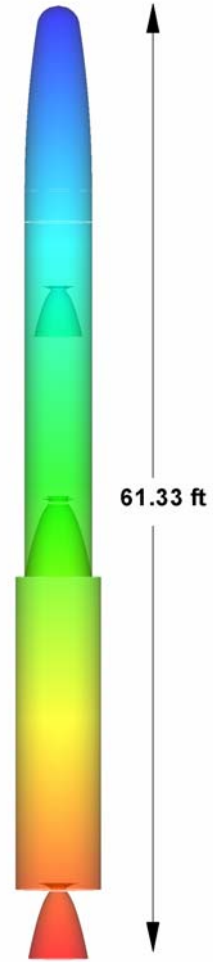


Figure 4-1. Three-Stage Solid Propellant Model vs. Minuteman III ICBM Schematic
(Ref. 52: http://www.globalsecurity.org/wmd/systems/images/us_nuke_minuteman3-01)

Table 4-3: Three-Stage Solid Propellant Model vs. Minuteman III ICBM Comparison

<u>Parameter</u>	<u>Model</u>	<u>Minuteman III ICBM</u>
Payload*	2,540 lbm	2,540 lbm
Total Vehicle Weight	75,870 lbm	79,432 lbm
Total Vehicle Length	61.33 ft	59.90 ft
Total Vehicle f_{prop}	0.9102	0.8925
Final Altitude	768,682 ft	750,000 ft
Final Velocity	22,071 ft/s	22,000 ft/s
<u>Stage 1</u>		
Stage Length*	295.20 in	295.20 in
Stage Diameter*	66.00 in	66.00 in
Propellants*	PBAA/AP/Al	PBAA/AP/Al
Total Stage Weight	49,882 lbm	50,486 lbm
m_{prop}	45,853 lbm	45,371 lbm
m_{inert}	4,029 lbm	5,115 lbm
f_{prop}	0.9192	0.8987
Burnout Time	67.72 s	61.00 s
Burnout Altitude	119,963 ft	100,000 ft
<u>Stage 2</u>		
Stage Length*	184.00 in	184.00 in
Stage Diameter*	52.00 in	52.00 in
Propellants*	PBAA/AP/Al	PBAA/AP/Al
Total Stage Weight	15,514 lbm	15,432 lbm
m_{prop}	13,993 lbm	13,669 lbm
m_{inert}	1,521 lbm	1,764 lbm
f_{prop}	0.9020	0.8857
Burnout Time	130.23 s	126.00 s
Burnout Altitude	406,931 ft	300,000 ft
<u>Stage 3</u>		
Stage Length*	90.00 in	90.00 in
Stage Diameter*	52.00 in	52.00 in
Propellants*	PBAA/AP/Al	PBAA/AP/Al
Total Stage Weight	7,666 lbm	9,520 lbm
m_{prop}	6,897 lbm	7,055 lbm
m_{inert}	769 lbm	882 lbm
f_{prop}	0.8997	0.8889
Burnout Time	189.23 s	191.00 s
Burnout Altitude	768,682 ft	750,000 ft
Burnout Velocity	22,071 ft/s	22,000 ft/s

A good match between the model and the Minuteman III ICBM has been obtained. The primary difference is that the three-stage solid propellant vehicle model

weighs about 3,500 pounds less than the Minuteman III ICBM. This weight difference comes about due to lower values of the inert mass in the model. This also causes the propellant mass fractions of the model to be approximately 2% higher than the propellant mass fractions of the Minuteman III ICBM. The model does not fully account for all the inert mass components thus resulting in lower values of the inert mass for each stage. This limitation on the mass properties model has implications for the actual design optimizations. Since the model underestimates the inert mass, an adjustment to the results of the validation model and the optimized vehicles would be required. For this study, an adjustment to the model was not performed. Future work to address this issue could be in the form of an updated mass properties model or incorporation of a correction factor into the existing mass properties model. Since the values of the propellant mass are quite accurate when compared to the Minuteman III ICBM, lower values of inert mass will cause higher propellant mass fractions. However, the propellant mass fractions of the model are still accurate for a solid propellant launch vehicle.

The strength of this model is its ability to reproduce the performance characteristics of the Minuteman III ICBM. This can be seen in the values generated for the final altitude (768,682 ft vs. 750,000 ft) and final velocity (22,071 ft/s vs. 22,000 ft/s). The model accurately predicts the payload position and velocity at burnout similar to the conditions of the Minuteman III ICBM. The burnout times and burnout altitudes for the different stages also match the published trajectory of the Minuteman III ICBM. Figure 4-2 shows a diagram of the Minuteman III ICBM ballistic flight profile. The vehicle is being modeled up until the point in the diagram that says “Third Stage Jettison” (approximately the first 191 seconds of flight). The vehicle flight profile for the

validation model is shown in Figure 4-3. The burnout altitudes and burnout times for both vehicles match fairly closely. However, the Minuteman III ICBM comes out of its launch facility at a much steeper launch angle than the validation model. The reason for this is that the 6DOF flight dynamics simulator used with the validation model is not configured to perform a programmed pitch-over maneuver.

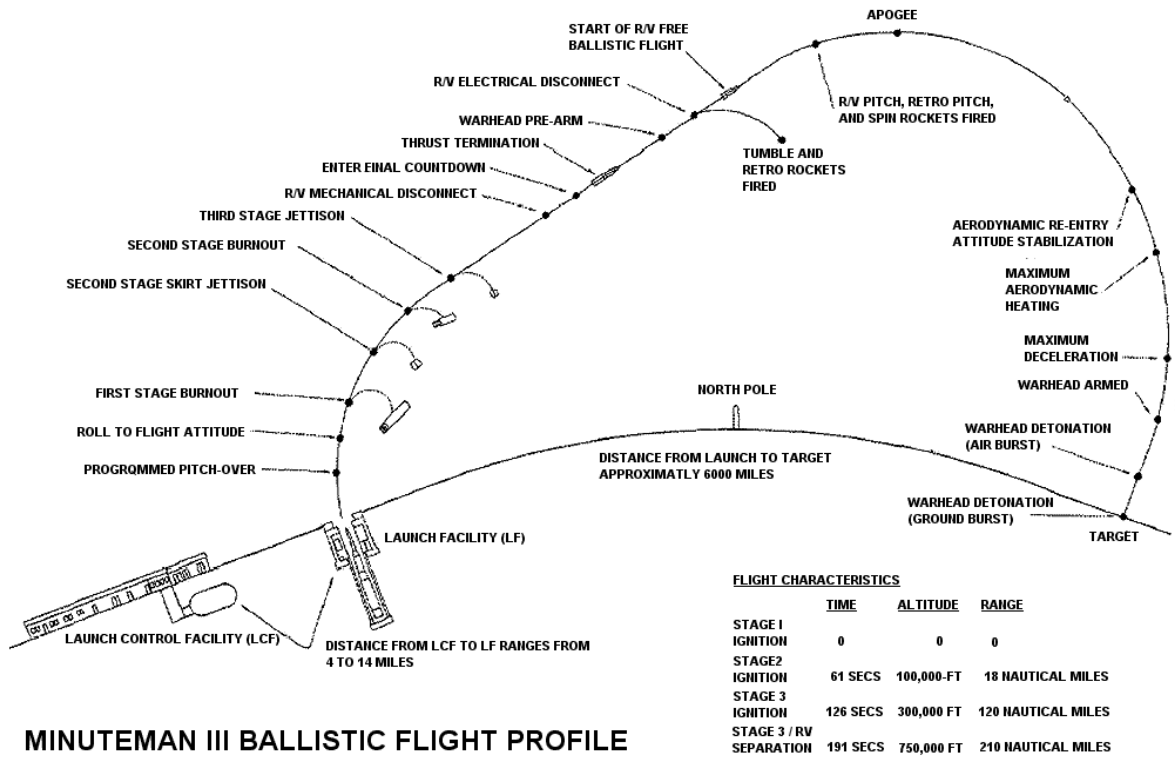


Figure 4-2. Minuteman III ICBM Ballistic Flight Profile
 (Ref. 53: http://www.geocities.com/minuteman_missile/diagrams.htm)

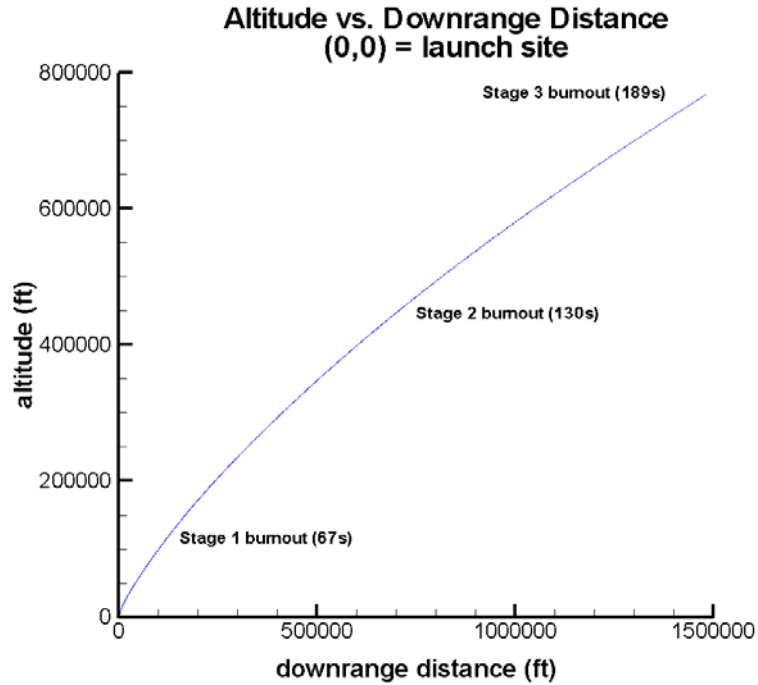


Figure 4-3. Validation Model Ballistic Flight Profile

4.4 Four-Stage Solid Propellant Vehicle vs. Minotaur I SLV

Like the three-stage solid propellant launch vehicle, the objective function for the four-stage solid propellant launch vehicle model has been manipulated using the known values of a real world system. The real world comparison vehicle chosen for this case is the Minotaur I Space Launch Vehicle (SLV). The Minotaur I SLV is a four-stage solid propellant launch vehicle used to carry small to medium payloads into low Earth orbit. The Minotaur I SLV has been launched from both the east and west coasts of the United States. For this validation, the west coast launch site, Vandenberg AFB, CA, has been chosen.

The Minotaur I SLV is owned and operated by Orbital Sciences Corporation. According to the Minotaur I SLV User's Guide,⁵⁴ "The Minotaur I launch vehicle was developed by Orbital for the United States Air Force (USAF) to provide a cost effective,

reliable and flexible means of placing small satellites into orbit.” This launch vehicle utilizes surplus stages of decommissioned Minuteman II ICBMs along with stages from Orbital Sciences Corporation’s air-launched Pegasus launch vehicle.

A schematic showing the four-stage solid propellant vehicle generated by the model and the Minotaur I SLV is shown in Figure 4-4. Another good match between the two vehicles has been obtained. However, one of the differences in the two vehicles is that the skirt between the first and second stages has not been included in the model. Also, the model uses a single nozzle for the first stage while the Minotaur I SLV has four nozzles which is the configuration on the first stage of the Minuteman III ICBM. The reason for this is that the propulsion system model for solid propellant motors was created for a single nozzle rocket. This is not a significant difference for this preliminary design study.

The comparison between the characteristics of the four-stage solid propellant launch vehicle model generated using the objective function and the Minotaur I SLV is shown in Table 4-4 and Table 4-5. The **bold*** values were direct inputs into the objective function based on the published characteristics of the Minotaur I SLV.

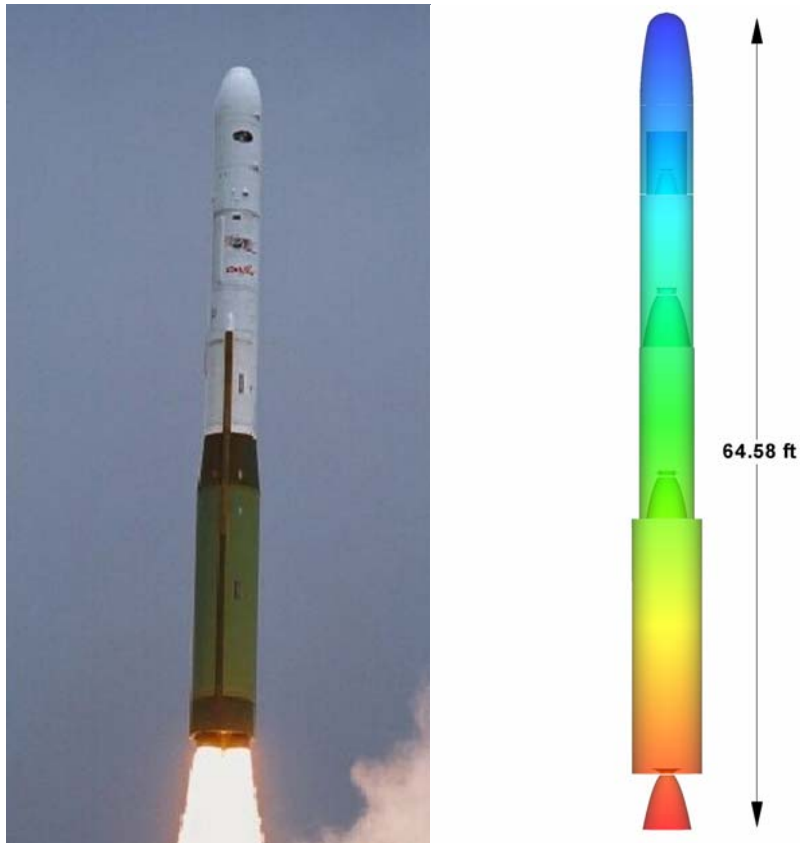


Figure 4-4. Four-Stage Solid Propellant Model vs. Minotaur I SLV Schematic
 (Ref. 55: <http://www.orbital.com/SpaceLaunch/Minotaur/index.html>)

Table 4-4: Four-Stage Solid Propellant Model vs. Minotaur I SLV Comparison

Parameter	Model	Minotaur I SLV
Payload*	738 lbm	738 lbm
Total Vehicle Weight	78,090 lbm	79,800 lbm
Total Vehicle Length	64.58 ft	63.02 ft
Total Vehicle f_{prop}	0.9185	0.8998
Final Altitude	2,425,999 ft	2,430,000 ft
Final Velocity	25,002 ft/s	25,004 ft/s
Cost per Launch	\$51.95 million	\$52.05 million
Adjusted Cost per Launch		\$29.76 million
Advertised Cost per Launch		\$20.00 million

Table 4-5: Four-Stage Solid Propellant Model Individual Stage Comparison

<u>Parameter</u>	<u>Model</u>	<u>Minotaur I SLV</u>
<u>Stage 1</u>		
Stage Length*	295.20 in	295.20 in
Stage Diameter*	66.00 in	66.00 in
Propellants*	PBAA/AP/Al	PBAA/AP/Al
Total Stage Weight	49,882 lbm	50,486 lbm
f_{prop}	0.9192	0.8987
Burnout Time	68.32 s	61.30 s
Burnout Altitude	123,706 ft	103,968 ft
Burnout Velocity	5,078 ft/s	4,919 ft/s
<u>Stage 2</u>		
Stage Length*	162.00 in	162.00 in
Stage Diameter*	52.00 in	52.00 in
Propellants*	PBAA/AP/Al	PBAA/AP/Al
Total Stage Weight	15,840 lbm	15,432 lbm
f_{prop}	0.9131	0.8857
Burnout Time	130.73 s	128.10 s
Burnout Altitude	440,142 ft	382,669 ft
Burnout Velocity	10,267 ft/s	9,512 ft/s
<u>Stage 3</u>		
Stage Length*	145.20 in	145.20 in
Stage Diameter*	50.00 in	50.00 in
Propellants*	HTPB/AP/Al	HTPB/AP/Al
Total Stage Weight	9,396 lbm	9,520 lbm
f_{prop}	0.9136	0.9086
Burnout Time	201.62 s	203.50 s
Burnout Altitude	976,766 ft	801,054 ft
Burnout Velocity	19,694 ft/s	19,208 ft/s
<u>Stage 4</u>		
Stage Length*	60.00 in	60.00 in
Stage Diameter*	38.00 in	38.00 in
Propellants*	HTPB/AP/Al	HTPB/AP/Al
Total Stage Weight	1,957 lbm	1,966 lbm
f_{prop}	0.8719	0.8642
Burnout Time	554.33 s	763.80 s
Burnout Altitude	2,425,999 ft	2,430,000 ft
Burnout Velocity	25,002 ft/s	25,004 ft/s

A good match has been obtained for the four-stage solid propellant vehicle model and its corresponding real world example. In this case, the model produces a vehicle

very similar to the Minotaur I SLV. The total weight of the vehicle produced by the model is about 1,700 pounds less than the weight of the Minotaur I SLV. Again, this difference is most likely due to the bias error in the mass properties model. There is also a large difference in the Stage 4 burnout time for the model versus the Minotaur I SLV. During the firing of the first three stages, the model and the Minotaur I SLV match burnout time, burnout velocity and burnout altitude very well. After the third stage burns out, the Minotaur I SLV uses a coast phase of about 400 seconds before firing the fourth stage for orbit insertion. Using the model, the value for this coast phase was determined to be 200 seconds in order to achieve the required orbital parameters.

As with the three-stage solid propellant model, the propellant mass fractions of the four-stage solid propellant model match the propellant mass fractions of the Minotaur I SLV within about 2% for each stage. Again, the model produces mass fractions that are slightly higher than the actual values of the Minotaur I SLV.

While the vehicle model being used in this study provides a reasonably high fidelity analysis of system performance, it cannot fully reproduce a real world system down to the specifics of individual components. Sutton⁶⁰ describes the eight components that make up the first stage of the Minuteman ICBM. These components are the propellant, internal and external insulation, the liner, the igniter, the nozzle, the motor case, and other miscellaneous components. Assuming that the other three stages of a four-stage solid propellant launch vehicle have the same components then the total number of components rises to 32. The total number of components becomes 35 when the nosecone, the payload and an electronics/avionics package are included. For a liquid propellant launch vehicle, the total number of vehicle components would be even higher.

An important point to remember is that the vehicle models being generated in this study represent a preliminary design level model. As a result, it would be quite difficult for the model to produce a very detailed representation of each vehicle component. This type of component analysis is usually done during later stages of the design engineering process.

Next, the subjective nature of vehicle cost is apparent in the cost comparison. Using the published mass values for the Minotaur I SLV and applying the cost model developed for this study, the cost per launch of the Minotaur I SLV is \$52.05 million in 2003 dollars. This is roughly about the same as the cost per launch of the vehicle generated by the model (\$51.95 million vs. \$52.05 million). In reality, there is no recurring cost for the first two stages of the Minotaur I SLV since those stages come from the surplus Minuteman II ICBMs that have already been built. An adjustment to the cost model to allow for this yields a cost per launch of the Minotaur I SLV to be \$29.76 million. Finally, the advertised cost per launch of the Minotaur I SLV is given as \$20.00 million.⁵² There is currently no data in an open source format that explains how the \$20.00 million value is determined. Overall, the results obtained for the performance characteristics and the mass properties are sufficient for this preliminary design study.

4.5 Two-Stage Liquid Propellant Vehicle vs. Titan II SLV

The historical data have shown that for a liquid propellant vehicle, the inert mass fraction is used rather than the propellant mass fraction. As stated in Humble et al.,⁵⁰ the inert mass fraction for a multi-stage, liquid propellant launch vehicle typically falls in the range of 0.04 to 0.14. Other data from Humble et al.⁵⁰ shows that the average value for f_{inert} for liquid propellant rockets is around 0.17. The same principals of mass fraction and total impulse apply to a liquid propellant vehicle as is done for a solid propellant

vehicle. Enough propellant mass is needed to launch the payload into the required orbit. The ideal rocket equation (Equation 4.4) drives this calculation.

As in the case of the solid propellant launch vehicle, the objective function for a liquid propellant launch vehicle has been manipulated and the characteristics of the resulting vehicle have been analyzed. Initial attempts to validate the multi-stage liquid propellant vehicle model focused on a three-stage liquid propellant launch vehicle. However, finding a real-world three-stage liquid propellant launch vehicle similar to the one being analyzed in the current study was a difficult task. One real world example, the Zenit-3SL,⁶² proved difficult to model due to incomplete information on the vehicle's launch trajectory.

Thus, the focus changed to using a two-stage liquid propellant launch vehicle for the model validation. There are numerous current, as well as previously built and flown, two-stage liquid propellant space launch vehicles on the market. One launch vehicle proved to be the best real world example to use for model validation. The Titan II SLV was chosen for the availability of information on the vehicle. The Titan II launch vehicle dates back to the 1960's when it was first used as an ICBM. It was also used by NASA to launch manned capsules into orbit as part of the Gemini program. According to the United States Air Force Titan II Space Launch Vehicle Profile Fact Sheet⁵⁶ "The Titan II Space Launch Vehicle is a modified Titan II ICBM that can lift approximately 4,200 pounds into polar orbit." The Titan II SLV has been retired in favor of the Delta IV and Atlas V launch vehicles. The Delta IV and Atlas V were developed under the USAF's evolved expendable launch vehicle (EELV) program. The last Titan II SLV was

launched in 2004. The launch site for these liquid propellant launch vehicles has been chosen to be Cape Canaveral AFS, FL.

Figure 4-5 shows a schematic comparing the launch vehicle generated by the model and the Titan II SLV. The stage diameter is the same for both the first and second stages. Also, the nosecone of the Titan II SLV is a more blunt shape than the nosecone on the model. This is due to the blunted ogive model used by the mass properties model.

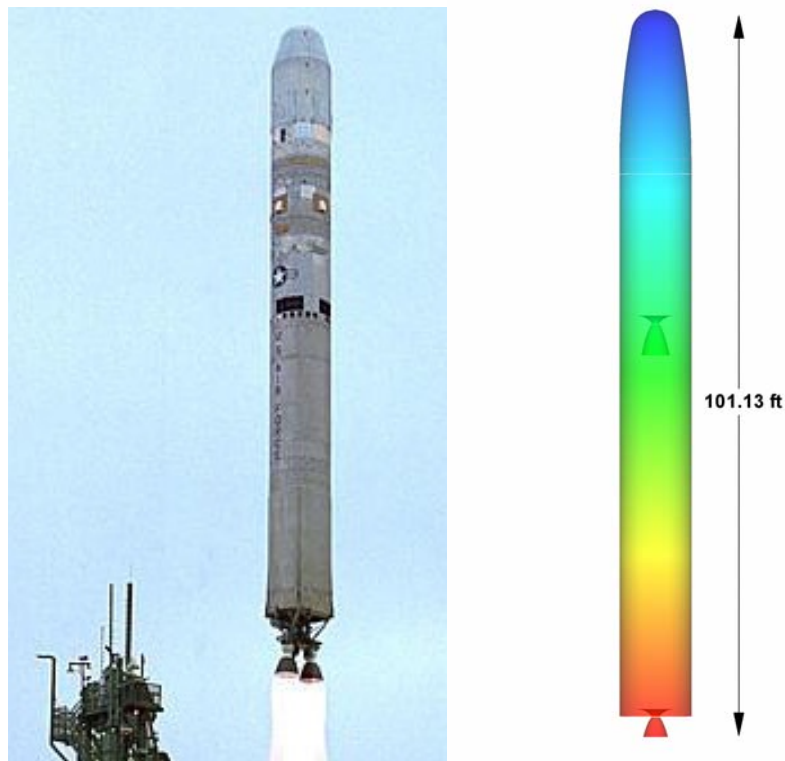


Figure 4-5. Two-Stage Liquid Propellant Model vs. Titan II SLV Schematic
(Ref. 57: <http://www.globalsecurity.org/space/systems/t2.htm>)

The comparison between the characteristics of the two-stage liquid propellant launch vehicle model and the Titan II SLV are shown in Table 4-6. The **bold*** values were direct inputs into the objective function based on the published characteristics of the Titan II SLV.

Table 4-6: Two-Stage Liquid Propellant Model vs. Titan II SLV Comparison

<u>Parameter</u>	<u>Model</u>	<u>Titan II SLV</u>
Payload*	7,000 lbm	7,000 lbm
Initial Vehicle Weight	290,499 lbm	339,000 lbm
Total Vehicle Length	101.13 ft	103.00 ft
Total Vehicle f_{inert}	0.0819	0.0818
Final Altitude	608,431 ft	607,000 ft
Final Velocity	26,248 ft/s	25,600 ft/s
<u>Stage 1</u>		
Burn Time*	140.00 s	140.00 s
Stage Diameter*	10.00 ft	10.00 ft
Propellants*	N2O4/Hydrazine	N2O4/Hydrazine
Total Stage Weight	220,836 lbm	259,850 lbm
m_{prop}	207,544 lbm	245,000 lbm
m_{inert}	13,293 lbm	14,850 lbm
f_{inert}	0.0602	0.0571
Stage Vacuum Thrust	480,556 lbf	488,337 lbf
<u>Stage 2</u>		
Burn Time*	180.00 s	180.00 s
Stage Diameter*	10.00 ft	10.00 ft
Propellants*	N2O4/Hydrazine	N2O4/Hydrazine
Total Stage Weight	57,357 lbm	63,939 lbm
m_{prop}	52,629 lbm	58,640 lbm
m_{inert}	4,728 lbm	5,299 lbm
f_{inert}	0.0824	0.0829
Stage Vacuum Thrust	100,569 lbf	100,000 lbf

The validity of the liquid propellant launch vehicle model is established in the strong comparison between the two-stage liquid propellant model and the Titan II SLV. The inert mass fractions are typical values for liquid propellant vehicles and the thrust characteristics of each stage are almost exactly those of the Titan II SLV. As with both solid propellant vehicle models, there are differences in the total vehicle mass of the two liquid propellant vehicles that are being compared. The model designs the vehicle to be about 48,500 pounds lighter than the Titan II SLV. This is seen in the difference in the total amount of fuel and oxidizer propellant in the first stage of the two launch vehicles

(207,544 lbm vs. 245,000 lbm). All the other physical and performance characteristics of the two-stage liquid propellant model closely match those of the Titan II SLV.

4.6 Air-Launched, Two-Stage Liquid Propellant Vehicle vs. QuickReach™

In order to provide additional validation of the liquid propellant launch vehicle model, an air-launched, two-stage liquid propellant case has been analyzed. Like the previous multi-stage liquid propellant vehicle, finding a real-world example of an air-launched, two-stage liquid propellant vehicle was not possible. However, currently, there is an air-launched, two-stage liquid propellant launch vehicle in development by a company known as AirLaunch LLC. The QuickReach™ launch vehicle⁵⁸ is designed to be a responsive small-lift vehicle used to launch small satellites into Low Earth Orbit (LEO) within a 24 hour call-up for a launch price of \$5 million.

The QuickReach™ launch vehicle is air-launched from the cargo bay of a C-17 transport aircraft. Some performance characteristics of this vehicle have been published. However, the specific mass properties of the QuickReach™ launch vehicle are not available so only a limited comparison can be made. Specifically, the values for inert mass and propellant mass would allow for a more direct comparison to the vehicle generated using the system model.

A schematic showing a test article of the QuickReach™ launch vehicle being deployed from a C-17 and the launch vehicle designed by the system model are shown in Figure 4-6. One important difference can be seen in the size of the first stage nozzle. The first stage nozzle for the QuickReach™ launch vehicle is much larger than the one generated in the model. Additional work on the model's generation of the first stage

nozzle would need to be done once more specific information on the QuickReach™ launch vehicle becomes available.

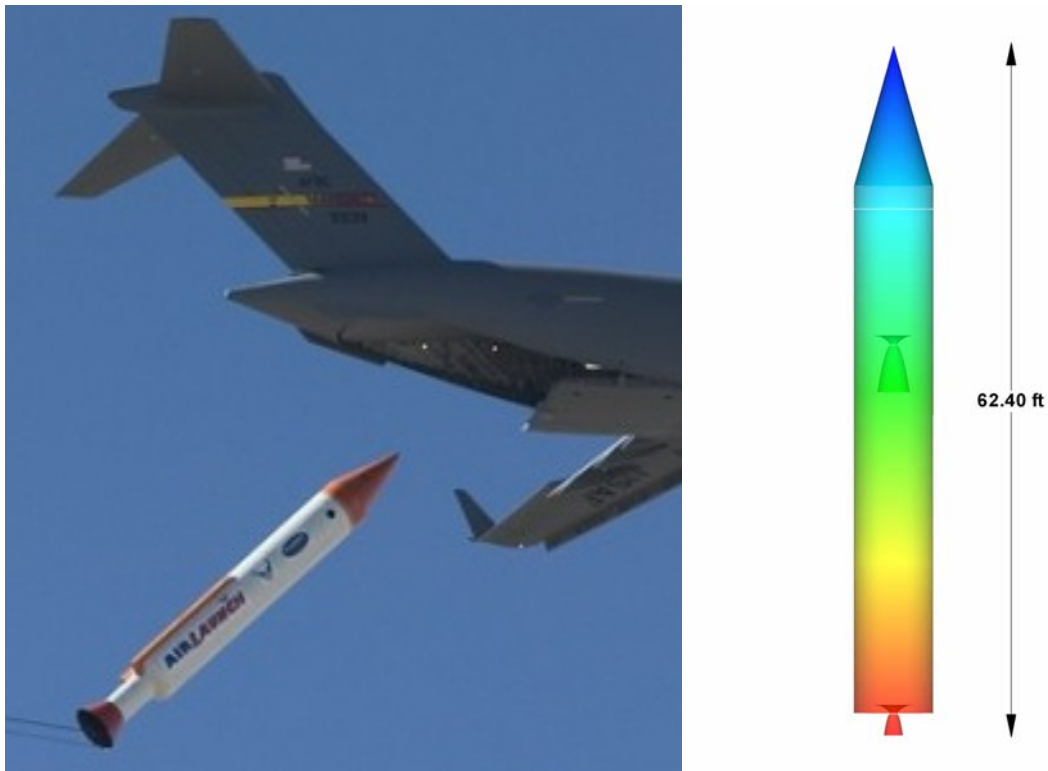


Figure 4-6. Air Launched, Two-Stage Liquid Propellant Model vs. QuickReach™ Launch Vehicle Schematic
(Ref. 59: <http://www.designation-systems.net/dusrm/app4/quickreach-slv.jpg>)

Table 4-7 shows the characteristics of the air launched, two-stage liquid propellant launch vehicle model with the QuickReach™ launch vehicle. Because the QuickReach™ launch vehicle is relatively new, there is not a large amount of information on the specifics of the vehicle. However, enough data exist to make the comparison a useful one. The validity of the liquid propellant model is also strengthened through this comparison.

Table 4-7: Air Launched, Two-Stage Liquid Propellant Model vs. QuickReach™ Launch Vehicle Comparison

<u>Parameter</u>	<u>Model</u>	<u>QuickReach™ Launch Vehicle</u>
Payload*	1,000 lbm	1,000 lbm
Initial Altitude*	35,000 ft	35,000 ft
Initial Velocity*	760 ft/s	760 ft/s
Total Vehicle Weight	74,633 lbm	72,000 lbm
Total Vehicle Length	62.40 ft	66.00 ft
Total Vehicle f_{inert}	0.12	unknown
Final Altitude	738,783 ft	700,000 ft
Final Velocity	25,619 ft/s	25,532 ft/s
<u>Stage 1</u>		
Stage Diameter*	7.00 ft	7.00 ft
Propellants*	LOX/Kerosene	LOX/Propane
m_{prop}	60,796 lbm	unknown
m_{inert}	5,130 lbm	unknown
f_{inert}	0.08	unknown
Stage Vacuum Thrust	171,825 lbf	172,000 lbf
<u>Stage 2</u>		
Stage Diameter*	7.00 ft	7.00 ft
Propellants*	LOX/Kerosene	LOX/Propane
m_{prop}	3,945 lbm	unknown
m_{inert}	1,516 lbm	unknown
f_{inert}	0.27	unknown
Stage Vacuum Thrust	25,333 lbf	24,000 lbf

As with the previous model validation cases, the objective function has been manipulated in order to generate a vehicle for the purposes of matching the real world example. Table 4-7 shows that a good match was obtained in total vehicle weight and performance characteristics between the model and the QuickReach™ launch vehicle. The total vehicle mass of the model is slightly higher than the total vehicle mass of the QuickReach™ launch vehicle (74,633 lbm vs. 72,000 lbm). However, the final altitude and the final velocity of the model are higher but still relatively close to the QuickReach™ launch vehicle. This provides confidence in the ability of the vehicle generated by the model to reach the desired orbit. Also, the values for vacuum thrust of

each stage are very similar. The Stage 1 thrust for the model is slightly lower than the QuickReach™ launch vehicle (171,825 lbf vs. 172,000 lbf) whereas the Stage 2 thrust is slightly higher (25,333 lbf vs. 24,000 lbf).

The inert mass fractions for this liquid propellant launch vehicle, also shown in Table 4-7, fall within the desired range of typical inert mass fraction values published in Humble et al.⁵⁰

4.7 Mass Fractions for Three-Stage Solid/Liquid/Liquid Propellant Vehicle

In addition to traditional launch vehicle configurations, the case of a mixed propellant system has been analyzed. This case is a three-stage vehicle that employs a solid propellant first-stage along with liquid propellant second and third stages. There are numerous real world examples of mixed propellant systems. Most use solid propellant motors as thrust augmentation to a first-stage liquid propellant rocket engine. The Space Shuttle solid rocket boosters (SRBs) are used to provide the lift-off thrust for the shuttle stack. The Delta II SLV uses up to nine graphite epoxy solid motors (GEMs) during operation of the liquid propellant first-stage. However, the case of a purely solid propellant first-stage along with liquid propellant second and third stages is a unique one. A real world example currently being developed by the National Aeronautics and Space Administration (NASA) is the Ares I Crew Launch Vehicle (CLV). NASA has proposed a two-stage; first stage solid/second stage liquid combination launch vehicle for the Ares I CLV. The Ares I CLV would provide a good real world example for any future model validation attempts.

Even though no real world examples exist for the three-stage solid/liquid/liquid launch vehicle, analysis of the mass fractions will give validity to the model being used.

The historical data of Humble et al.⁵⁰ will continue to be referenced in order to compare the results from the model with previously designed and flown vehicles. The solid propellant first stage will use the propellant mass fraction and the liquid propellant second and third stages will use the inert mass fraction. The reason for using two types of mass fractions is that the historical data used by Humble et al.⁵⁰ focuses on the propellant mass fraction for solids and the inert mass fraction for liquids.

For this case, two pure design optimizations using the GA were performed. There were three goals involved in each optimization. The first two were for the vehicle to attain the desired low-Earth orbit. The third goal was to minimize the total vehicle mass. Design optimizations have been performed for launch out of Vandenberg AFB, CA and Cape Canaveral AFS, FL. Table 4-8 summarizes the vehicle mass fraction for each of the three stages of the two vehicle models produced by the GA.

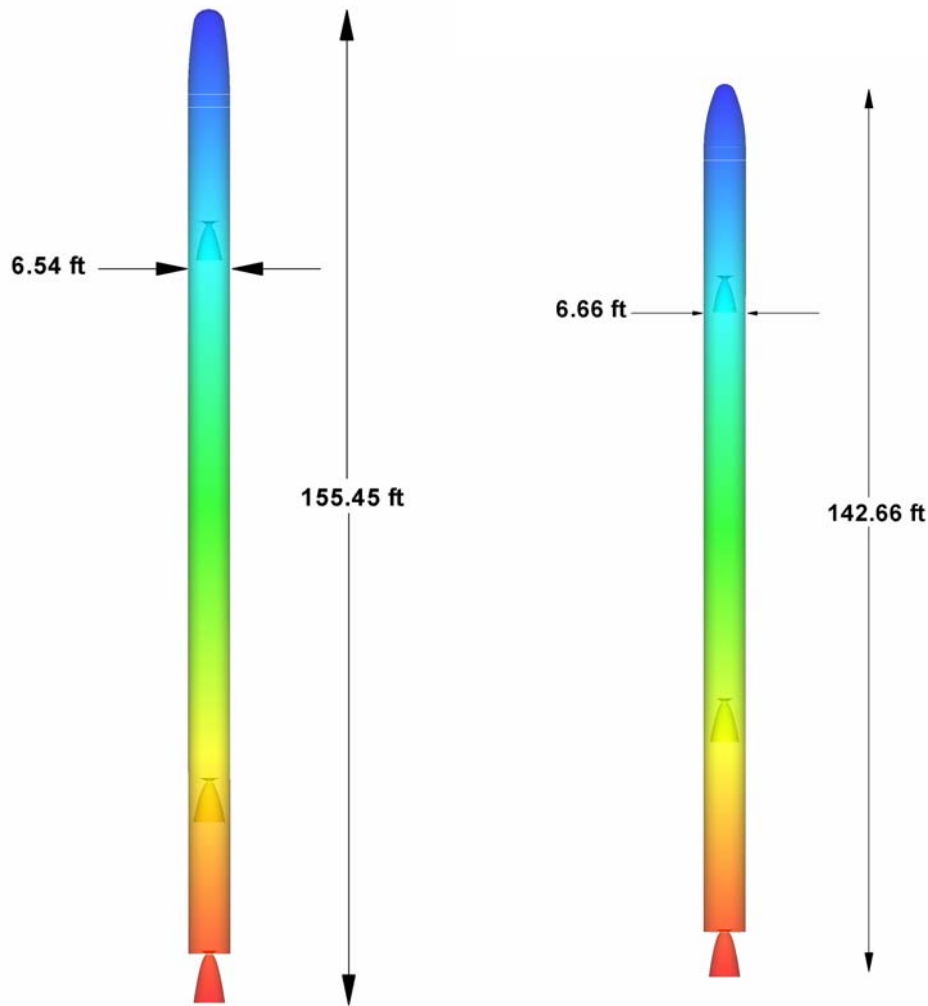
Table 4-8: Three-Stage Solid/Liquid/Liquid Propellant Vehicle Mass Fractions

	<u>3-Stage Solid/Liquid/Liquid (Vandenberg Launch)</u>	<u>3-Stage Solid/Liquid/Liquid (Cape Canaveral Launch)</u>
Stage 1 (solid)		
f_{prop}	0.8991	0.8699
Stage 2 (liquid)		
f_{inert}	0.1274	0.0748
Stage 3 (liquid)		
f_{inert}	0.0957	0.1128

Schematics of the resulting launch vehicles are shown in Figure 4-7. Both vehicles are very similar in geometry as well as their mass fractions. While not ideal, the mass fractions listed in Table 4-8 are consistent with the values published in Humble et al.⁵⁰ The propellant mass fraction for Stage 1 of both vehicles is slightly lower than the desired value of 0.90 for solid rocket motors. Since this value is lower than 0.90, the

inert mass for this stage is probably too high. This indicates some adjustment to the modeling of the Stage 1 inert mass needs to be done in order to bring the propellant mass fractions closer to 0.90. The inert mass fractions of the two liquid stages fall within the expected range (0.04 to 0.14) for liquid propellant rocket engines.

Overall, the model for this three-stage solid/liquid/liquid propellant launch vehicle configuration appears to be accurate. It should be emphasized that these three-stage solid/liquid/liquid propellant launch vehicles have not been compared to any existing experimental data. The validity of the model is limited to the comparison of the mass fractions of the individual vehicle stages. Certainly, future real world examples would help strengthen the current model's validity. The use of variable diameter stages might also provide additional insight into the modeling of this type of launch vehicle. As previously stated, the Ares I CLV is proposed to have a solid propellant first stage and a liquid propellant second stage along with a second stage diameter that is larger than the first stage diameter.



Vandenberg Launch

Cape Canaveral Launch

Figure 4-7. Three-Stage Solid/Liquid/Liquid Propellant Launch Vehicles Schematic

4.8 Summary of Validation Efforts

Four successful model validations have been performed for four different types of launch vehicles. The validity of the system models used in the objective functions has been established through the use of comparisons with real world examples. While the launch vehicle models do not exactly match their respective real world counterparts, the results are encouraging. These validation efforts should instill confidence that the launch vehicle models have produced realistic designs at this preliminary design level.

4.8.1 Three-Stage Solid Propellant Launch Vehicle

The three-stage solid propellant launch vehicle model has been validated against the Minuteman III ICBM. A good match between these two vehicles has been made with the model producing a vehicle with a lower weight than the Minuteman III ICBM. This difference is likely related to the ability of the model to reproduce individual system components.

The performance values for the vehicle model and the Minuteman III ICBM match very well. This can be seen in the values generated for the final altitude of the model versus the Minuteman III ICBM (768,682 ft vs. 750,000 ft) and the final velocity (22,071 ft/s vs. 22,000 ft/s).

4.8.2 Four-Stage Solid Propellant Launch Vehicle

For the validation of the four-stage solid propellant launch vehicle, the Minotaur I SLV has been used as the real world example. Again, a good match has been obtained between the vehicle model and the Minotaur I SLV. The model generates a vehicle within 1,700 pounds of the total vehicle mass of the Minotaur I SLV.

In terms of performance, the first three stages of the vehicle model match the velocity and altitude of the Minotaur I SLV. However, after Stage 3 burnout, the Minotaur I SLV goes into a coast phase for approximately 400 seconds. Upon completion of the coast phase, Stage 4 is fired for orbit insertion. For the vehicle model, the same type of trajectory was modeled. However, the vehicle model produced a coast phase of 240 seconds. A recommended improvement of the 6DOF flight dynamics simulator would be to incorporate an orbit insertion burn for future design optimization work. This recommendation will be discussed further in Chapter 8.

4.8.3 Two-Stage Liquid Propellant Launch Vehicle

The Titan II SLV has been chosen to validate the two-stage liquid propellant launch vehicle model. As in the previous two cases, the vehicle model successfully reproduced the characteristics of the Titan II SLV with some slight differences.

Comparing the performance of the model versus the Titan II SLV, the vehicle model was very accurate in final altitude (608,431 ft vs. 607,000 ft) and final velocity (26,248 ft/s vs. 25,600 ft/s).

One important difference was the total vehicle mass with the model coming in at about 40,000 pounds lighter than the Titan II SLV. This is seen in the difference in the amount of propellant in the first stage (207,543 pounds vs. 245,000 pounds). Additional work could be done to investigate the parameters (such as mass flow rate and fuel-to-oxidizer ratio) used to calculate the propellant mass. These parameters could then be compared to the same parameters of the Titan II SLV.

4.8.4 Air-Launched, Two-Stage Liquid Propellant Launch Vehicle

An additional validation of the liquid propellant model has been performed using the QuickReach™ launch vehicle as the real world example. The QuickReach™ launch vehicle is still in its initial development stages so detailed information about the vehicle is currently unavailable. However, enough information is available to make a comparison with the vehicle model. A good match has been obtained between the vehicle model and the QuickReach™ launch vehicle.

Vehicle performance was again the strength of the launch vehicle model versus the QuickReach™ launch vehicle. The system model was able to accurately match the final altitude (738,783 ft vs. 700,000 ft) and final velocity (25,619 ft/s vs. 25,532 ft/s) of

the two launch vehicles. Also, the values of vacuum thrust for each stage were similar to the published values of the QuickReach™ launch vehicle (Stage 1: 171,825 lbf vs. 172,000 lbf and Stage 2: 25,333 lbf vs. 24,000 lbf). The main difference was the size of the Stage 1 nozzle. The nozzle on the QuickReach™ launch vehicle is much larger than the nozzle generated in the model. This is an area where additional work on the model can be performed. Also, when more specific data on the QuickReach™ launch vehicle is published, the system model will be improved upon.

4.8.5 Three-Stage Solid/Liquid/Liquid Propellant Launch Vehicle

A basic validation of three-stage solid/liquid/liquid propellant launch vehicles has been performed. A real world example launch vehicle does not exist for this type of launch vehicle configuration. Two pure design optimizations have been performed for each of the two launch vehicles based on the choice of launch site (Vandenberg AFB, CA and Cape Canaveral AFS, FL). As a result, a comparison of the propellant and inert mass fractions has been performed for the resulting best performers from the design optimization processes. The mass fractions of these two launch vehicles match well the established values for propellant and inert mass fraction for space launch vehicle systems.

5.0 OPTIMIZATION RESULTS

5.1 Introduction

The motivation behind the current study is to support the important national security effort of assured access to space. The results demonstrate the feasibility of designing launch vehicles using a genetic algorithm (GA). In addition, one overall goal has been to investigate the possibility of improving launch vehicle design. The results also have the added benefit of tying a cost model to the design optimization effort.

The philosophy behind choosing different cases is to provide a wide-range of space launch vehicle types for the purposes of finding an optimum design. The thirteen cases that were accomplished encompass different types of propulsion systems as well as launches from the two primary United States Air Force (USAF) space launch sites: Cape Canaveral AFS, FL (CCAFS) and Vandenberg AFB, CA (VAFB).

The cases are broken down into five different sets of results. The first section encompasses the initial launch vehicle optimizations that demonstrate the feasibility of the process. Next, solid propellant rockets have been optimized for both three and four-stage configurations. The third section covers the optimization of two and three-stage liquid propellant rockets. Two-stage, air-launched vehicles were then analyzed using liquid propellant systems. Finally, three-stage vehicles with a solid propellant first stage and liquid propellant second and third stages have been optimized.

The results show the positive and negative aspects of each type of launch vehicle design. Cost per launch values along with performance and physical characteristics are summarized for each vehicle that has been optimized. In certain cases, the results are summarized to show how these vehicles have demonstrated improvement in cost and performance over their real world example counterpart launch vehicle. Information describing some of the important characteristics of the design optimization cases is presented in Table 5-1.

Table 5-1: Space Launch Vehicle Design Optimization Cases

	<u>Case #</u>	<u>1st Stage</u>	<u>2nd Stage</u>	<u>3rd Stage</u>	<u>4th Stage</u>	<u>Goal(s)</u>	<u>Launch Site</u>
<u>Initial Vehicles</u>							
5.2.1	1	solid	solid	solid		Get to orbit	VAFB
5.2.2	2	solid	solid	solid		Min. mass	VAFB
<u>Solids</u>							
5.3.1	3	solid	solid	solid		Min. cost	VAFB
5.3.2	4	solid	solid	solid		Min. cost	CCAFS
5.3.3	5	solid	solid	solid	solid	Min. cost	VAFB
5.3.4	6	solid	solid	solid	solid	Min. cost	CCAFS
<u>Liquids</u>							
5.4.1	7	liquid	liquid	liquid		Min. cost	VAFB
5.4.2	8	liquid	liquid	liquid		Min. cost	CCAFS
5.4.3	9	liquid	liquid			Min. cost	VAFB
5.4.4	10	liquid	liquid			Min. cost	CCAFS
<u>Air-Launch</u>							
5.5.1	11	air-launch	liquid	liquid		Min. cost	CCAFS
<u>Mixed</u>							
5.6.1	12	solid	liquid	liquid		Min. cost	VAFB
5.6.2	13	solid	liquid	liquid		Min. cost	CCAFS

5.2 Initial Launch Vehicles

The design optimization of space launch vehicles begins with two cases that represent initial vehicles optimized using the system models along with the genetic algorithm (GA). These initial vehicles provide insight to the optimization process and show how well the GA works at meeting the desired goals. These cases are not meant to be the best solutions to the launch vehicle preliminary design problem. The reason for

this is that the system models used for these initial vehicles have not gone through the model validation process.

For this initial analysis, the three-stage solid propellant launch vehicle has been chosen for the design optimization process. Additionally, a typical low-Earth orbit has been chosen for the mission with the launch site being Vandenberg AFB, CA. The launch direction is due North in order to obtain a polar orbit. A nominal 1,000 pound payload provides the mass to be carried into orbit by the launch vehicle. The two cases analyzed in this section use slightly different goals for the GA to optimize.

5.2.1 Case 1: Three-Stage Solid Propellant Launch Vehicle with Two Goals

The purpose of this initial design optimization is to determine if a three-stage solid propellant rocket can be designed that will achieve a low-Earth orbit. The desired mission statistics for this vehicle are listed in Table 5-2.

Table 5-2: Initial Launch Vehicles Mission Statistics

Payload Mass	1,000 lbm
Launch Site	Vandenberg AFB, CA (34.6° N, 120.6° W)
Launch Direction	Due North (0° Azimuth or i=90°/polar orbit)
Desired Orbital Velocity	24,550 ft/s
Desired Orbital Altitude	2,430,000 ft

The two goals for this optimization are:

Goal #1: minimize the difference between the desired orbital velocity and the actual velocity of the vehicle

Goal #2: minimize the difference between the desired orbital altitude and the actual altitude of the vehicle

These goals assume that all the vehicle propellant has been consumed upon reaching the desired orbital parameters. Note that this first case is merely a demonstration of the

feasibility of finding a workable solution using the GA. The design optimization for this three-stage solid propellant rocket uses a population size of 400 members. The reason for the large population size is due to the large number of design variables (34 for the three-stage solid propellant launch vehicle). The number of design variables, along with their particular range of values, results in a relatively long chromosome string (over 100 bits). As previously mentioned, Anderson¹⁶ used Equation (3.3) to determine the population size for his design optimizations. Thus, in order to maintain sufficient genetic diversity and to avoid falling into a local optimum, the large population size is required. Also, the value of 400 members was the maximum value available for use in the GA.

The design optimization was intended to run for 150 generations but the optimum solution that met both goals was actually achieved by generation #43 (see Figures 5-1 and 5-2). Figures 5-1 and 5-2 show how the best performer improved as each generation proceeded. In Figure 5-1, the velocity goal was met by generation #23, while in Figure 5-2, the altitude goal was met by generation #43.

The behavior of the best performer in Figures 5-1 and 5-2 is interesting in that, during certain generations, there is a large change in performance. For example, there is significant improvement in the best performer's ability to meet the altitude goal from generation #22 to generation #23. This improvement highlights the powerful GA operators of crossover and mutation. These operators allow the GA to choose values of the different design variables that facilitate better vehicle performance. In addition, the complexities of launch vehicle design can also be seen in the improvement of the altitude and velocity goals. The right change in a particular variable (like nozzle throat area) at the right place and at the right time can greatly affect vehicle performance.

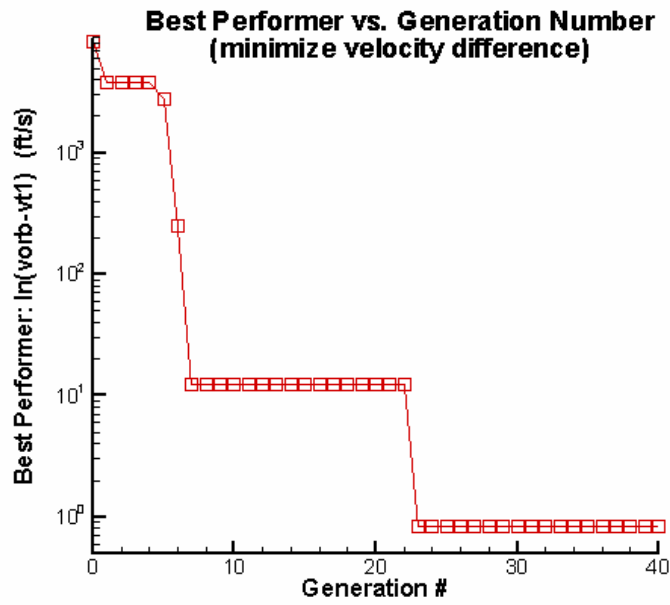


Figure 5-1. Progress of Best Performer to Meet Goal #1

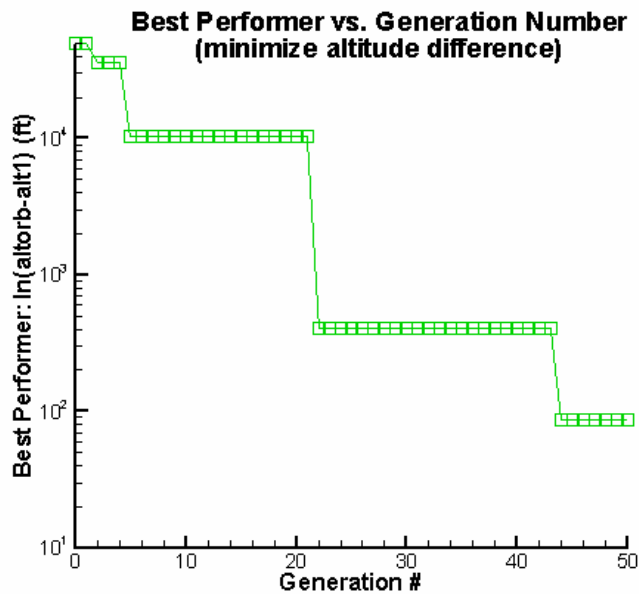


Figure 5-2. Progress of Best Performer to Meet Goal #2

The best performing vehicle of the final generation was used to display the actual performance of the optimum design. This vehicle would thus be the three-stage solid rocket that most closely meets the desired performance goals. The design variables (i.e.

the 34 GA variables) that created the best performer were run in a single-run format to generate data files which are summarized in the following paragraphs and figures.

Figures 5-3 thru 5-7 show the important performance parameters of this vehicle. Looking at Figure 5-3, it appears that the GA selected very similar dimensions for the 1st and 2nd stages of the rocket and a relatively small sized 3rd stage in order to meet both design goals. The ballistic flight trajectory of the vehicle is shown in Figure 5-4 where the altitude has reached the orbital altitude at the top of the parabolic trajectory. The next three figures display the changes in vehicle performance with time. Figure 5-5 shows the Thrust vs. Time characteristics. Three distinct “humps” in the curve show where the thrust in each stage tails off and then the next stage abruptly starts. There is no delay between the end of one stage and the start of another. Figure 5-6 (Vehicle Mass vs. Time) shows how the mass of the vehicle continuously decreases until burnout of Stage 3 at approximately 107 seconds. Finally, the Velocity vs. Time plot in Figure 5-7 displays the increase in velocity during powered flight and then the slight decrease in velocity during ballistic flight to maximum altitude.

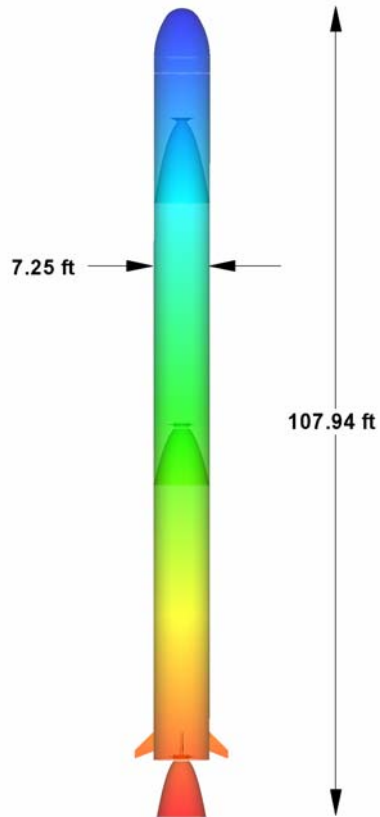


Figure 5-3. Three-Stage Solid Propellant Launch Vehicle Schematic

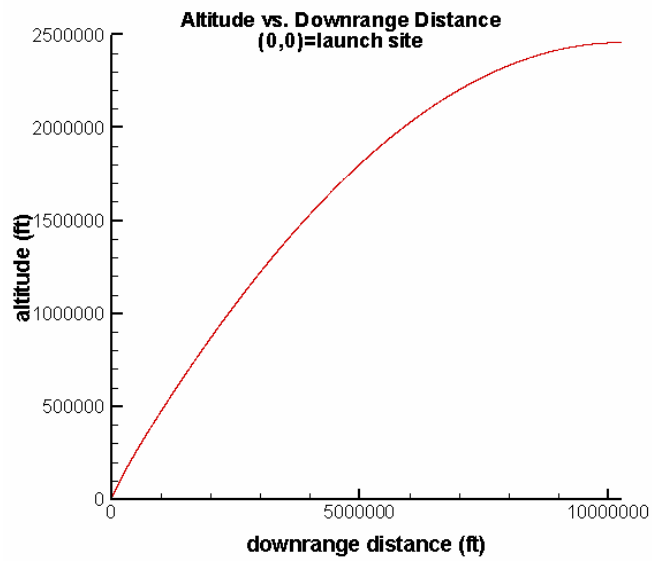


Figure 5-4. Altitude vs. Downrange Distance for Best Performer

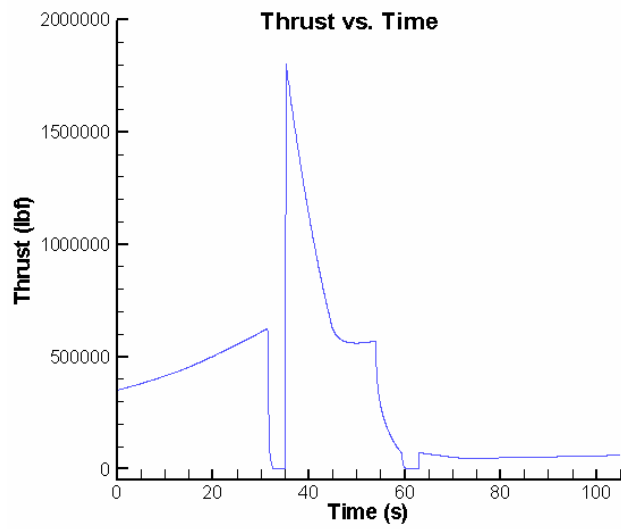


Figure 5-5. Thrust vs. Time for Best Performer

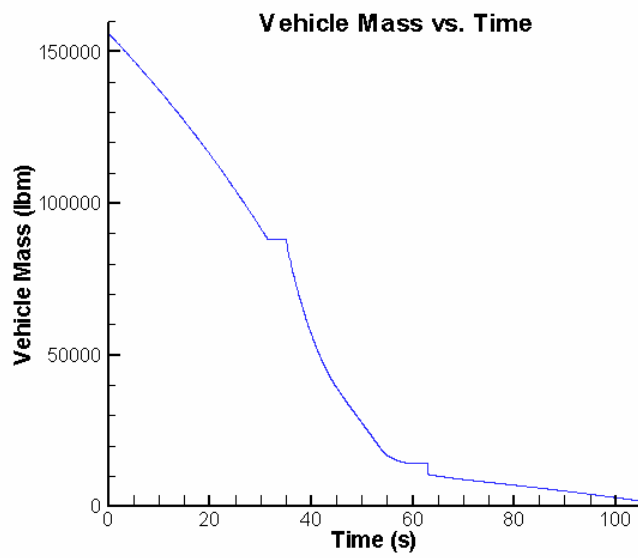


Figure 5-6. Vehicle Mass vs. Time for Best Performer

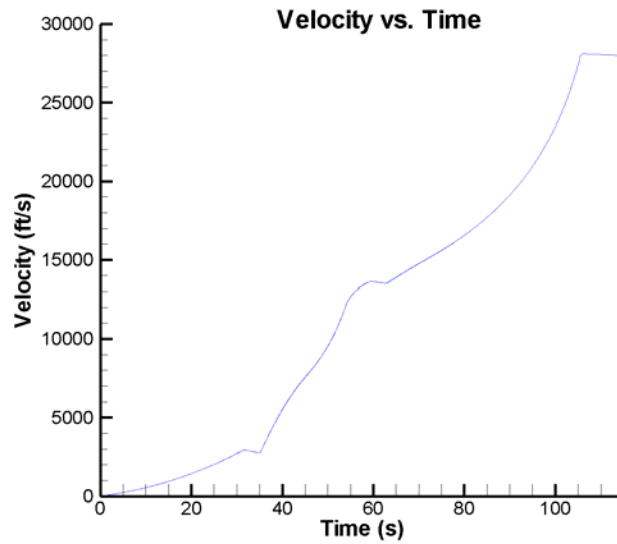


Figure 5-7. Velocity vs. Time for Best Performer

5.2.2 Case 2: Three-Stage Solid Propellant Launch Vehicle with Three Goals

The second design optimization demonstration again uses a three-stage solid propellant launch vehicle with a third goal added. The first two goals are the same as the goals used in Case 1. However, in addition to getting to orbit, it would be useful to minimize the total vehicle mass at lift-off. Thus, the third goal is to minimize the system mass while still attaining the desired orbital parameters. For these initial launch vehicles, the cost model has not been included in the design optimization process. The goal at this point is to focus on minimization of the total vehicle mass.

Also, with the addition of the third goal, a slightly different optimization process has been used. Instead of trying to meet the goals individually, a single, global solution is found. This global solution attempts to optimize the design to produce a single vehicle that meets all three design goals. However, not all three goals are weighted equally. The two orbital goals (velocity and altitude) have a higher priority because if these goals are not met (i.e. the vehicle does not get to the desired orbit) then the mission is a failure.

Finally, in order to make the GA perform better, the goals are normalized by dividing each of the three differences by their particular desired value. This prevents the GA from trying to optimize one goal which could have differences of 5,000 ft/s (velocity goal) and another goal which could have differences of 150,000 ft (altitude goal). The GA is also configured in a non-pareto format so that one overall fitness function is used in the optimization process.

Goal #1: minimize the difference between the desired orbital velocity and the actual velocity of the vehicle divided by the desired orbital velocity

Goal #2: minimize the difference between the desired orbital altitude and the actual altitude of the vehicle divided by the desired orbital altitude

Goal #3: minimize the difference between a desired minimum mass and the total vehicle mass divided by the desired minimum mass

Some interesting results have been obtained for this case. Two different design optimization runs were performed. The first run was configured for the objective function to throw out any vehicles that had final velocity and final altitude values that were below the desired orbital values. The second run relaxed this restriction and allowed for off-design vehicles to be considered in the optimization process. It was theorized that the goal minimization in the GA would account for the differences and ensure that the desired orbital values would be met. The results for these runs are summarized in Table 5-3.

Table 5-3: Case 2 Runs Comparison/Three-Stage Solid Propellant Launch Vehicles

	Run #1	Run #2
Actual Altitude	2,433,559 ft	2,439,733 ft
Actual Velocity	24,820 ft/s	23,944 ft/s
Total Vehicle Mass	115,068 lbm	104,553 lbm
Total Vehicle Diameter	6.59 ft	5.74 ft
Total Vehicle Length	109.37 ft	110.66 ft

These results show that the optimum vehicle for each run is very similar.

However, in order to meet the velocity requirement, a slightly larger rocket is required.

The differences in total vehicle mass and vehicle diameter show that attaining the desired orbital velocity is driven by vehicle mass. The difference is an additional 10,000 pounds which, as a result, will most likely add to the cost per launch of the vehicle.

Also, normalizing the goals forces the GA to choose reasonable values for the various design parameters. For the members of each generation, the three answers corresponding to each of the three goals are within a factor of 10 of each other due to this normalization process. This ensures that the GA attempts to minimize all three goals in a consistent manner. Figures 5-8 and 5-9 show the schematics for the two different vehicles analyzed in the Case 2 design optimization runs.

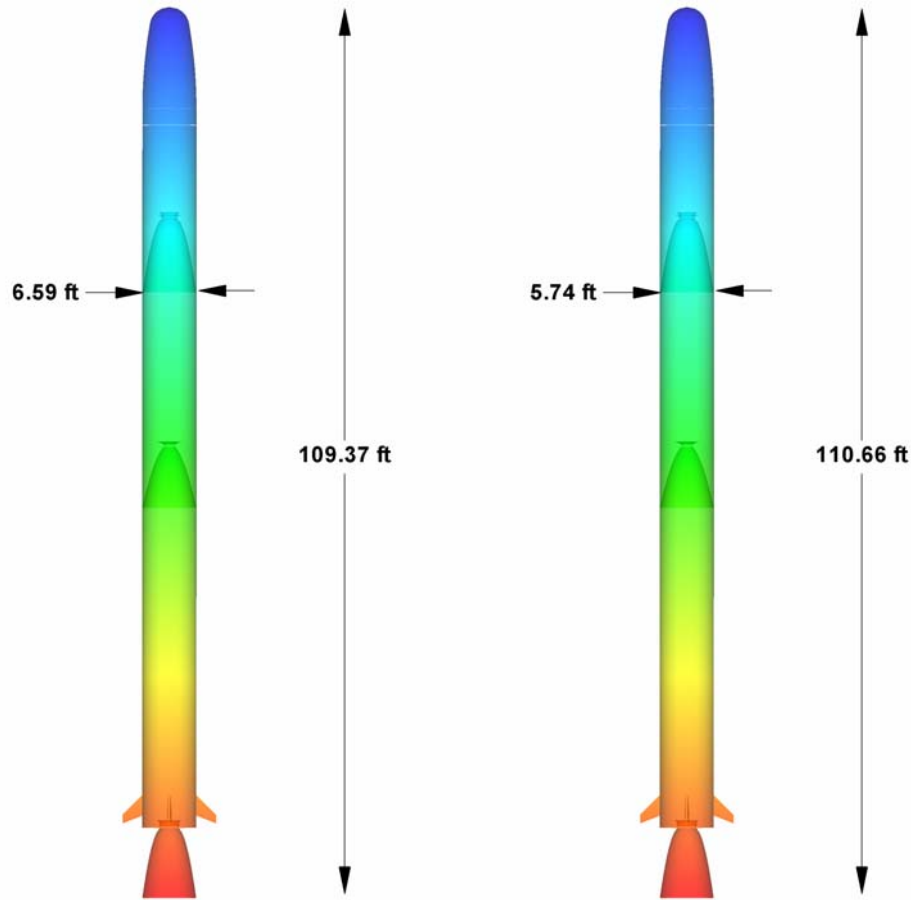


Figure 5-8. Three-Stage Solid Propellant Launch Vehicle Schematic (Case 2/Run 1) Figure 5-9. Three-Stage Solid Propellant Launch Vehicle Schematic (Case 2/Run2)

5.2.3 Conclusions: Initial Launch Vehicle Design Optimizations

Initial design optimizations for three-stage solid propellant launch vehicles have been performed. These optimizations served two purposes. The first was to demonstrate that the objective function and the GA together could be used to design a launch vehicle that achieves the desired low-Earth orbit. This was done successfully with the first case where the best performer met both design goals in a relatively small number of generations.

The second purpose was to still meet the desired orbital altitude and orbital velocity goals but also to add an additional goal of minimizing the total vehicle mass.

Two different design optimization runs were accomplished for this second case. The first run produced an optimized vehicle that met the desired altitude and velocity goals well and reduced the total vehicle mass from the previous case (115,068 lbm vs. 155,853 lbm). The second run did not quite meet the desired altitude and velocity goals as well as the first run but lowered the total vehicle mass to 104,553 pounds. Thus, it has been shown that the trend toward reducing the total vehicle mass and still meeting the performance requirements can be accomplished.

For comparison purposes, the three-stage Minuteman III ICBM has a total vehicle mass of 79,432 pounds and the four-stage solid propellant Minotaur I SLV has a total vehicle mass of 79,800 pounds. The three-stage solid propellant launch vehicles analyzed here have significantly higher values of total vehicle mass. The reason for this is that these launch vehicles are preliminary design optimization runs. The vehicle model used for these runs has not been through the model validation process.

Thus, the next step will be to implement the previously discussed model validation work and use the objective function and GA to investigate the improvement of the real world launch vehicle examples.

5.3 Solid Propellant Vehicles

The results for the design optimization of three and four-stage solid propellant launch vehicles are presented in this section. The four cases investigated for these solid propellant launch vehicles are an extension of the analysis performed during model validation. The models developed during the validation efforts have been used in the design optimization process with the goal of improving on the real world examples.

Table 5-4 shows the mission statistics for the four different solid propellant launch vehicles that have been optimized. The payloads (1,000 lbm) for both three-stage solid vehicles are different than the payload used for the model validation (2,540 lbm). The reason for this is that the real world example for the three-stage solid propellant vehicles is the Minuteman III ICBM. The payload of the Minuteman III ICBM is the reentry system which weighs 2,540 pounds. However, the Minuteman III ICBM is not an orbital vehicle. Thus, a more typical payload (1,000 lbm) for the three-stage orbital vehicles has been chosen. The payload for the four-stage solid/VAFB matches the typical payload of the Minotaur I SLV (738 lbm). In an attempt to expand the performance of the four-stage solid/CCAFS vehicle, the payload mass was increased to 1,000 pounds.

The low-Earth orbit parameters for all four cases are essentially the same except for the four-stage solid/VAFB. The desired orbital velocity for this case (25,004 ft/s) is slightly higher than the desired orbital velocities of the other three cases (24,550 ft/s). The reason for this is that certain launches out of VAFB are slightly retrograde in order to attain a sun-synchronous orbit. This orbit requires the vehicle to attain a higher velocity in order to overcome the eastward rotation of the Earth. Thus, the velocity goal of the four-stage solid/VAFB is to match the 25,004 feet per second value.

Table 5-4: Solid Propellant Launch Vehicles Mission Statistics

	<u>Three-Stage Solid</u>	<u>Three-Stage Solid</u>	<u>Four-Stage Solid</u>	<u>Four-Stage Solid</u>	<u>Minotaur I SLV</u>
Payload	1,000 lbm	1,000 lbm	738 lbm	1,000 lbm	738 lbm
Launch Site	VAFB	CCAFS	VAFB	CCAFS	VAFB
Launch Direction	Due North 0° Azimuth	Due East 90° Azimuth	Due North 0° Azimuth	Due East 90° Azimuth	Slightly Northwest
Orbit Type	i=90° polar orbit	i=28.4° prograde orbit	i=90° polar orbit	i=28.4° prograde orbit	i=97.5° sun-sync orbit
Desired Orbital Altitude	2,430,000 ft	2,430,000 ft	2,430,000 ft	2,430,000 ft	2,430,000 ft
Desired Orbital Velocity	24,550 ft/s	24,550 ft/s	25,004 ft/s	24,550 ft/s	25,004 ft/s

Upon completion of the analysis of the initial launch vehicles, the next step in the design optimization of solid propellant launch vehicles is to incorporate the cost model described in Chapter 3, the *TRANSCost 7.1* cost model, into the design optimization process. This is essentially a minor modification to the sequence of operations in the objective function. The information from the mass properties model is used in the *TRANSCost 7.1* cost model and the cost per launch of the vehicle is determined. Also, Goal #3 is changed to a straight minimization of the system mass rather than a minimization of the differences between two values. Since the *TRANSCost 7.1* cost model is mass-based, the decision has been made for Goal #3 to minimize the total vehicle mass rather than the cost per launch value. A minimized total vehicle mass should produce the minimum cost per launch vehicle. The three goals are listed below.

Goal #1: minimize the difference between the desired orbital velocity and the actual velocity of the vehicle divided by the desired orbital velocity

Goal #2: minimize the difference between the desired orbital altitude and the actual altitude of the vehicle divided by the desired orbital altitude

Goal #3: minimize the total vehicle system mass divided by a desired total vehicle system mass

As in the previous design optimizations, the velocity and altitude goals are weighted higher than the total vehicle mass goal. This is to ensure that, at a minimum, the vehicle reaches the desired orbital values.

5.3.1 Case 3: Three-Stage Solid Propellant Launch Vehicle (VAFB)

A successful design optimization of a three-stage solid propellant launch vehicle has been performed. Figure 5-10 shows a schematic of the best performer resulting from the design optimization of the three-stage solid propellant vehicle. The launch vehicle was designed to carry a 1,000 pound payload and the launch site was chosen to be Vandenberg AFB, CA. Additional mission statistics for this launch vehicle are described in Table 5-4.

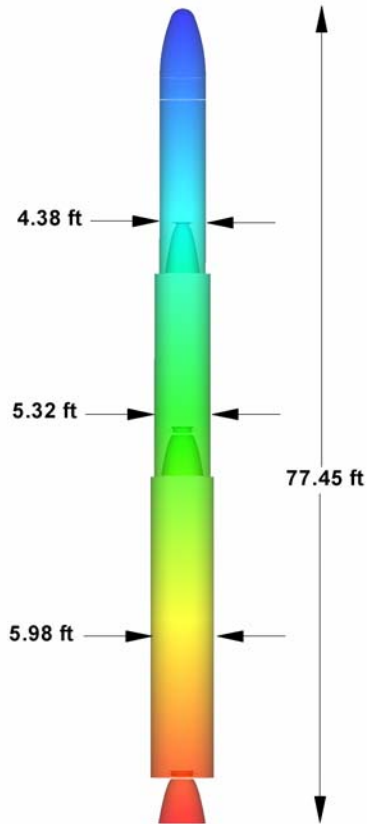


Figure 5-10. Three-Stage Solid Propellant Launch Vehicle Schematic (VAFB)

The important characteristics of the optimized three-stage solid propellant vehicle are shown in Table 5-5. The final altitude of the vehicle is within 10,000 feet of the desired orbital altitude. The final velocity is slightly above the desired orbital velocity which ensures the payload reaches orbit. Thus, the optimized vehicle meets the required orbital parameters thus reaching orbit and ensuring mission success.

The GA chose different propellants for each of the three solid propellant stages. The first stage solid propellant is polybutadiene-acrylic acid (PBAA)/ammonium perchlorate (AP)/aluminum (Al). Sutton⁶⁰ describes this type of propellant as a composite propellant that forms a heterogeneous grain. The AP is used as the crystalline

oxidizer and the PBAA is the fuel. In addition, solid aluminum (Al) powder is added to enhance combustion. The AP and Al are held together in the matrix with the PBAA as the binder. The PBAA/AP/Al propellant is one of the more common solid propellants because of its relatively high I_{sp} (260s-265s) and moderate density (0.064 lbm/in³). The second stage also uses a composite propellant with the same oxidizer and fuel as the first stage but with a different binder. The GA chooses the polysulfide/ammonium perchlorate/aluminum (PS/AP/Al) propellant for this stage. Finally, an energetic propellant that is based on the solid propellant used in the Star 37 solid rocket motor has been developed. This motor has a high I_{sp} (292.6s) for a solid propellant which makes it an attractive choice for performance reasons. Knowing that the Star 37 solid propellant is based on the hydroxyl-terminated polybutadiene (HTPB)/AP/Al propellant, the necessary data was determined and loaded into the appropriate solid propellant model. The GA chose this propellant for the third stage of the optimized vehicle.

From a mass fraction perspective, the entire vehicle as well as the individual stages, all closely match the desired value of propellant mass fraction (0.90) given by Humble et al.⁵⁰ The propellant mass fraction (f_{prop}) for the entire vehicle is 0.9072 which is as expected. For each of the three individual stages (Stage 1: 0.9139, Stage 2: 0.8882, Stage 3: 0.9241), reasonable values for the propellant mass fraction have been produced.

The first stage thrust provides the initial high thrust (331,972 lbf) required to lift the vehicle off the ground with a thrust-to-weight ratio of over 3-to-1. The Stage 2 and Stage 3 thrust values drop off but still provide the necessary force to get the payload into the desired low-Earth orbit.

Finally, the cost per launch of \$49.71 million in 2003 dollars is a moderate price for an expendable launch vehicle. It is not exceptionally cheap but it also is not prohibitively expensive. The total vehicle mass of 89,906 pounds is the reason for this particular price. This value of the total vehicle mass is an improvement over the vehicles optimized in Cases 1 and 2. However, this value is over 10,000 pounds heavier than the Minuteman III ICBM (79,432 lbm) and the Minotaur I SLV (79,800 lbm). The Minuteman III ICBM is not an orbital vehicle. This would suggest that an additional 10,000 pounds is required to enable the launch vehicle to go from sub-orbital speed (22,000 ft/s) to orbital velocity (24,550 ft/s). Additionally, the actual vehicle flight trajectory might also play a factor in attaining the desired orbital velocity. The sequence of powered flight/coast phase/orbit insertion burn has been used for existing launch vehicles to provide the final velocity boost into orbit.

Table 5-5: Summary of Three-Stage Solid Propellant Launch Vehicle Characteristics (VAFB)

Entire Vehicle		Stage 1	
Final Altitude	2,439,276 ft	Stage Length	33.05 ft
Final Velocity	24,595 ft/s	Stage Diameter	5.98 ft
Total Vehicle Mass	89,906 lbm	Stage Weight	53,550 lbm
Total Vehicle Length	77.45 ft	Initial Thrust	331,972 lbf
Total Vehicle f_{prop}	0.9072	Propellants	PBAA/AP/Al
Nosecone Length	6.61 ft	m_{prop}	48,939 lbm
Cost per Launch	\$49.71 million	m_{inert}	4,611 lbm
		f_{prop}	0.9139
		Stage 2	
		Stage Length	19.28 ft
		Stage Diameter	5.32 ft
		Stage Weight	21,351 lbm
		Initial Thrust	82,093 lbf
		Propellants	PS/AP/Al
		m_{prop}	18,965 lbm
		m_{inert}	2,386 lbm
		f_{prop}	0.8882
		Stage 3	
		Stage Length	16.50 ft
		Stage Diameter	4.38 ft
		Stage Weight	13,801 lbm
		Initial Thrust	67,192 lbf
		Propellants	Energetic Star 37
		m_{prop}	12,754 lbm
		m_{inert}	1,047 lbm
		f_{prop}	0.9241

The progress of the design optimization of this three-stage solid propellant launch vehicle is shown in Figures 5-11 thru 5-13. These three figures show how the GA progressed from one generation to the next in order to meet each of the three design optimization goals. The reason for the jagged nature of the plots is that only a small sampling of the over 200 generations was used to generate the plots. Analyzing each generation would have been a work intensive effort that would not have yielded significantly different results. The overall trend of each plot is the important information

that should be taken away. Figure 5-11 shows how the initial generations produced a launch vehicle with a final velocity of around 22,000 feet per second. As the optimization progressed, the GA was able to create vehicles that were much closer to the desired orbital velocity of 24,550 feet per second. Finally, the best performer of generation #221 produced a launch vehicle with a final velocity of 24,595 feet per second.

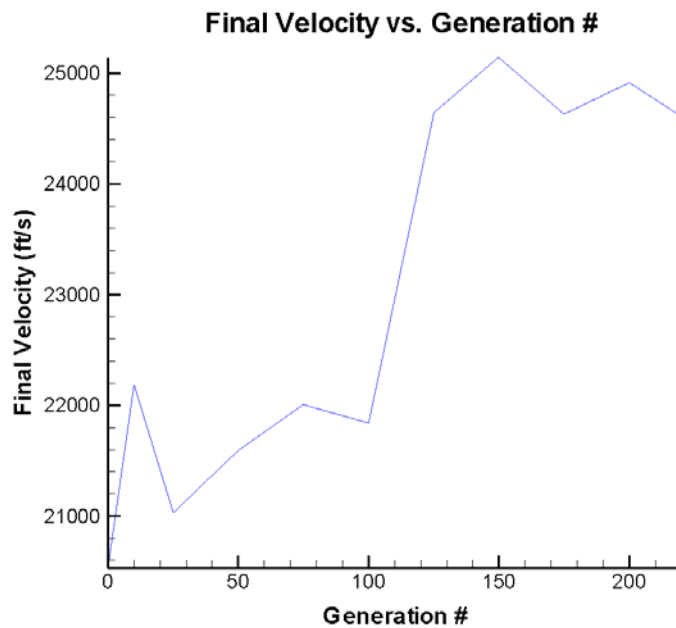


Figure 5-11. Velocity vs. Generation # for Three-Stage Solid Propellant Launch Vehicle

The trend for the final altitude, shown in Figure 5-12, was the opposite of the trend for the final velocity. Initially, the GA designed launch vehicles that had a final altitude of over 4,000,000 feet. Again, as the optimization progressed, the GA was able to meet the final velocity goal while, at the same time, reducing the final altitude to the desired value of 2,430,000 feet. The best performer for this optimization produced a final altitude of 2,439,276 feet which is a good match for the desired orbital altitude.

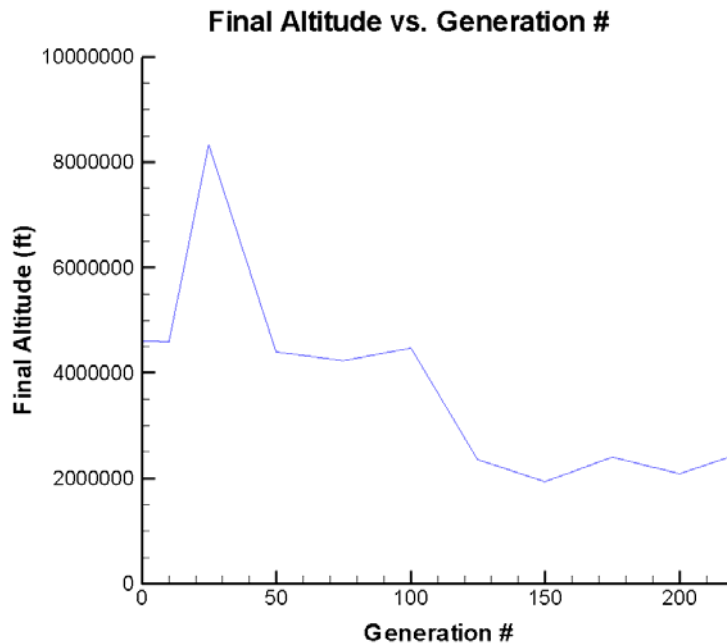


Figure 5-12. Altitude vs. Generation # for Three-Stage Solid Propellant Launch Vehicle

For the total vehicle mass, the GA was simply trying to minimize this value while still meeting the desired orbital parameters. Thus, the trend, as shown in Figure 5-13, should be for decreasing values of total vehicle mass. The optimization starts with a total vehicle mass of over 120,000 pounds and by generation #221, the mass has been reduced to 89,906 pounds. Overall, the design optimization is a success due to the GA's ability to match the desired orbital goals while minimizing the total vehicle mass.

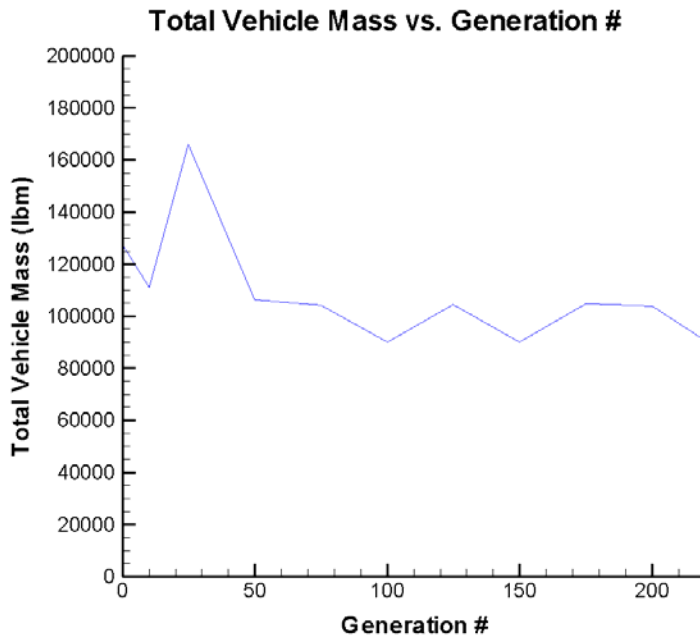


Figure 5-13. Total Vehicle Mass vs. Generation # for Three-Stage Solid Propellant Launch Vehicle

The design optimization for this three-stage solid propellant launch vehicle ran for 221 generations. This was sufficient to produce a vehicle that met the desired orbital parameters and minimized the total vehicle mass. A closer look at a few of the members of this generation provides additional insight into the results generated by the GA. Figures 5-14 thru 5-16 show the values of final velocity, final altitude and total vehicle mass for three members from generation #221. The “best” member represents the best performer of the design optimization process. The results for this best performer are summarized in Table 5-5. The member that made it through the objective function and was ranked lowest within the population was chosen as the “worst” member. Finally, the average member was a randomly chosen member with results that were between the best and worst members.

The results for the best member have been previously discussed. Both the final velocity and the final altitude of the average member are fairly close to the desired orbital parameters. The reason for this is because the goals for the orbital parameters are weighted more heavily than the total vehicle mass goal. However, the total vehicle mass of the average member is well above the total vehicle mass of the best member. This justifies why the average member is not ranked higher within the population. Finally, all the results of the worst member differ considerably from the results of the best member. While the design parameters of the worst member produce a workable launch vehicle, the design does not meet the mission requirements and, as a result, would result in mission failure.

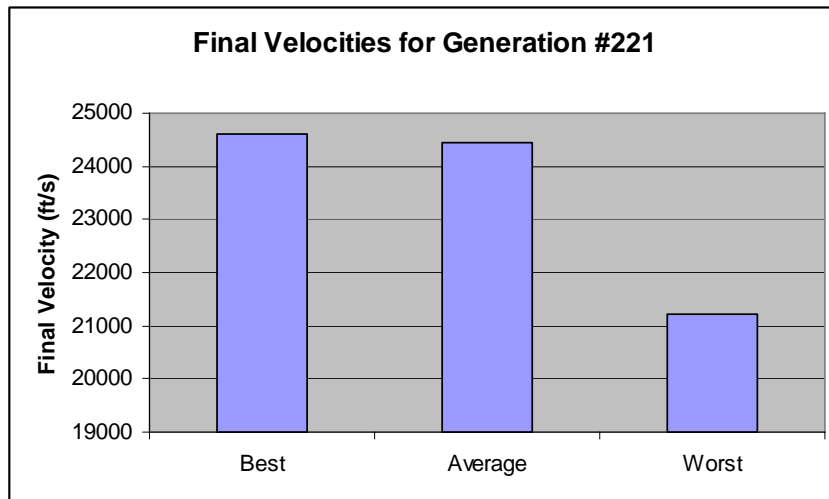


Figure 5-14. Final Velocity for Best, Worst, and Average Members of Generation #221

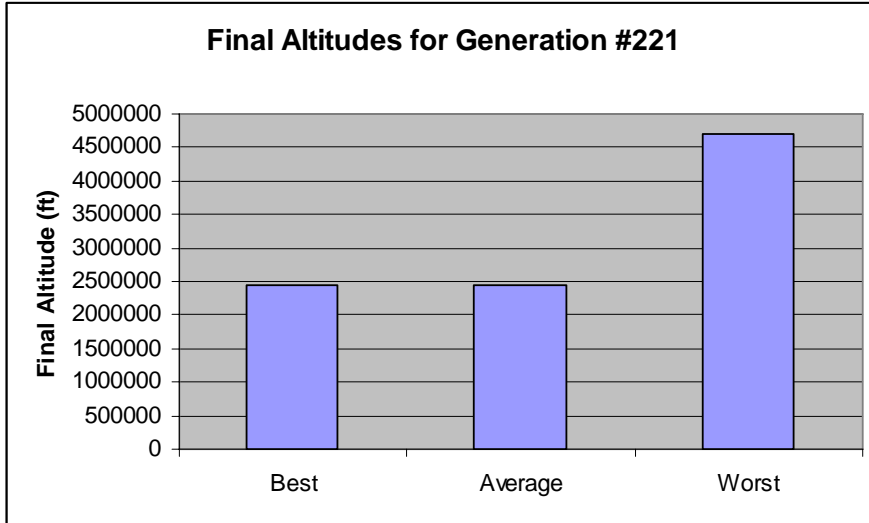


Figure 5-15. Final Altitude for Best, Worst, and Average Members of Generation #221

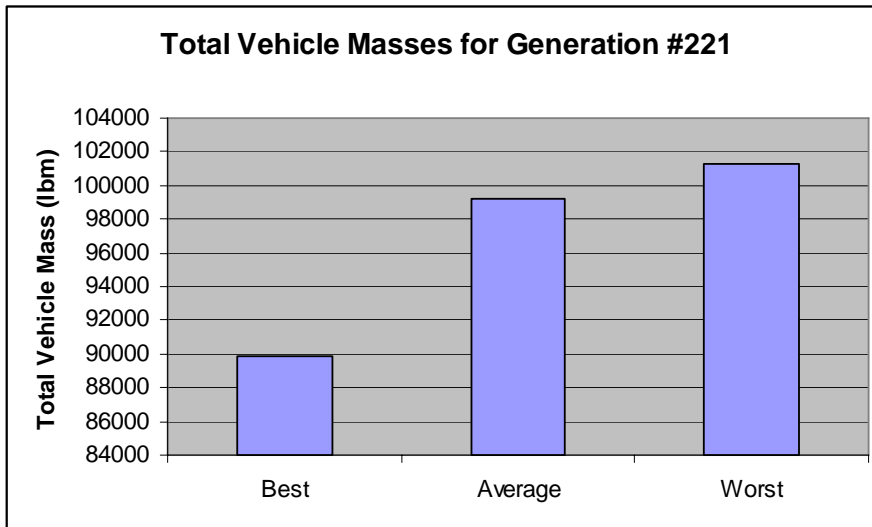


Figure 5-16. Total Vehicle Mass for Best, Worst, and Average Members of Generation #221

5.3.2 Case 4: Three-Stage Solid Propellant Launch Vehicle (CCAFS)

The same approach for the Vandenberg launch design optimization is performed for the Cape Canaveral launch. The main difference is the direction of launch and the subsequent benefit received due to the Earth's eastward rotation. Up until this point in the design optimizations, the vehicles have been analyzed using Vandenberg AFB, CA as the launch site. Typical space launches out of Vandenberg follow a polar trajectory either due North/South or slightly retrograde. For these launches, the eastward rotation of the Earth provides no initial velocity benefit. In fact, for the slightly retrograde launches, the Earth's rotation is a hindrance.

Eastward launches out of Cape Canaveral AFS, FL are popular for the initial velocity boost imparted to a launch vehicle simply because the Earth is rotating in the direction of launch. Sellers⁶¹ writes this velocity boost as given by Equation 5.1:

$$V_{Earth} = \left(0.4651 \frac{km}{s} \right) \cos(L_o) \quad (5.1)$$

where L_o is the launch site latitude. From this equation, it should be noted that the greatest velocity boost comes from an eastward launch at the equator where $L_o = 0^\circ$.

For the design optimization of space launch vehicles being launched out of Cape Canaveral AFS, FL, Equation 5.1 has been incorporated into the six-degree-of-freedom (6DOF) flight dynamics simulator model. In the end, this velocity boost should result in some improvement in total vehicle mass over a similar launch vehicle performing the same mission out of Vandenberg AFB, CA.

Figure 5-17 shows a schematic of the best performer of the design optimization of the three-stage solid propellant launch vehicle for a due East launch out of Cape Canaveral AFS, FL.

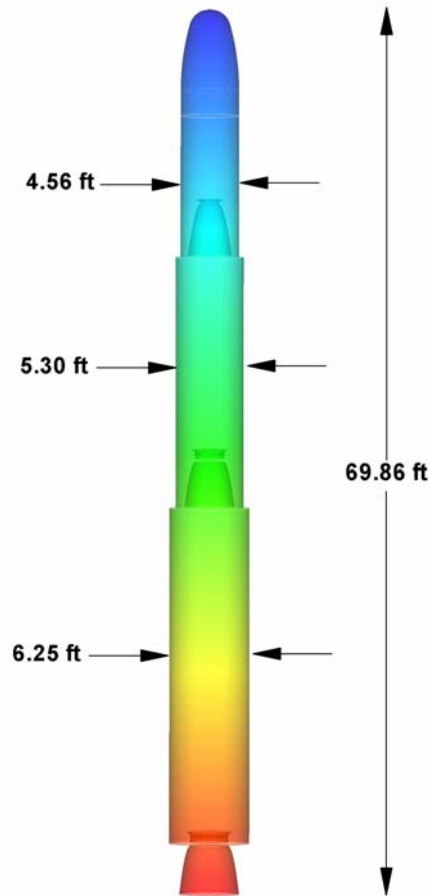


Figure 5-17. Three-Stage Solid Propellant Launch Vehicle Schematic (CCAFS)

The results of the best performer for the design optimization process involving launch out of Cape Canaveral AFS, FL are shown in Table 5-6. There is some cost (\$48.48 million vs. \$49.71 million) and mass (89,884 lbm vs. 89,906 lbm) savings for this case as compared to the previous case but overall the two vehicles are very similar. The main difference is that the GA designed this vehicle to be about seven feet shorter than the Vandenberg vehicle.

The GA also chose different propellants for Stage 1 and Stage 2 of the Cape Canaveral vehicle. For Stage 1, the polybutadiene-acrylic acid-acrylonitrile terpolymer (PBAN)/ammonium perchlorate (AP)/aluminum (Al) composite propellant was chosen. This propellant has very similar characteristics to the PBAA/AP/Al propellant combination. The hydroxyl-terminated polybutadiene (HTPB)/AP/Al propellant was chosen for the second stage and according to Sutton,⁶⁰ this propellant has better performance characteristics than the PBAN binder. The energetic Star 37 propellant was chosen again for Stage 3. The conclusion here is that the GA is looking for a propellant with high I_{sp} characteristics in order to get into orbit. The higher I_{sp} of the energetic Star 37 is the best choice for this application among all the available solid propellants.

Like the Vandenberg vehicle, this optimized vehicle has excellent values of propellant mass fraction. The overall vehicle propellant mass fraction of 0.9111 makes it a very realistic system for Earth-to-orbit missions. All three individual stages also have very good values of propellant mass fraction (Stage 1: 0.9190, Stage 2: 0.9027, Stage 3: 0.9056).

The cost per launch and total vehicle mass savings are not as dramatic as one would have liked. This is likely because the eastward launch out of Cape Canaveral does not provide as significant a boost that could result in significant mass savings.

Table 5-6: Summary of Three-Stage Solid Propellant Launch Vehicle Characteristics (CCAFS)

Entire Vehicle		Stage 1	
Final Altitude	2,448,695 ft	Stage Length	30.64 ft
Final Velocity	24,575 ft/s	Stage Diameter	6.25 ft
Total Vehicle Mass	89,884 lbm	Stage Weight	55,926 lbm
Total Vehicle Length	69.86 ft	Initial Thrust	417,563 lbf
Total Vehicle f_{prop}	0.9111	Propellants	PBAN/AP/Al
Nosecone Length	6.36 ft	m_{prop}	51,397 lbm
Cost per Launch	\$48.48 million	m_{inert}	4,530 lbm
		f_{prop}	0.9190
		Stage 2	
		Stage Length	21.99 ft
		Stage Diameter	5.30 ft
		Stage Weight	25,090 lbm
		Initial Thrust	112,301 lbf
		Propellants	HTPB/AP/Al
		m_{prop}	22,650 lbm
		m_{inert}	2,441 lbm
		f_{prop}	0.9027
		Stage 3	
		Stage Length	11.11 ft
		Stage Diameter	4.56 ft
		Stage Weight	7,658 lbm
		Initial Thrust	26,165 lbf
		Propellants	Energetic Star 37
		m_{prop}	6,935 lbm
		m_{inert}	723 lbm
		f_{prop}	0.9056

Finally, a comparison has been made for the three-stage solid propellant launch vehicles generated in Cases 1 thru 4 of this study. The improvements in total vehicle mass for these different cases are shown in Figure 5-18. This figure shows that when choosing to launch a 1,000 pound payload into a low-Earth orbit, the preliminary design of a possible launch vehicle can and should go through a number of iterations to find the optimum solution. The total vehicle mass improves from Case 1 to Case 4 as a step-by-step process is employed to work towards the best performer. For Case 1, the goal was

simply to reach the desired orbit. The two runs for Case 2 added the goal of minimizing the total vehicle mass while putting two constraints on the GA. The first run ignored vehicles with velocity and altitude performance that were not above the desired orbital values, The second run relaxed this restriction and allowed the GA to keep off-design members even though they didn't meet the desired parameters Finally, Cases 3 and 4 used the models from the validation efforts to optimize the three-stage solid propellant launch vehicle. The total vehicle mass of the Minuteman III ICBM is included for the sake of comparison. With a multi-variable design problem like a space launch vehicle, the odds of finding the single "best" solution of all the possible solutions are low. Thus, the focus here has been on improving the launch vehicle designs rather than on finding a single optimum solution.

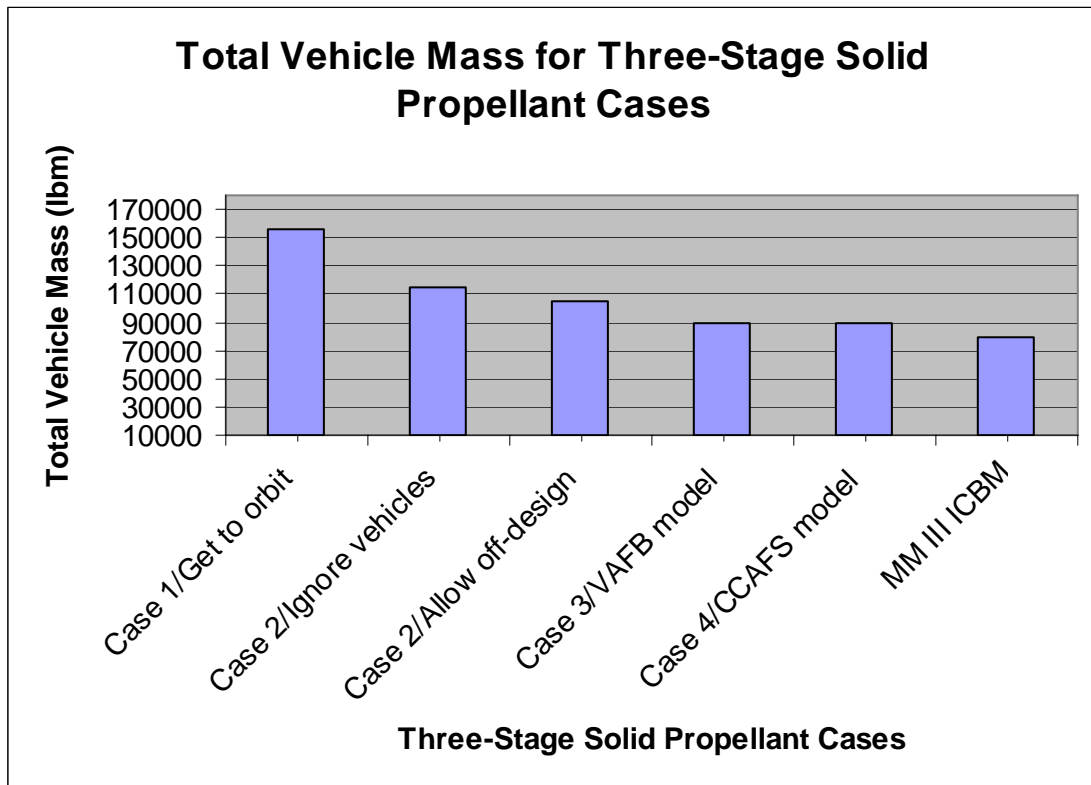


Figure 5-18. Mass Improvements for Three-Stage Solid Propellant Vehicles

5.3.3 Case 5: Four-Stage Solid Propellant Launch Vehicle (VAFB)

The design optimization for the four-stage solid propellant launch vehicles is quite similar to the three-stage solid propellant vehicles (Cases 1 thru 4). The launch sites and desired orbital velocity and orbital altitude values are described in Table 5-4. However, additional changes have been made in an attempt to mirror an existing, real world launch vehicle. The Minotaur I Space Launch Vehicle (SLV) is a four-stage solid propellant rocket operated by Orbital Sciences Corporation. The first two stages of the Minotaur I SLV consist of decommissioned Minuteman II ICBMs. The third and fourth stages employ the second and third stages of Orbital Sciences Corporation's Pegasus launch vehicle.

The four-stage solid propellant launch vehicle design optimization attempts to either match or improve upon the Minotaur I SLV design. A few modifications to the design parameters are incorporated to allow for the possibility of a launch vehicle to be generated by the GA that is similar to the Minotaur I SLV. In no way do these modifications ensure that the Minotaur I SLV design is chosen. It is left up to the GA and the objective function to choose the specific design parameters. Also, the four-stage solid propellant launch vehicle has some characteristics not found in the three-stage solid launch vehicle. These differences are listed below:

- the payload mass is changed to 738 lbm for Vandenberg launch
- use of coast period after Stage 3 burnout
- Stage 4 is located inside the nosecone fairing

Figure 5-19 shows a schematic of the four-stage solid propellant launch vehicles analyzed in the current study. The launch site of all three vehicles was chosen to be

Vandenberg AFB, CA. The left image is the Minotaur I SLV in flight. The middle schematic is the vehicle produced in the model validation process. The optimized vehicle is shown on the right. A comparison summary of these four-stage solid propellant launch vehicles is shown in Table 5-7. The results of the design optimization of this vehicle are summarized in Table 5-8. These results show significant improvement over the Minotaur I SLV.

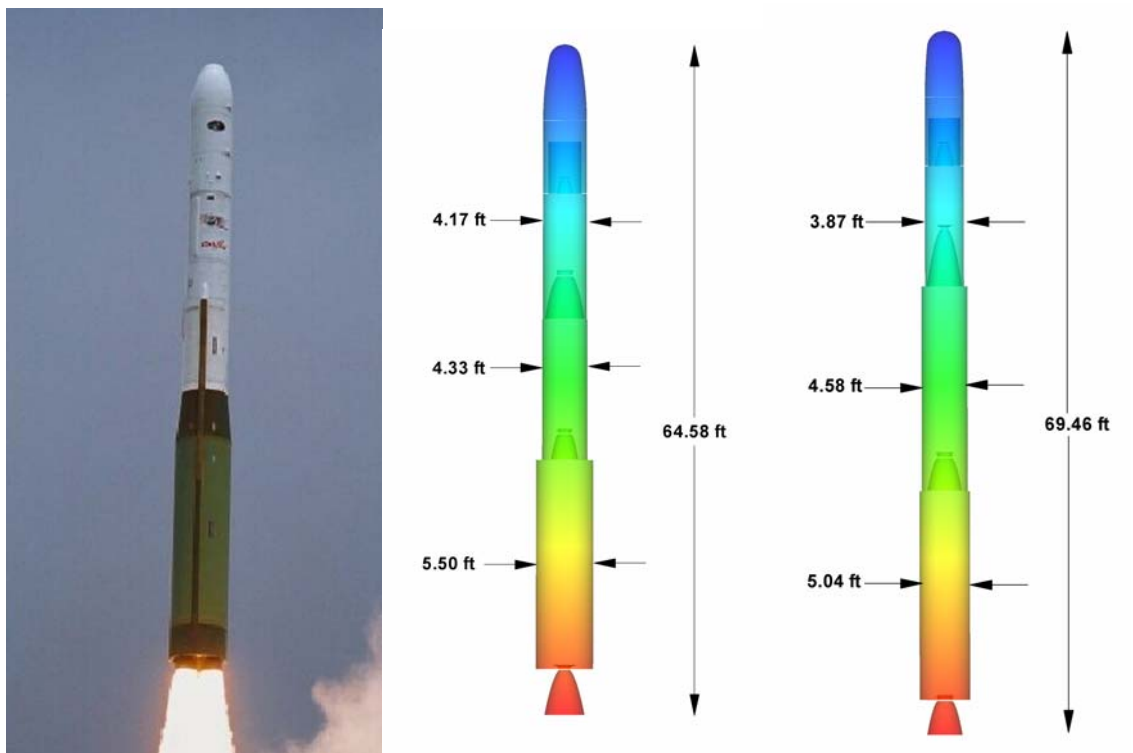


Figure 5-19. Four-Stage Solid Propellant Launch Vehicles Schematic (VAFB)
(Ref. 55: <http://www.orbital.com/SpaceLaunch/Minotaur/index.html>)

Table 5-7: Four-Stage Solid Propellant Launch Vehicles Comparison

	<u>Minotaur I SLV</u>	<u>Validation Model</u>	<u>Optimized Vehicle</u>
Payload	738 lbm	738 lbm	738 lbm
Total Vehicle Weight	79,800 lbm	78,090 lbm	60,690 lbm
Total Vehicle Length	63.02 ft	64.58 ft	69.46 ft
Total Vehicle f_{prop}	0.8998	0.9185	0.8976
Final Altitude	2,430,000 ft	2,425,999 ft	2,430,505 ft
Final Velocity	25,004 ft/s	25,002 ft/s	25,036 ft/s
Cost per Launch	\$52.05 million	\$51.95 million	\$46.07 million
Advertised Cost per Launch	\$20.00 million		

The best performer from the design optimization of the four-stage solid propellant launch vehicle weighs 19,000 pounds less than the Minotaur I SLV. An important note concerning the mass properties model should be mentioned again. As was discussed in the model validation section, the mass properties model underestimates the inert mass values. Thus, the reduction in total vehicle mass is most likely not as high as described here. Future work on the mass properties model will address this issue. With that in mind, the design optimization of the four-stage solid propellant launch vehicle has still resulted in a fairly substantial mass savings.

The mass savings comes primarily from the difference in the mass of the Stage 1 propellants. The Stage 1 propellant mass in the optimized vehicle is 30,017 pounds versus 45,371 pounds for the Minotaur I SLV. This reduction in propellant mass was probably also aided by the choice of propellants for the individual stages. The GA chose fairly energetic composite and double-based propellants that possess a higher I_{sp} than some of the more common solid propellants (260s – 265s). The Stage 1 and Stage 2 propellants were chosen to be HTPB/AP/Al which has an I_{sp} , according to Sutton⁶⁰, of around 267s. The energetic Star 37 propellant was chosen for Stage 3. This propellant is

an HTPB/AP/Al derivative with an I_{sp} of 292.6s. Finally, an energetic double-based propellant, DB/AP-HMX/Al, was chosen for Stage 4 of the vehicle. From Sutton,⁶⁰ this propellant uses HMX mixed into the propellant thus reducing the amount of AP. The HMX is a crystalline nitramine or explosive that provides higher performance for this type of solid propellant ($I_{sp}=275s$). The conclusion regarding these propellants is that the higher I_{sp} provides higher performance for the vehicle and thus reduces the amount of propellant required to achieve orbit.

The optimized vehicle also provides about a \$6 million savings in cost per launch over the Minotaur I SLV. Using the *TRANSCost 7.1* cost model for the mass values of the Minotaur I SLV resulted in a cost per launch of \$52.05 million. The optimized four-stage solid propellant launch vehicle yielded a cost per launch of \$46.07 million. It should be noted that the advertised cost per launch of the Minotaur I SLV is \$20 million. This is attributed to the use of decommissioned Minuteman II ICBMs for the first two stages of the Minotaur I SLV.

The performance characteristics for the optimized vehicle also closely match the desired orbital altitude and orbital velocity parameters. The total vehicle propellant mass fraction of 0.8976 is right in line for the mass fraction of a solid propellant launch vehicle. The propellant mass fractions of the individual stages also produce excellent results (Stage 1: 0.9137, Stage 2: 0.9000, Stage 3: 0.8250, Stage 4: 0.8448).

There is a difference in the coast times for the orbit insertion burn of the two vehicles. After Stage 3 burnout, the Minotaur I SLV uses a coast time of 400s before Stage 4 ignites to put the payload into its final orbit. The GA chose a coast time of 55s between Stage 3 burnout and Stage 4 ignition. The issue of coast time will be addressed

in future work associated with the recommended improvements of the 6DOF flight dynamics simulator.

Table 5-8: Summary of Four-Stage Solid Propellant Launch Vehicle Characteristics (VAFB)

Entire Vehicle		Stage 1	
Final Altitude	2,430,505 ft	Stage Length	24.10 ft
Final Velocity	25,036 ft/s	Stage Diameter	5.04 ft
Total Vehicle Mass	60,690 lbm	Stage Weight	32,852 lbm
Total Vehicle Length	69.46 ft	Initial Thrust	239,820 lbf
Total Vehicle f_{prop}	0.8976	Propellants	HTPB/AP/Al
Nosecone Length	6.54 ft	m_{prop}	30,017 lbm
Cost per Launch	\$46.07 million	m_{inert}	2,835 lbm
		f_{prop}	0.9137
		Stage 2	
		Stage Length	20.21 ft
		Stage Diameter	4.58 ft
		Stage Weight	21,609 lbm
		Initial Thrust	98,829 lbf
		Propellants	HTPB/AP/Al
		m_{prop}	19,448 lbm
		m_{inert}	2,161 lbm
		f_{prop}	0.9000
		Stage 3	
		Stage Length	11.84 ft
		Stage Diameter	3.87 ft
		Stage Weight	3,743 lbm
		Initial Thrust	35,065 lbf
		Propellants	Energetic Star 37
		m_{prop}	3,088 lbm
		m_{inert}	655 lbm
		f_{prop}	0.8250
		Stage 4	
		Stage Length	4.76 ft
		Stage Diameter	3.21 ft
		Stage Weight	1,490 lbm
		Initial Thrust	18,459 lbf
		Propellants	DB/AP-HMX/Al
		m_{prop}	1,259 lbm
		m_{inert}	231 lbm
		f_{prop}	0.8448

5.3.4 Case 6: Four-Stage Solid Propellant Launch Vehicle (CCAFS)

The approach for the design optimization of the four-stage solid propellant launch vehicle with launch out of Cape Canaveral AFS, FL was slightly different than the Vandenberg launch. Since the eastward launch out of Cape Canaveral provides a slight velocity boost, the payload for this case has been increased to 1,000 pounds. The vehicle should have a higher payload carrying capacity due to the Earth's eastward rotation. Also, since the target orbit is a typical low-Earth orbit, the desired orbital velocity (24,550 ft/s) corresponds to the desired orbital altitude (2,430,000 ft). A schematic showing the optimized vehicle for this case is shown in Figure 5-20. The results of the design optimization of this vehicle are summarized in Table 5-9.

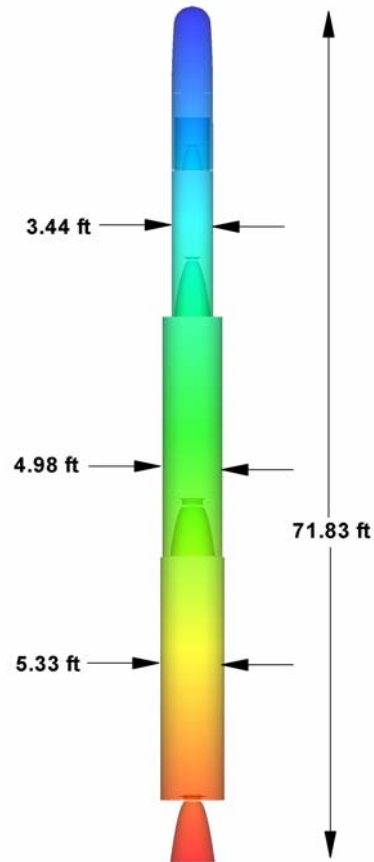


Figure 5-20. Four-Stage Solid Propellant Launch Vehicle Schematic (CCAFS)

Another successful design optimization has been obtained for the four-stage solid propellant launch vehicle. The total vehicle mass (72,080 lbm) comes in at 7,700 pounds less than the Minotaur I SLV (79,800 lbm). The same issue with the mass properties model is applicable here as well. Thus, even with an increase in payload mass, the design optimization still improves on the total vehicle mass characteristics of the Minotaur I SLV. As in the previous case, the GA chose more energetic propellants for the Stage 3 and Stage 4. The DB/AP-HMX/Al propellant was chosen for Stage 3 and the HTPB/AP/Al was chosen for Stage 4.

The performance characteristics of the optimized vehicle essentially match exactly the desired orbital altitude and the desired orbital velocity. As in the previous case, the propellant mass fractions are all appropriate values for a solid propellant launch vehicle. The propellant mass fraction of the total vehicle is 0.8894 which is only slightly lower than the ideal 0.90 value.

The cost per launch (\$48.98 million) for the optimized vehicle is comparable for a typical expendable launch vehicle. As with the total vehicle mass, the cost per launch for the optimized vehicle is lower than the cost per launch of the Minotaur I SLV (\$52.05 million). However, the cost per launch of the optimized vehicle does not approach the advertised cost per launch of the Minotaur I SLV which is \$20 million per launch.

The GA chose a very different coast time for this vehicle than the coast time of the Vandenberg launch vehicle. The coast time for the Cape Canaveral optimized vehicle is 301s which is much closer to the 400s of the Minotaur I SLV. This would seem to indicate that the use of Stage 4 for the orbit insertion burn requires additional analysis. Specifically, the operation of the 6DOF flight dynamics simulator and how it takes the coast time into account needs to be further investigated. The results of the design optimization for this vehicle provide an attractive four-stage solid propellant launch vehicle that meets the mission requirements.

Table 5-9: Summary of Four-Stage Solid Propellant Launch Vehicle Characteristics (CCAFS)

Entire Vehicle		Stage 1	
Final Altitude	2,432,143 ft	Stage Length	25.68 ft
Final Velocity	24,592 ft/s	Stage Diameter	5.33 ft
Total Vehicle Mass	72,0780 lbm	Stage Weight	38,958 lbm
Total Vehicle Length	71.83 ft	Initial Thrust	358,962 lbf
Total Vehicle f_{prop}	0.8894	Propellants	PBAA/AP/Al
Nosecone Length	7.27 ft	m_{prop}	34,500 lbm
Cost per Launch	\$48.48 million	m_{inert}	4,457 lbm
		f_{prop}	0.8856
		Stage 2	
		Stage Length	20.13 ft
		Stage Diameter	4.98 ft
		Stage Weight	26,422 lbm
		Initial Thrust	176,198 lbf
		Propellants	PBAN/AP/Al
		m_{prop}	24,130 lbm
		m_{inert}	2,292 lbm
		f_{prop}	0.9133
		Stage 3	
		Stage Length	12.29 ft
		Stage Diameter	3.44 ft
		Stage Weight	4,174 lbm
		Initial Thrust	129,442 lbf
		Propellants	DB/AP-HMX/Al
		m_{prop}	3,515 lbm
		m_{inert}	659 lbm
		f_{prop}	0.8420
		Stage 4	
		Stage Length	4.46 ft
		Stage Diameter	2.91 ft
		Stage Weight	1,279 lbm
		Initial Thrust	28,477 lbf
		Propellants	HTPB/AP/Al
		m_{prop}	1,077 lbm
		m_{inert}	202.50 lbm
		f_{prop}	0.8417

5.3.5 Conclusions: Solid Propellant Launch Vehicle Design Optimizations

Four successful design optimizations have been performed for three and four-stage solid propellant launch vehicles. All four vehicles meet the mission requirements and the optimization process generates improvements in total vehicle mass and cost per launch. In addition, the propellant mass fractions are consistent with the historical data for solid propellant vehicles. This fact further strengthens the argument that the preliminary designs are realistic and could be developed into real world systems.

The use of energetic solid propellants seems to be the key to meeting the performance parameters while at the same time minimizing total vehicle mass. Throughout the design optimizations, the GA consistently chose the more energetic propellants rather than propellants with lower density but less desirable I_{sp} .

5.4 Liquid Propellant Vehicles

The results for the design optimization of two and three-stage liquid propellant launch vehicles have also been investigated. Like the solid propellant cases, the liquid propellant launch vehicles have been analyzed for launch out of Vandenberg AFB, CA and Cape Canaveral AFS, FL. Model validation was performed for the two-stage liquid propellant case, so the design optimization of these vehicles was an attempt to improve on the real world example. General comments were made on the results for the three-stage liquid propellant cases and how those results compared to real world examples. However, the model validation applies to both types of liquid propellant launch vehicles.

The mission statistics for the liquid propellant launch vehicles that have been optimized are shown in Table 5-10. The payload, desired orbital altitude and desired orbital velocity for the three-stage vehicles were chosen as typical values for responsive

space-type missions. Also, these values allow the three-stage vehicles to be compared to other types of optimized launch vehicles currently being investigated in this study. For the two-stage liquid propellant cases, initially, the values of payload, desired orbital altitude and desired orbital velocity were chosen to mirror those same values used in the model validation. The two-stage liquid propellant launch vehicle model was validated using the Titan II SLV. However, during the design optimization process, it became necessary to adjust some of these values. Three different design optimization runs have been performed for both of the two-stage liquid propellant launch vehicle cases. The desired orbital altitude and the desired orbital velocity were the same values as those used to validate the Titan II SLV. However, the issue of attaining the desired orbit forced the payload mass to be changed from 7,000 pounds to 1,000 pounds.

The three goals for the design optimization of these vehicles were the same as those for the solid propellant launch vehicle cases. The first two goals were to minimize the differences between the desired orbital parameters and the actual vehicle performance parameters. The third goal was a direct minimization of the total vehicle mass. Using the *TRANSCost 7.1* cost model allowed for the minimization of the cost per launch since the total vehicle mass has been minimized. However, the results for these liquid propellant cases show that the decision to minimize the total vehicle mass rather than the cost per launch itself may have been an incorrect one.

Table 5-10: Liquid Propellant Launch Vehicles Mission Statistics

	<u>Three-Stage Liquid</u>	<u>Three-Stage Liquid</u>	<u>Two-Stage Liquid</u>	<u>Two-Stage Liquid</u>
Payload	1,000 lbm	1,000 lbm	1,000 lbm	1,000 lbm
Launch Site	VAFB	CCAFS	VAFB	CCAFS
Launch Direction	Due North 0° Azimuth	Due East 90° Azimuth	Due North 0° Azimuth	Due East 90° Azimuth
Orbit Type	i=90° polar orbit	i=28.4° prograde orbit	i=90° polar orbit	i=28.4° prograde orbit
Desired Orbital Altitude	2,430,000 ft	2,430,000 ft	656,000 ft	656,000 ft
Desired Orbital Velocity	24,550 ft/s	24,550 ft/s	25,532 ft/s	25,532 ft/s

5.4.1 Case 7: Three-Stage Liquid Propellant Launch Vehicle (VAFB)

The results for the design optimization of the three-stage liquid propellant launch vehicle are presented here. Figure 5-21 shows a schematic of the three-stage liquid propellant vehicle with Vandenberg AFB, CA as the launch site. The mission statistics are described in Table 5-10. From Figure 5-21, it can be seen that Stage 1 is the largest of the three stages while the other two stages are significantly smaller. The fin geometry has been pre-determined for aerodynamic stability purposes.

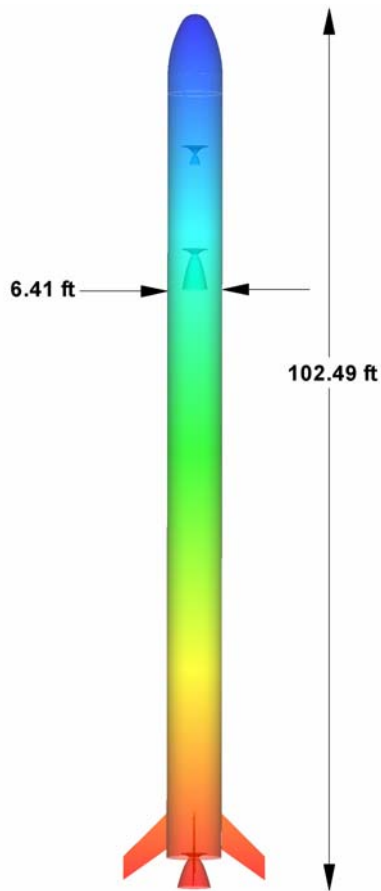


Figure 5-21. Three-Stage Liquid Propellant Launch Vehicle Schematic (VAFB)

The results of the design optimization for the three-stage liquid propellant rocket are shown in Table 5-11. In terms of total vehicle mass and cost per launch, this rocket is much heavier and more expensive than the three-stage solid propellant vehicle launched out of Vandenberg. The additional weight of engine structure, propellant tanks and separate fuel and oxidizer are just a few of the reasons for this difference. Liquid propellant launch vehicles are also known to be more expensive to design and build and this is reflected in the results for the cost per launch. Yet, \$100.11 million is a relatively moderate cost for a liquid propellant vehicle. For the sake of comparison, a current,

operational three-stage liquid propellant launch vehicle, the Zenit-3SL, has an advertised cost per launch of \$90 million.⁶²

The choices of liquid propellants available for the design optimization have been limited to accommodate the calculations in the cost model. The only option for the oxidizer is liquid oxygen (LOX) and the options for fuels are restricted to storable fuel types (Hydrazine, RP-1, etc.). Liquid hydrogen (LH2) is not an option because it requires special consideration in the cost model. The *TRANSCost 7.1* cost model employs separate development and recurring Cost Estimating Relationships (CERs) for launch vehicles using LH2 as the fuel. These CERs result in much higher development and recurring costs for LH2 fueled vehicles. Since one of the goals of this study is to minimize vehicle cost per launch, the choice has been made not to use LH2 as an option. Of course, the combination of LOX/LH2 provides close to the highest I_{sp} for all liquid fueled systems. Future design optimizations should look at using only LOX/LH2 as the launch vehicle's propellants. Then, a comparison of the resulting total vehicle mass and cost per launch values for the best performers can be made with the results of other types of liquid propellants.

From the results in Table 5-11, the GA chose LOX/Hydrazine as the oxidizer/fuel combination of all three stages for the optimized vehicle. The choice of LOX/Hydrazine in this case represents the propellant combination with the highest sea-level I_{sp} (313.0s) and thus makes sense for the design optimization process for this three-stage liquid propellant launch vehicle.

In addition, the performance characteristics of the optimized vehicle (final altitude and final velocity) closely match the desired orbital values. As a result, this launch vehicle performs well in launching the required payload to its intended low-Earth orbit.

Table 5-11: Summary of Three-Stage Liquid Propellant Launch Vehicle Characteristics (VAFB)

Entire Vehicle		Stage 1	
Final Altitude	2,545,061 ft	Stage Length	70.26 ft
Final Velocity	24,732 ft/s	Stage Diameter	6.41 ft
Total Vehicle Mass	130,136 lbm	Stage Weight	119,267 lbm
Total Vehicle Length	102.49 ft	Initial Thrust	387,903 lbf
Total Vehicle f_{inert}	0.1094	Propellants	LOX/Hydrazine
Nosecone Length	7.31 ft	Stage 2	
Cost per Launch	\$100.11 million	Stage Length	14.63 ft
		Stage Diameter	6.41 ft
		Stage Weight	6,358 lbm
		Initial Thrust	35,207lbf
		Propellants	LOX/Hydrazine
		Stage 3	
		Stage Length	8.29 ft
		Stage Diameter	6.41 ft
		Stage Weight	2,310 lbm
		Initial Thrust	7,125 lbf
		Propellants	LOX/Hydrazine

5.4.2 Case 8: Three-Stage Liquid Propellant Launch Vehicle (CCAFS)

Again, similar to the three-stage solid propellant cases, a design optimization of a three-stage liquid propellant launch vehicle has been performed with launch out of Cape Canaveral AFS, FL. The mission statistics for this launch vehicle are described in Table 5-10. Launching eastward out of Cape Canaveral provides an initial velocity boost that, in theory, should produce a lower mass vehicle than the Vandenberg launch. Figure 5-22 shows a schematic of the best performer from the design optimization of this three-stage liquid propellant launch vehicle. The large size of the 1st stage is again evident with smaller 2nd and 3rd stages.

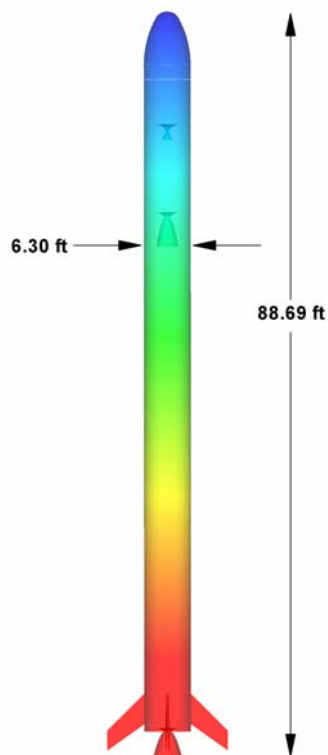


Figure 5-22. Three-Stage Liquid Propellant Launch Vehicle Schematic (CCAFS)

The results for the design optimization of the three-stage liquid propellant launch vehicle are shown in Table 5-12. The benefits of launching out of Cape Canaveral AFS, FL are apparent. The best performer weighs almost 26,000 pounds less than the Vandenberg vehicle. The cost per launch is also significantly less (\$93.68 million vs. \$100.11 million) than the Vandenberg vehicle. This brings the cost per launch of this vehicle more in line with existing liquid propellant launch vehicles.

Like the Vandenberg vehicle, the GA has chosen LOX/Hydrazine as the propellants for all three stages. These propellants provide the best performance and thus are the logical choice to aid in minimizing the mass and subsequently the cost of the vehicle. Geometrically, this vehicle has essentially the same body diameter as the

Vandenberg vehicle. However, the mass savings is a result mainly of a reduction in the length of the rocket. The Cape Canaveral vehicle is only 88.69 feet long whereas the Vandenberg vehicle is 102.49 feet long. This difference in length comes about due to the differences in the Stage 1 length of both vehicles.

Also, like the Vandenberg vehicle, the performance characteristics of this optimized vehicle match well the desired orbital parameters. This three-stage liquid propellant launch vehicle would be good choice for further development of the design into a real world system.

Table 5-12: Summary of Three-Stage Liquid Propellant Launch Vehicle Characteristics (CCAFS)

Entire Vehicle		Stage 1	
Final Altitude	2,433,952 ft	Stage Length	57.17 ft
Final Velocity	24,604 ft/s	Stage Diameter	6.30 ft
Total Vehicle Mass	104,354 lbm	Stage Weight	91,702 lbm
Total Vehicle Length	88.69 ft	Initial Thrust	321,273 lbf
Total Vehicle f_{inert}	0.1178	Propellants	LOX/Hydrazine
Nosecone Length	6.55 ft	Stage 2	
Cost per Launch	\$93.68 million	Stage Length	14.91 ft
		Stage Diameter	6.30 ft
		Stage Weight	8,256 lbm
		Initial Thrust	35,537 lbf
		Propellants	LOX/Hydrazine
		Stage 3	
		Stage Length	8.06 ft
		Stage Diameter	6.30 ft
		Stage Weight	2,249 lbm
		Initial Thrust	8,567 lbf
		Propellants	LOX/Hydrazine

5.4.3 Case 9: Two-Stage Liquid Propellant Launch Vehicle (VAFB)

The results of the design optimization process of a two-stage liquid propellant launch vehicle launched out of Vandenberg AFB, CA are presented here. Two distinct design optimization runs have been performed with changes in each one due to vehicle

performance. A schematic of the resulting optimized launch vehicles from these two runs is shown in Figure 5-23. The overall trend seen in these runs was the challenge of meeting the desired orbital altitude and orbital velocity requirements. A summary of the two runs is shown in Table 5-13. The results from Run #2, shown in Table 5-14, provided the best performing vehicle and produced the lowest total mass vehicle.

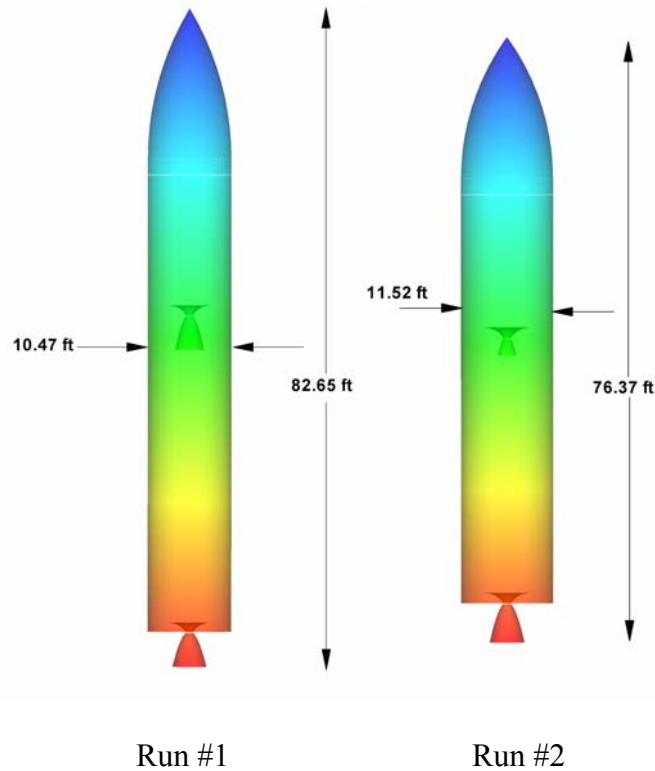


Figure 5-23. Two-Stage Liquid Propellant Launch Vehicles Schematic (VAFB)

Table 5-13: Summary of Two-Stage Liquid Propellant Launch Vehicle Runs (VAFB)

	Run #1	Run #2
Payload	7,000 lbm	1,000 lbm
Desired Altitude	656,000 ft	656,000 ft
Actual Altitude	653,691 ft	652,269 ft
Desired Velocity	25,532 ft/s	25,532 ft/s
Actual Velocity	22,667 ft/s	25,537 ft/s
Total Vehicle Mass	172,989 lbm	159,432 lbm
Cost per Launch	\$87.41 million	\$85.96 million

An initial design optimization that employed variable first and second stage diameters for the launch vehicle was performed. This optimization was an attempt to improve on the Titan II SLV that was used in the validation of the liquid propellant model. The run was very successful at improving on the vehicle mass of the Titan II SLV with the resulting vehicle having a mass (187,409 lbm) substantially lower than that of the Titan II SLV (339,000 lbm). However, while the optimized vehicle was able to reach the desired orbital altitude, the final velocity (23,145 ft/s) was less than the desired orbital velocity (25,532 ft/s). This would make it difficult for the payload to remain in its proper orbit and thus runs the risk of mission failure.

For the next design optimization (Run #1), the decision was made to eliminate the variable diameter aspect of the vehicle and employ a constant diameter configuration. This produced a more streamlined vehicle and reduced the total vehicle mass. Unfortunately, both the final altitude and final velocity for the vehicle were much lower than the desired orbital values. The constant diameter helped reduce the drag but it forced the second stage diameter to be the same as the first stage diameter. The use of more energetic liquid propellants is one possibility that may help solve this particular problem. The use of LOX/Kerosene in the first stage and LOX/Hydrazine in the second stage does not provide the highest I_{sp} for liquid propellants. Allowing the GA to use LOX/LH2 in the future would help improve the performance.

Since only storable liquid propellants were used in order to avoid the higher costs associated with using LH2, the decision was made to reduce the payload mass for the final design optimization run (Run #2) presented here. The vehicle model has already improved upon the design of the Titan II SLV even though the performance values were

not ideal. Using the value of 1,000 pounds for the payload mass allows the two-stage liquid propellant launch vehicle to be compared to other types of vehicles that have been optimized in this study. The optimized vehicle for this final run continued the trend of reducing the total vehicle length while increasing the vehicle diameter. This resulted in the performance parameters producing a good match with the desired performance values.

One other interesting note, both vehicles have a cost per launch of around \$85 million in 2003 dollars. The reason for this is that the inert mass of each vehicle is slightly different. The vehicle from Run #2 has the lowest inert mass of the two vehicles. The *TRANSCost 7.1* cost model does not use the propellant mass in the development and recurring cost models. The cost of the propellants would be considered in the ground and flight operations part of the cost model which was not considered for this study.

Overall, the design optimization of a two-stage liquid propellant launch vehicle has been successful. The results in Table 5-14 show that the optimized vehicle meets the mission requirements while significantly reducing total vehicle mass. The inert mass fractions of the total vehicle and the individual stages fall within the range of values expressed by Humble et al.⁵⁰ In terms of cost per launch, the optimized vehicle is more expensive than a solid propellant launch vehicle.

Table 5-14: Summary of Two-Stage Liquid Propellant Launch Vehicle Characteristics (VAFB-Run #2)

Entire Vehicle		Stage 1	
Final Altitude	652,267 ft	Stage Length	36.29 ft
Final Velocity	25,537 ft/s	Stage Diameter	11.52 ft
Total Vehicle Mass	159,432 lbm	Stage Weight	121,405 lbm
Total Vehicle Length	76.37 ft	Initial Thrust	245,399 lbf
Total Vehicle f_{inert}	0.1051	Propellants	LOX/Kerosene
Nosecone Length	17.84 ft	m_{prop}	112,993 lbm
Cost per Launch	\$85.96 million	m_{inert}	8,412 lbm
		f_{inert}	0.0693
		Stage 2	
		Stage Length	20.24 ft
		Stage Diameter	11.52 ft
		Stage Weight	32,912 lbm
		Initial Thrust	54,574 lbf
		Propellants	LOX/Ammonia
		m_{prop}	28,783 lbm
		m_{inert}	4,129 lbm
		f_{inert}	0.1255

5.4.4 Case 10: Two-Stage Liquid Propellant Launch Vehicle (CCAFS)

The design optimization of two-stage liquid propellant launch vehicles launched out of Cape Canaveral AFS, FL followed the same approach as the previously described Vandenberg case. Again, two distinct optimization runs have been performed with minor differences between each one. A schematic of the resulting best performers from these two runs is shown in Figure 5-24. With the eastward launch and accompanying velocity boost, there was some savings in total vehicle mass. However, the overall trend seen in these two runs was still the challenge of meeting the desired orbital altitude and orbital velocity requirements. A summary of the two runs is shown in Table 5-15. The results from Run #2, shown in Table 5-16, provided the best performing vehicle and produced the lowest total mass vehicle.

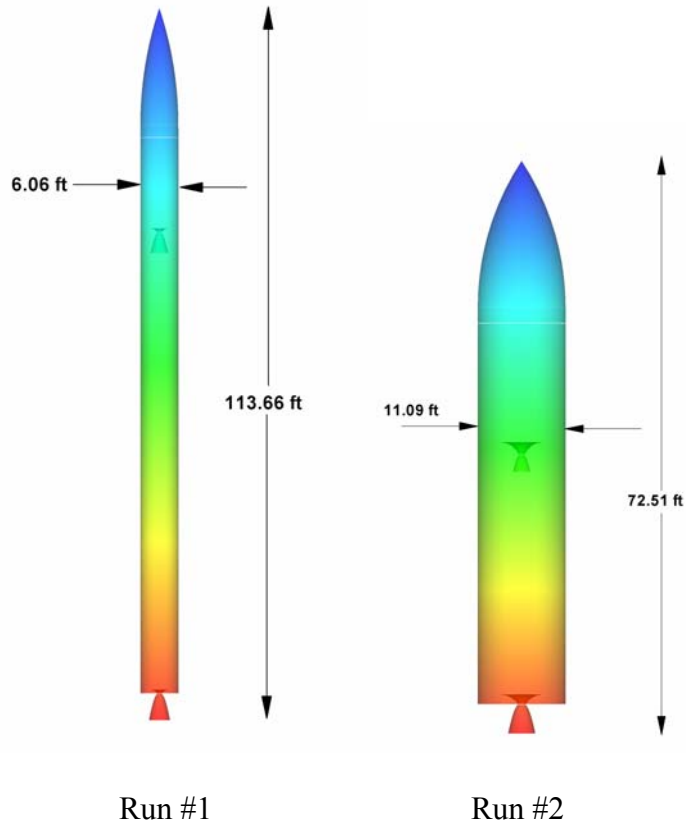


Figure 5-24. Two-Stage Liquid Propellant Launch Vehicles Schematic (CCAFS)

Table 5-15: Summary of Two-Stage Liquid Propellant Launch Vehicle Runs (CCAFS)

	Run #1	Run #2
Payload	7,000 lbm	1,000 lbm
Desired Altitude	656,000 ft	656,000 ft
Actual Altitude	622,405 ft	660,170 ft
Desired Velocity	25,532 ft/s	25,532 ft/s
Actual Velocity	25,294 ft/s	25,531 ft/s
Total Vehicle Mass	141,046 lbm	135,121 lbm
Cost per Launch	\$79.53 million	\$79.04 million

As with the previous case, the design conditions have been changed in order to incorporate a constant diameter launch vehicle. This change for Run #1 resulted in further reduction in the total vehicle mass but the performance values for the final altitude

(622,405 ft) and the final velocity (25,294 ft/s) were reduced. It is interesting that for this optimized vehicle, the GA chose to increase the overall length of the vehicle.

Finally, the second design optimization (Run #2) produced an optimized vehicle that matched well the desired altitude and velocity parameters while reducing the total vehicle mass further. This vehicle was also the least expensive (\$79.04 million) of all the two-stage liquid propellant launch vehicles being analyzed. Of course, a decrease in payload mass from 7,000 pounds to 1,000 pounds should produce much better performance and the results in Table 5-15 show this.

Table 5-16: Summary of Two-Stage Liquid Propellant Launch Vehicle Characteristics (CCAFS-Run #2)

Entire Vehicle		Stage 1	
Final Altitude	660,170 ft	Stage Length	33.25 ft
Final Velocity	25,531 ft/s	Stage Diameter	11.09 ft
Total Vehicle Mass	135,121 lbm	Stage Weight	104,492 lbm
Total Vehicle Length	72.51 ft	Initial Thrust	201,370 lbf
Total Vehicle f_{inert}	0.1124	Propellants	LOX/Kerosene
Nosecone Length	18.53 ft	m_{prop}	97,074 lbm
Cost per Launch	\$79.04 million	m_{inert}	7,419 lbm
		f_{inert}	0.0710
		Stage 2	
		Stage Length	18.72 ft
		Stage Diameter	11.09 ft
		Stage Weight	25,521 lbm
		Initial Thrust	39,513 lbf
		Propellants	LOX/Ammonia
		m_{prop}	21,965 lbm
		m_{inert}	3,556 lbm
		f_{inert}	0.1393

5.4.5 Conclusions: Liquid Propellant Launch Vehicle Design Optimizations

A number of successful design optimizations of two and three-stage liquid propellant launch vehicles have been performed. All four vehicles meet the mission

requirements for their respective orbital altitude and orbital velocity constraints. Also, the inert mass fractions meet the required values for liquid propellant systems.

As was the case in the solid propellant vehicles, the use of higher I_{sp} propellants can have an effect on vehicle performance and sizing. Future work in the design optimization of liquid propellant launch vehicles should look at the use of LOX/LH2 as a possible propellant combination. Also, the use of a variable diameter design seemed to complicate the design of the two-stage liquid vehicles more than the solid propellant vehicles. Of course, the GA chose a much more dramatic difference in the stage diameters of the liquid vehicles versus the solid vehicles. Additional work in the modeling of the aerodynamics of variable diameter vehicles would prove useful for future design optimization endeavors.

5.5 Air-Launched Vehicles

A design optimization has been performed for an air-launched, Earth-to-orbit launch vehicle system. This system employs a two-stage liquid propellant launch vehicle deployed from the cargo bay of a USAF C-141 transport aircraft. In addition, the air-launched, two-stage liquid propellant launch vehicle has a real world counterpart, the QuickReachTM launch vehicle, which was used in the model validation efforts.

Table 5-17 summarizes the mission statistics for this case. Payload, desired orbital altitude and desired orbital velocity are typical for a low-Earth orbit mission. They are essentially the same as the values used in the design optimizations of the three and four-stage solid propellant launch vehicles and the two and three-stage liquid propellant launch vehicles.

Table 5-17: Air-Launched Vehicle Mission Statistics

	<u>Two-Stage Air-Launched Liquid</u>
Payload	1,000 lbm
Launch Site	C-141 Cargo Bay
Launch Direction	Due East 90° Azimuth
Orbit Type	i=28.4° prograde orbit
Desired Orbital Altitude	2,430,000 ft
Desired Orbital Velocity	24,550 ft/s

5.5.1 Case 11: Air-Launched, Two-Stage Liquid Propellant Launch Vehicle (CCAFS)

The results of the design optimization of an air-launched, two-stage solid propellant launch vehicle are presented here. The concept of an air-launched vehicle is as follows: one stage of the launch vehicle is replaced with an aircraft platform that would act as the “launch site” or, what is commonly called Stage 0, of the rocket. This concept is not new. Orbital Sciences Corporation deploys its Pegasus space launch vehicle from the underside of a modified L-1011 aircraft. The Pegasus is a three-stage solid propellant launch vehicle that has been quite successful to date. Also, a similar effort is currently on-going where the QuickReach™ launch vehicle is being developed by AirLaunch LLC.⁵⁷ The QuickReach™ launch vehicle is a two-stage, liquid propellant vehicle as opposed to a solid propellant vehicle. Additionally, the QuickReach™ launch vehicle is to be deployed from the cargo bay of an unmodified USAF C-17A transport aircraft. In recent months, a full-scale mock-up of this launch vehicle has been successfully drop tested.

The current study involves a demonstration of the feasibility of finding a workable solution using the GA. The goals of this design optimization are the same as

previous cases: minimize orbital velocity and orbital altitude differences along with minimizing total vehicle mass. The *TRANSCost 7.1* cost model has again been used but it only estimates the cost per launch of the launch vehicle itself. The cost of the airborne platform would also need to be considered in order to get a more accurate cost estimate.

When considering the cost of the airborne platform, there are different options that can be taken. First, an aircraft can be specifically designed and built to accommodate the launch vehicle to be employed. This option provides the most flexibility but is probably the most expensive. Second, an existing aircraft can be modified for use specifically for the launch vehicle. This option is probably not as expensive but will impose some restrictions on the design of the launch vehicle. The vehicle must be designed to accommodate specific aircraft physical characteristics. Finally, an existing, unmodified aircraft can be chosen and the launch vehicle can be designed and built specifically for launch on this aircraft. This is the approach that AirLaunch LLC is taking for their QuickReachTM launch vehicle.

For a design optimization using the GA, any of these airborne platform options will work. However, the objective function requires some initial conditions in order to analyze the flight trajectory of the rocket. Those conditions are the airspeed of the aircraft and the cruise altitude. An existing aircraft has been used to provide that data for use in the 6DOF flight dynamics simulator. The USAF C-141 transport aircraft is a good candidate for this application. Since these aircraft have been retired, the possibility exists that one or more C-141s could be obtained by a launch vehicle provider for a reduced cost and used as the launch platform for this particular launch vehicle (similar to the Minotaur I SLV's use of decommissioned Minuteman II ICBMs).

In order to properly configure the objective function, a few other assumptions have been made. Again, the 6DOF flight dynamics simulator needs initial information in order to analyze the flight of the vehicle. Specifically, the latitude and longitude of the launch site are required inputs. For an air-launched case, technically, the aircraft could fly almost anywhere in the world to launch the rocket (provided the aircraft can be refueled). For example, the aircraft could fly down to the equator and launch the rocket in an eastward direction to maximize the benefit of the Earth's rotation. However, for the sake of consistency with other design optimizations that have been performed, the latitude and longitude values have been chosen to be the same as Cape Canaveral AFS, FL. Also, it is assumed that the C-141 moves out of the way essentially instantly in order for the rocket to fire its first stage motor. Lastly, it is assumed that a system will be available to orient the vehicle to its initial launch angle instantly after deployment from the cargo bay of the C-141 aircraft. Certain design parameters for the GA are specified in such a way so that the rocket fits into the cargo bay of the C-141. Vehicle length and diameter are restricted so that the GA cannot choose values that would result in a rocket larger than the aircraft's cargo bay. Table 5-18 summarizes the characteristics of the C-141 transport aircraft used in this study. It is assumed that the aircraft is flying directly over the Cape Canaveral launch pads at an altitude of 35,000 feet and with a velocity of 733.33 feet per second in the direction of launch.

Table 5-18: C-141 Transport Aircraft Characteristics

Cargo Bay Dimensions	93 ft (length) x 10 ft (width) x 9 ft (height)
Cargo Bay Load Capacity	70,000 lbm
Launch Altitude	35,000 ft
Launch Velocity	733.33 ft/s

A successful design optimization has been performed for an air-launched, two-stage liquid propellant launch vehicle. The mission statistics are described in Table 5-17 and the C-141 transport aircraft is used as the airborne platform. In addition, a direct comparison to the QuickReach™ launch vehicle can be made because it is also a two-stage liquid propellant launch vehicle. Figure 5-25 shows a schematic of the air-launched two-stage liquid propellant launch vehicles that have been analyzed. The left image shows a mock-up of the QuickReach™ launch vehicle being deployed from a C-17A transport aircraft. The middle schematic is the launch vehicle produced in the validation process. The best performer from the design optimization process is shown in the schematic on the right. Table 5-19 summarizes the important characteristics of the optimized launch vehicle.

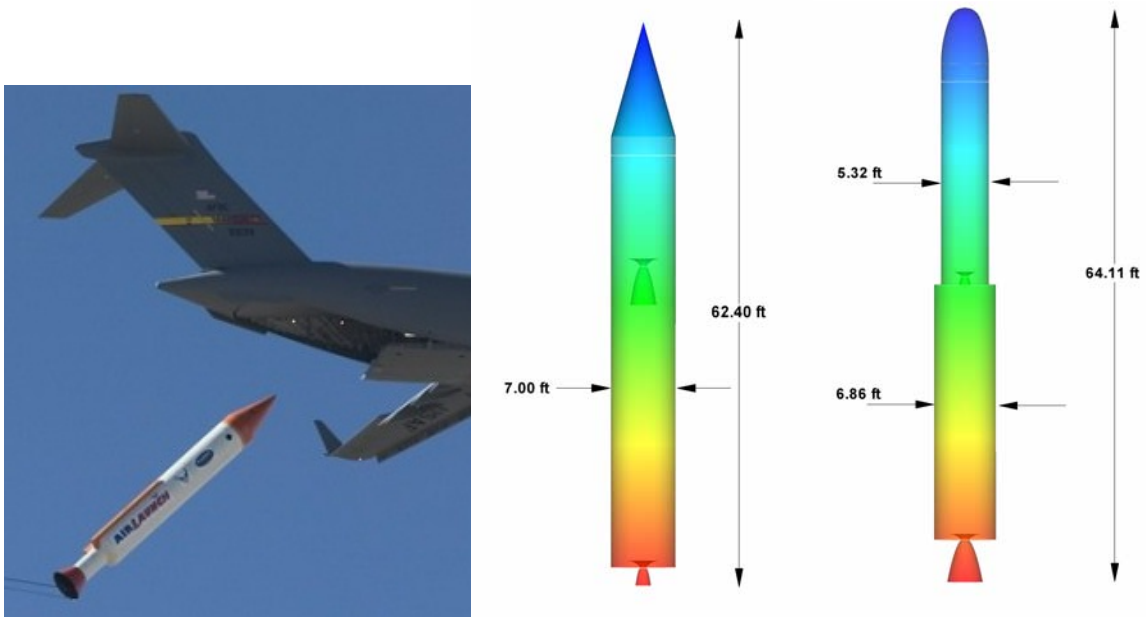


Figure 5-25. Air Launched, Two-Stage Liquid Propellant Launch Vehicles Schematic (CCAFS)

(Ref. 59: <http://www.designation-systems.net/dusrm/app4/quickreach-slv.jpg>)

The launch vehicle resulting from the design optimization process is very similar to the QuickReachTM launch vehicle with some improvements in the physical characteristics. Both launch vehicles have essentially the same total vehicle mass (72,049 lbm vs. 72,000 lbm). However, the optimized vehicle shows improvement in both total vehicle length and the individual stage diameters. The QuickReachTM launch vehicle has a total length of 66 feet whereas the optimized vehicle's total length is 64.11 feet. The diameter of both stages of the QuickReachTM launch vehicle is 7 feet. The optimized vehicle has a 6.86 feet diameter for Stage 1 and a 5.32 feet diameter for Stage 2. These improvements are important since the launch vehicle has to fit into the small confines of a C-141's cargo bay.

As with previous liquid propellant launch vehicles, the GA chose LOX/Hydrazine as the oxidizer/fuel combination for Stage 1. These propellants have the highest I_{sp} of the

available choices so this makes sense for the GA to choose the best performing propellants. However, the GA chose the LOX/Ammonia combination for Stage 2 of the launch vehicle. This is an interesting choice since the sea-level I_{sp} of LOX/Ammonia (294.0s) is much lower than the sea-level I_{sp} of LOX/Hydrazine (313.0s).

In addition, the inert mass fractions for this case match well the typical values for liquid propellant engines. The total vehicle inert mass fraction is 0.1029 which falls in the accepted range of values.

Table 5-19: Summary of Air-Launched, Two-Stage Liquid Propellant Launch Vehicle Characteristics (CCAFS)

Entire Vehicle		Stage 1	
Final Altitude	699,990 ft	Stage Length	33.21 ft
Final Velocity	25,532 ft/s	Stage Diameter	6.86 ft
Total Vehicle Mass	72,049 lbm	Stage Weight	49,991 lbm
Total Vehicle Length	64.11 ft	Initial Thrust	127,081 lbf
Total Vehicle f_{inert}	0.1029	Propellants	LOX/Hydrazine
Nosecone Length	6.25 ft	m_{prop}	45,951 lbm
Cost per Launch	\$61.99 million	m_{inert}	4,039 lbm
		f_{inert}	0.0808
		Stage 2	
		Stage Length	22.65 ft
		Stage Diameter	5.32 ft
		Stage Weight	20,118 lbm
		Initial Thrust	72,412 lbf
		Propellants	LOX/Ammonia
		m_{prop}	17,783 lbm
		m_{inert}	2,335 lbm
		f_{inert}	0.1161

A comparison between the air-launched, two-stage liquid propellant launch vehicle resulting from the design optimization and the QuickReach™ launch vehicle are shown in Table 5-20. The optimized vehicle closely matches the physical characteristics of the QuickReach™ launch vehicle. Also, the optimized vehicle is able to attain the same desired orbital parameters as the QuickReach™ launch vehicle. There are some

differences in the vacuum thrust of both stages of each vehicle. The GA has designed a much more powerful Stage 2 thrust for the optimized vehicle (72,412 lbf vs. 24,000 lbf).

Table 5-20: Air-Launched, Two-Stage Liquid Propellant Launch Vehicles Comparison

	<u>QuickReach™ Launch Vehicle</u>	<u>Validation Model</u>	<u>Optimized Vehicle</u>
Payload	1,000 lbm	1,000 lbm	1,000 lbm
Total Vehicle Weight	72,000 lbm	74,633 lbm	72,049 lbm
Total Vehicle Length	66.00 ft	62.40 ft	64.11 ft
Final Altitude	700,000 ft	738,783 ft	699,990 ft
Final Velocity	25,532 ft/s	25,619 ft/s	25,532 ft/s
Stage 1 Vacuum Thrust	172,000 lbf	171,825 lbf	127,081 lbf
Stage 2 Vacuum Thrust	24,000 lbf	25,333 lbf	72,412 lbf

5.5.2 Conclusions: Air-Launched Vehicle Design Optimization

The design optimization of an air-launched, two-stage liquid propellant launch vehicle has been performed. This optimization has shown the feasibility of this system and the fact that the objective function and GA can meet the mission requirements. The optimized liquid propellant launch vehicle can fit into the cargo bay of the C-141 transport aircraft. However, the total vehicle mass of the optimized vehicle is slightly higher than the payload capacity of the C-141.

The cost per launch of the optimized launch vehicle is quite attractive (\$61.99 million). This cost per launch value is lower than all the other liquid propellant launch vehicles. This cost per launch does not include the cost of the airborne platform. Of course, using existing transport aircraft like the C-141 or C-17 should keep this cost at a minimum.

Additional design optimizations for this system should include using different combinations of liquid propellants. Consideration should be made for the fact that these

launch vehicles are launched from an airborne platform. This would have an affect on the choice of propellants since they would have special transport requirements. Also, design optimizations should investigate launching the vehicle from locations other than Cape Canaveral AFS, FL. Flying the transport aircraft down to the equator and launching in an eastward direction would provide additional useful information on the preliminary design of this type of launch vehicle. Finally, the case of an air-launched, two-stage solid propellant launch vehicle should be investigated.

5.6 Mixed Propellant Vehicles

The last two cases analyzed in the current study are mixed propellant launch vehicles with larger payloads and different desired orbital parameters. These launch vehicles employ a unique configuration of a first stage solid propellant motor along with second and third stage liquid propellant rocket engines. The use of mixed propellant systems on space launch vehicles is not a new idea. Strap-on solid rocket motors are often used to provide thrust augmentation at lift-off for a variety of launch vehicles (like the Space Shuttle and Delta II). However, in the current study, the 1st stage solid propellant motor is designed to provide all the lift-off thrust for the vehicle. Then, the two liquid propellant stages take over and accelerate the payload to orbit.

In order to investigate the characteristics of a medium to heavy lift launch vehicle capability, the payload mass has been increased to 10,000 pounds. In addition, most of the previous design optimizations have used a relatively high value for the desired orbital altitude of 700 km (2,430,000 ft). For these final two cases, the desired orbital altitude has been lowered to an altitude of 300 km (984,252 ft). As a result of this lower orbit, the desired orbital velocity requirement has increased to 25,328 feet per second in

accordance with the appropriate orbital mechanics calculations. Table 5-21 summarizes the mission statistics for the two launch vehicles being optimized.

Table 5-21: Mixed Propellant Launch Vehicles Mission Statistics

	<u>Three-Stage Solid/Liquid/Liquid</u>	<u>Three-Stage Solid/Liquid/Liquid</u>
Payload	10,000 lbm	10,000 lbm
Launch Site	VAFB	CCAFS
Launch Direction	Due North 0° Azimuth	Due East 90° Azimuth
Orbit Type	i=90° polar orbit	i=28.4° prograde orbit
Desired Orbital Altitude	984,252 ft	984,252 ft
Desired Orbital Velocity	25,328 ft/s	25,328 ft/s

5.6.1 Case 12: Three-Stage Solid/Liquid/Liquid Propellant Launch Vehicle (VAFB)

The results for the design optimization of a three-stage solid/liquid/liquid propellant launch vehicle with launch out of Vandenberg AFB, CA are presented here. The schematic of the best performer from the optimization process for this vehicle is shown in Figure 5-26. The choice of a constant diameter vehicle was chosen prior to the start of the design optimization process. The fairly large 2nd stage can be seen in the schematic as well as the relatively smaller 1st and 3rd stages. Also, this vehicle is longer (155.45 ft) than all the other previously optimized vehicles investigated in this study. The large launch vehicle size is to be expected due to the increase in the payload mass-to-orbit requirement.

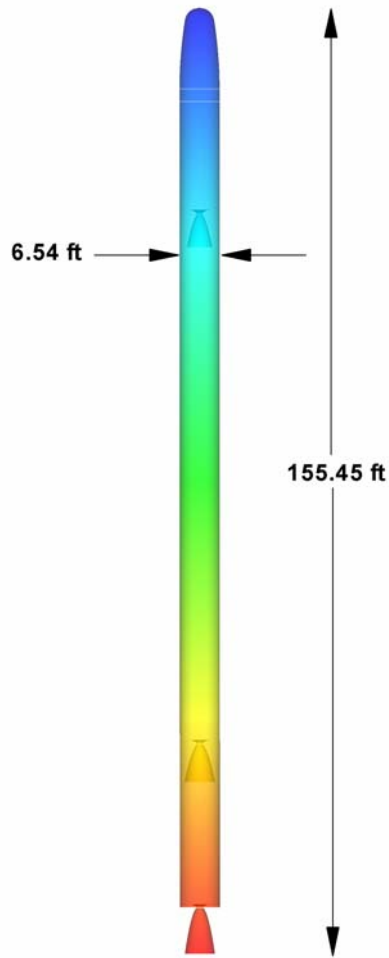


Figure 5-26. Three-Stage Solid/Liquid/Liquid Propellant Launch Vehicle Schematic (VAFB)

The important characteristics of the optimized three-stage solid/liquid/liquid propellant launch vehicle are shown in Table 5-22. Two design optimizations have been run for this case. The first run produced a launch vehicle with some generally good characteristics. However, the optimized vehicle failed to meet one of the desired goals. The final velocity of this vehicle (23,595 ft/s) was well below the desired orbital velocity (25,328 ft/s). As a result, this design optimization was declared an unusable solution. A second design optimization was prepared with one important change in the optimization

process. The previous design optimization run limited the choice of available liquid propellants for the GA. The reason for this was to facilitate the operation of the *TRANSCost 7.1* cost model by using only storable liquid propellants. These liquid propellants (like LOX/Kerosene and LOX/Hydrazine) do not have as good performance characteristics as other propellants (like LOX/LH2). For the second design optimization run, it was decided to open up the available choices for the GA to include higher I_{sp} liquid propellants (like LOX/LH2 and LF2/LH2). The *TRANSCost 7.1* cost model was adjusted in order to account for the possibility of the GA choosing these types of liquid propellants.

The success of this decision is seen in the performance characteristics of the optimized vehicle. The final altitude (984,726 ft) and final velocity (25,330 ft/s) closely match the desired orbital parameters. The total vehicle mass (180,673 lbm) also has been reduced significantly from the total vehicle mass of the previous run (226,589 lbm). The choice of higher sea-level I_{sp} propellants definitely has made the difference. The GA chose LF2/LH2 ($I_{sp}= 410s$) for the Stage 2 propellants and LF2/Hydrazine ($I_{sp}= 363s$) for the Stage 3 propellants. These propellants are excellent choices to increase the performance of the optimized launch vehicle. However, there is a downside to using these propellants. The toxicity of LF2 makes it highly undesirable as a propellant. Also, the *TRANSCost 7.1* cost model was adjusted for the use of these propellants and the result was a higher cost per launch (\$125.08 million) than the previous run (\$109.75 million).

Overall, this design optimization has produced a successful launch vehicle that closely matches the desired orbital parameters. The mass fractions for this optimized vehicle are also desirable and all three values fall within the range for the desired mass fractions for solid and liquid propellant launch vehicles.

Table 5-22: Summary of Three-Stage Solid/Liquid/Liquid Propellant Launch Vehicle Characteristics (VAFB)

<u>Entire Vehicle</u>		<u>Stage 1 (solid)</u>	
Final Altitude	984,726 ft	Stage Length	28.26 ft
Final Velocity	25,330 ft/s	Stage Diameter	6.54 ft
Total Vehicle Mass	180,673 lbm	Stage Weight	64,874 lbm
Total Vehicle Length	155.45 ft	Initial Thrust	623,082 lbf
Nosecone Length	13.36 ft	Propellants	DB/AP/Al
Cost per Launch	\$125.08 million	m_{prop}	58,330 lbm
		m_{inert}	6,545 lbm
		f_{prop}	0.8991
		<u>Stage 2 (liquid)</u>	
		Stage Length	87.83 ft
		Stage Diameter	6.54 ft
		Stage Weight	73,606 lbm
		Initial Thrust	221,433 lbf
		Propellants	LF2/LH2
		m_{prop}	64,226 lbm
		m_{inert}	9,380 lbm
		f_{inert}	0.1274
		<u>Stage 3 (liquid)</u>	
		Stage Length	24.00 ft
		Stage Diameter	6.54 ft
		Stage Weight	29,851 lbm
		Initial Thrust	101,114 lbf
		Propellants	LF2/Hydrazine
		m_{prop}	26,994 lbm
		m_{inert}	2,858 lbm
		f_{inert}	0.0957

5.6.2 Case 13: Three-Stage Solid/Liquid/Liquid Propellant Launch Vehicle (CCAFS)

The results for the final design optimization case of the current study are presented here. This three-stage solid/liquid/liquid propellant launch vehicle has been optimized for launch out of Cape Canaveral AFS, FL. In addition, the mission statistics for this vehicle are described in Table 5-21. The schematic of the best performer from the optimization process for this vehicle is shown in Figure 5-27. This optimized vehicle is very similar to the Vandenberg launch vehicle. The 2nd stage is the largest stage and the overall vehicle length is large (142.66 ft).

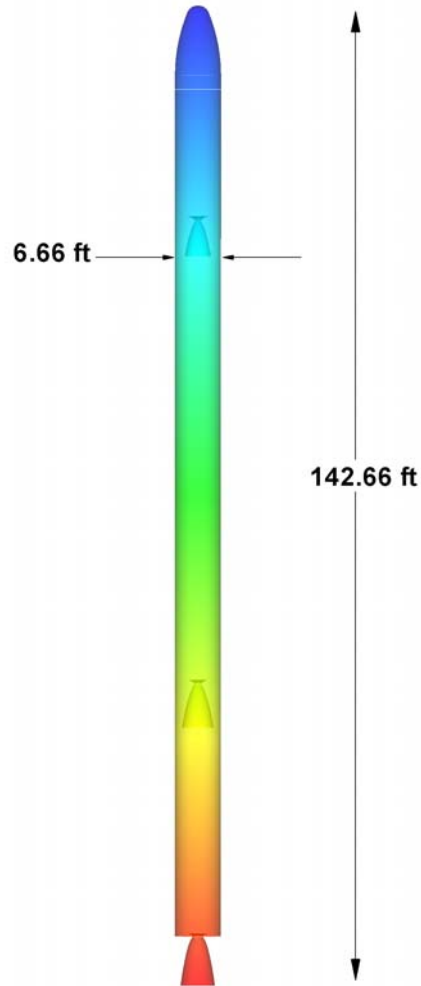


Figure 5-27. Three-Stage Solid/Liquid/Liquid Propellant Launch Vehicle Schematic (CCAFS)

The important characteristics of the optimized three-stage solid/liquid/liquid propellant launch vehicle are shown in Table 5-23. The benefits of launching in the eastward direction are clearly seen in the performance results. The final altitude (985,320 ft) and the final velocity (25,377 ft/s) of this optimized vehicle both closely match the desired orbital altitude and desired orbital velocity values. Thus, the slight velocity boost given by the Earth's rotation provides the difference for getting to orbit.

The other performance characteristics of the optimized vehicle yield good results. The propellant mass fraction of the solid propellant 1st stage is a respectable 0.8699. The inert mass fractions of the two liquid propellant stages (Stage 2: 0.0748 & Stage 3: 0.1128) also fall within the acceptable range for these types of engines. These results show that this particular launch vehicle model is a good one and the results are realistic.

The only possible draw back to this vehicle is the cost per launch (\$117.21 million). While still less expensive than the Vandenberg vehicle, the cost per launch for this optimized vehicle is higher than the cost per launch values of all the other previously optimized cases. Of course, the payload mass for the solid/liquid/liquid propellant launch vehicles (10,000 lbm) is ten times greater than the payload mass (1,000 lbm) of the previous cases. Because of this larger payload, a larger and more expensive launch vehicle should be expected.

Table 5-23: Summary of Three-Stage Solid/Liquid/Liquid Propellant Launch Vehicle Characteristics (CCAFS)

Entire Vehicle		Stage 1 (solid)	
Final Altitude	985,320 ft	Stage Length	37.64 ft
Final Velocity	25,377 ft/s	Stage Diameter	6.66 ft
Total Vehicle Mass	242,884 lbm	Stage Weight	82,915 lbm
Total Vehicle Length	142.66 ft	Initial Thrust	1,781,882 lbf
Nosecone Length	10.17 ft	Propellants	PBAN/AP/Al
Cost per Launch	\$117.21 million	m_{prop}	72,128 lbm
		m_{inert}	10,786 lbm
		f_{prop}	0.8699
		Stage 2 (liquid)	
		Stage Length	68.51 ft
		Stage Diameter	6.66 ft
		Stage Weight	121,273 lbm
		Initial Thrust	283,503 lbf
		Propellants	LOX/Hydrazine
		m_{prop}	112,203 lbm
		m_{inert}	9,070 lbm
		f_{inert}	0.0748
		Stage 3 (liquid)	
		Stage Length	24.33 ft
		Stage Diameter	6.66 ft
		Stage Weight	27,045 lbm
		Initial Thrust	109,584 lbf
		Propellants	LOX/Hydrazine
		m_{prop}	23,993 lbm
		m_{inert}	3,052 lbm
		f_{inert}	0.1128

5.6.3 Conclusions: Mixed Propellant Vehicle Design Optimizations

Two successful design optimizations of a unique three-stage solid/liquid/liquid launch vehicle have been performed. The results provide some interesting insight into the challenge of meeting mission requirements (orbital altitude and orbital velocity) while at the same time reducing total vehicle mass and cost per launch. There are certainly many parameters to consider and the GA provides an effective tool to aid in the analysis of space launch vehicles.

The optimized vehicle for the Vandenberg launch initially did not match the desired orbital velocity and this prompted an analysis of vehicle mass and propellant choice considerations. Allowing for the use of more energetic propellants to increase performance and reduce weight was proposed as a possible solution. As a result, a second design optimization was performed that allowed for the choice of other liquid propellants. This proved to be successful as the new optimized vehicle closely matched the desired orbital values. The downside was that the cost per launch for this vehicle rose substantially.

The optimized vehicle for the Cape Canaveral launch met the desired orbital parameters most likely due to the velocity boost provided by the Earth's eastward rotation. The same argument of variable diameter stages and more energetic propellants applies to the Cape Canaveral launch vehicle in order to reduce total vehicle mass while maintaining vehicle performance.

5.7 Launch Vehicle Comparisons

5.7.1 Launch Vehicles Comparison of 1,000 lbm Payload Cases

The first comparison of the launch vehicles produced by the various design optimizations performed in this study is presented here. In order to make a useful comparison, all the launch vehicles being considered for this comparison should have a common reference point. In this comparison, the common reference point is the payload mass launched into orbit. The payload mass is a direct input to the objective function and an important variable in the design optimization process. Of the thirteen different design optimizations performed in this study, eight cases used the value of 1,000 lbm for the payload mass. These eight cases are summarized in Table 5-24.

Table 5-24: Optimized Cases for 1,000 lbm Payload Mass

Case #	Optimized Launch Vehicle
3	Three-Stage Solid (VAFB)
4	Three-Stage Solid (CCAFS)
6	Four-Stage Solid (CCAFS)
7	Three-Stage Liquid (VAFB)
8	Three-Stage Liquid (CCAFS)
9	Two-Stage Liquid (VAFB)
10	Two-Stage Liquid (CCAFS)
11	Air-Launched, Two-Stage Liquid (CCAFS)

The comparison of the total vehicle mass for these eight cases is shown in Figure 5-28. This comparison shows that the liquid propellant vehicles tend to have the highest total vehicle mass of all the launch vehicles being compared; the one exception is the air-launched two-stage liquid propellant vehicle (72,049 lbm).

All of the solid propellant vehicles weigh around 80,000 pounds whereas all of the liquid cases weigh over 100,000 pounds (the air-launched two-stage liquid being the one exception). Thus, in general, the broad conclusion can be made that in order to achieve a particular low-Earth orbit with a 1,000 pound payload, the total mass of the launch vehicle will need to be at least 70,000 pounds.

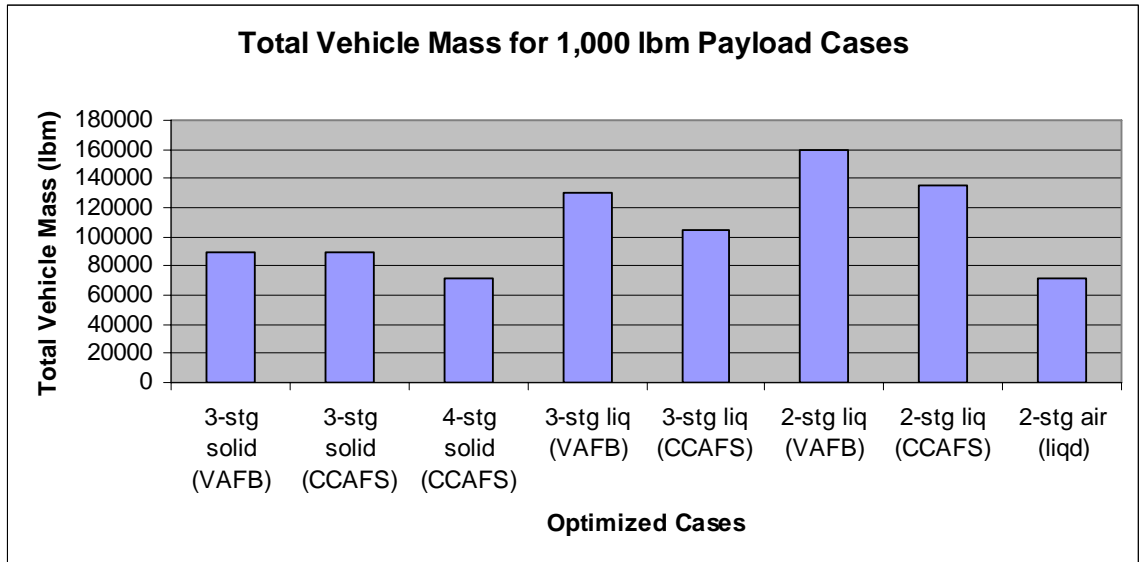


Figure 5-28. Total Vehicle Mass Comparison

The comparison of the cost per launch values for these same nine cases is shown in Figure 5-29. Since the cost estimating relationships (CERs) used in the *TRANSCost 7.1* cost model are mass-based, the less expensive launch vehicles are the solid propellant vehicles because they weigh less than the liquid propellant vehicles. What is interesting is the cost per launch values of the two and three-stage liquid propellant vehicles. The three-stage liquid propellant vehicles have a lower total vehicle mass than the two-stage liquid propellant vehicles. However, the three-stage liquid propellant vehicles are more expensive than the two-stage liquid propellant vehicles. This implies that, for the liquid propellant vehicles, minimizing the total vehicle mass did not result in a minimized cost per launch. Future work should be done where the third design goal is a direct minimization of the cost per launch.

The reason for this is the use of the system engineering/integration factor (f_{0d}) in the Development Cost Submodel and the system management/vehicle integration/checkout factor (f_{0p}) used in the Production Cost Submodel. These two

factors address the cost associated with developing a multi-stage vehicle along with the complexities of producing it and integrating the different stages. Thus, both of these factors are dependent on the number of stages of the vehicle. The equations used for these two factors are written by Koelle⁴¹ as:

$$f_{0d} = 1.04^{nstg} \quad (5.2)$$

$$f_{0p} = 1.025^{nstg} \quad (5.3)$$

where *nstg* is the number of stages in the vehicle. Equations 5.2 and 5.3 show that a three-stage launch vehicle could have a higher cost than a two-stage vehicle even if the total mass of the three-stage vehicle is lower than the total mass of the two-stage vehicle.

Figure 5-29 also shows that, overall, liquid propellant launch vehicles are more expensive than solid propellant launch vehicles. Thus, if cost is a driving concern in the design of a launch vehicle, solid propellant systems probably should be considered early on in the systems engineering process.

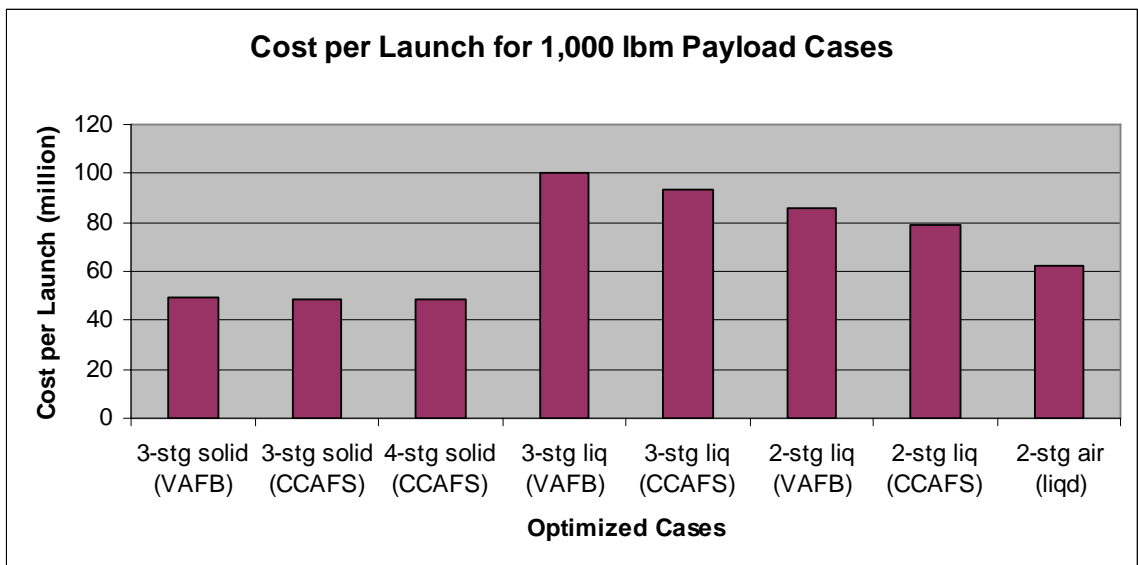


Figure 5-29. Cost per Launch Comparison

5.7.2 Launch Vehicles Comparison of Propellant Mass Fractions

The next comparison involves the propellant mass fractions (f_{prop}) that were determined for all the solid propellant launch vehicles. As previously explained in Humble et al.,⁵⁰ the propellant mass fraction is used to size solid propellant launch vehicles. The preferred value for propellant mass fraction, as determined from previously flown and built launch vehicles, is 0.90 for solid propellant vehicles. Thus, one goal of the design optimizations that have been performed was to ensure that the propellant mass fractions for the various optimized launch vehicles met the desired propellant mass fraction criteria.

Figure 5-30 shows the propellant mass fractions for the various solid propellant launch vehicle cases optimized in the current study. These values represent the propellant mass fraction of the entire vehicle stack. The propellant mass fractions for all the optimized vehicles fall within the range of 0.89 to 0.90. Overall, these values of propellant mass fraction closely match the desired value.

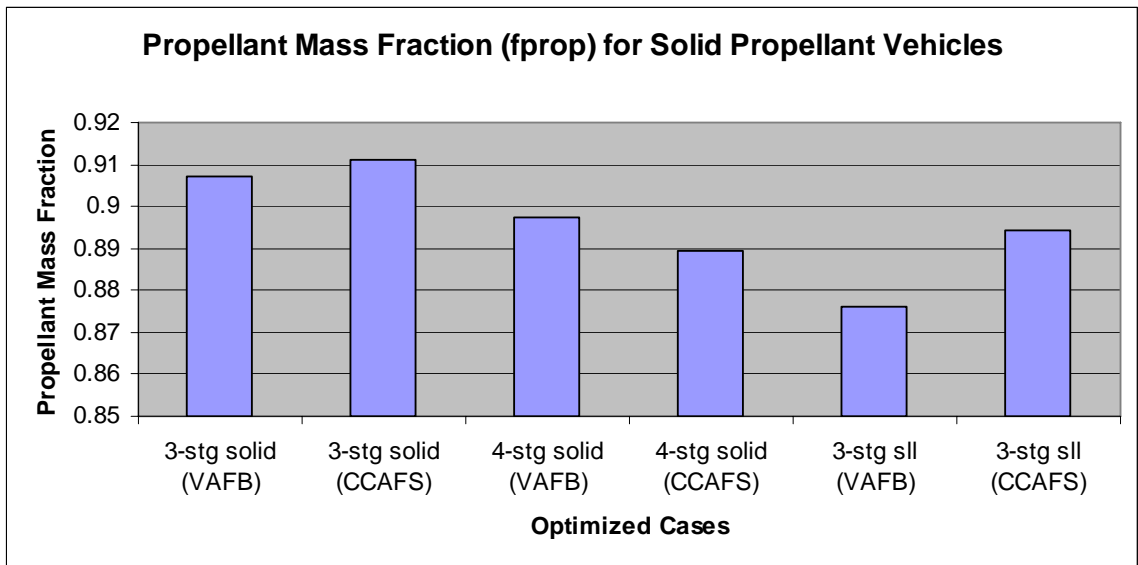


Figure 5-30. Propellant Mass Fractions (f_{prop}) Comparison

5.7.3 Launch Vehicles Comparison of Inert Mass Fractions

Figure 5-31 shows the inert mass fractions for the various liquid propellant launch vehicles optimized in the current study. All of these results are well within the required range and produce very good inert mass fractions for the liquid propellant launch vehicles. This makes their high degree of accuracy similar to the accuracy of the solid propellant launch vehicles. Thus, the mass fractions for both solid and liquid propellant launch vehicles compare very well to real world launch vehicles.

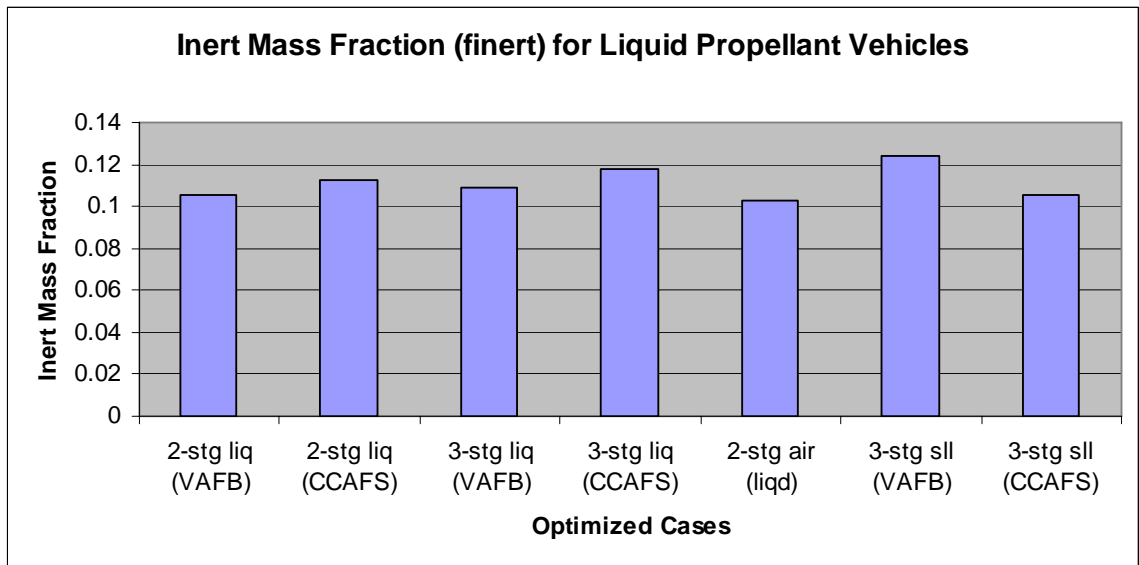


Figure 5-31. Inert Mass Fractions (f_{inert}) Comparison

5.7.4 Launch Vehicles Comparison of Cost per Launch Values

Finally, one of the main goals of the current study was to attempt to minimize the cost per launch of Earth-to-orbit launch vehicles. A variety of optimizations were performed in order to investigate the feasibility of lowering launch costs for space launch vehicles. While the results presented here are promising, the cost per launch values did not produce a truly economical launch vehicle. Many factors must be considered when determining cost and certainly not all were considered in the cost model used. Yet, the

TRANSCost 7.1 cost model provides a very powerful tool for analysis at this preliminary design level. The least expensive cost per launch (\$46.07 million) is a fairly good price for an expendable launch vehicle. However, it is also much higher than the \$5 million cost per launch desired by the USAF Operationally Responsive Space (ORS) program.

The costs per launch values, in millions of dollars, for all the launch vehicles considered in this study are shown in Figure 5-32. One item to note is that not all the launch vehicles considered used the same payload mass and not all attained the same low-Earth orbit. However, this comparison does show the overall trend that solid propellant vehicles tend to be less expensive than liquid propellant launch vehicles. Also, when solids and liquids are combined (as in the three-stage solid/liquid/liquid cases) the cost per launch is even higher than for single propellant types of systems. Thus, if possible, careful consideration should be taken for launch vehicle designs that employ different types of propellants since higher costs are likely.

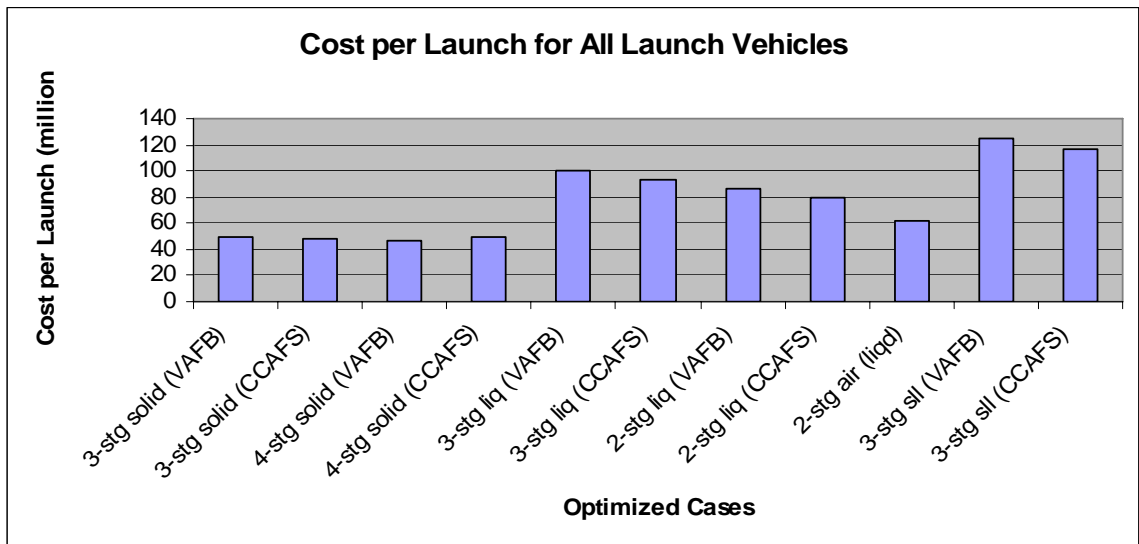


Figure 5-32. Cost per Launch Comparison for All Launch Vehicles

6.0 CONCLUSIONS

6.1 Introduction

A variety of design optimizations have been performed in an attempt to demonstrate the possibility for improvement upon current space launch vehicle design. The analysis from these optimizations has shown encouraging results with regards to the possibility for improvement of launch vehicle systems.

The design optimization processes undertaken in this study provide insight into possible launch vehicle design improvement. The focus has been on generating useful results that can aid the systems engineering process at the preliminary design level. The goals of the optimization process have been to minimize total launch vehicle mass and cost per launch while at the same time meeting the desired orbital parameters.

The genetic algorithm (GA), in conjunction with the objective function, provides a powerful tool for finding the optimum solution for a given set of design goals. For the highly complicated space launch vehicle system, the GA and objective function have been successfully implemented and some interesting launch vehicle designs have emerged. One unique aspect of this analysis is the implementation of a cost model used to predict the cost per launch of each optimized vehicle.

The optimized launch vehicle results are within the confines of the launch vehicle design class that has been modeled. The optimized vehicles fall into the class of launch vehicles categorized as small to medium lift vehicles. These vehicles also employ

conventional forms of propulsion based on heritage vehicle technology. It is likely that additional improvement in the design goals may be gained by the use of additional technology in the form of propulsion and vehicle shaping. The use of air-breathing propulsion systems along with lifting body shapes could bring about better performing and more cost effective space launch vehicles.

6.2 System Modeling and Validation

An entire multi-stage launch vehicle has been modeled using a suite of system models in the form of performance codes and then validated against real world systems. The propulsion characteristics, mass properties, aerodynamic characteristics and vehicle flight dynamics have been successfully integrated to analyze the launch vehicle performance from lift-off to orbit insertion. In addition, a mass-based cost model has been successfully added to provide cost per launch data on the optimized launch vehicle.

The important task of model validation has been performed on four specific launch vehicle types. A three-stage solid propellant vehicle, a four-stage solid propellant vehicle, a two-stage liquid propellant vehicle and an air-launched, two-stage liquid propellant vehicle have been validated against similar real world launch vehicles. The use of propellant and inert mass fractions also strengthened the validity of system models being used.

One important limitation has been identified in the model validation process. The mass properties model tended to underestimate the mass values of certain vehicle components. Specifically, the inert mass of the solid propellant launch vehicles was less than the inert mass of the real world examples. Precisely estimating the mass properties of space launch vehicles is a difficult task. Future work could address this issue by either

updating the mass properties model with the most current and detailed information available or including a correction factor for the inert mass in the current model.

6.3 Design Optimizations

The design optimizations performed in this study have produced informative results in the preliminary design of space launch vehicles. Thirteen different cases that covered a broad range of vehicle types showed the feasibility of minimizing total vehicle mass and cost per launch while meeting the specified orbital parameters. The resulting optimized vehicles are not only realistic but are also improvements on their real world counterparts.

Three specific trends have been noted throughout the results of these optimizations. First, propellant choice had a large effect on vehicle performance and meeting the desired goals. Often the GA would attempt to use the more energetic solid and liquid propellants in order to meet the desired orbital parameter goals. This would make sense since those goals were weighted higher than the third design goal.

Second, along the same lines as propellant choice, the payload mass for each launch vehicle played a large role in overall vehicle size and performance. All the vehicles that used a payload mass of less than 1,000 pounds were able to closely match the desired orbital parameters. In addition, the total vehicle mass and cost per launch for these vehicles fell within the typical range for this class of launch vehicles. A few vehicles were optimized using a payload mass of 7,000 lbm or higher. The challenge of lifting higher mass payloads into orbit was realized in the resulting higher total vehicle mass and cost per launch values obtained for these heavier lift vehicles.

Lastly, the cost per launch values for the optimized vehicles were good but did not result in breakthroughs in launch vehicle cost. The Operationally Responsive Space (ORS) program has the goal of getting launch costs down to \$5 million per launch for 1,000 pound payloads. The lowest cost per launch obtained from the results of this study is \$46.07 million for the four-stage solid propellant launch vehicle. A difference of over \$40 million exists between the desired ORS program launch cost and the results obtained here. From the design optimizations performed in this study, the likelihood of achieving the \$5 million per launch value does not seem feasible. A significant breakthrough in propulsion or materials technology would be required to bring the cost per launch down to that price. As a result, additional work still needs to be done in order to reduce the cost of access to space.

One final note should be made on the issue of cost and the choice of design goals. Early in the process, the decision was made to minimize the total vehicle mass as the third design optimization goal. Since the cost model being used was mass-based, this seemed like a logical choice that would result in a minimized cost per launch value. For the most part, the results of the design optimization supported this choice. However, the analysis of the liquid propellant launch vehicles resulted in a different conclusion. In the end, a fourth goal should have been added that directly minimized the cost per launch value.

To summarize, the purpose of the current effort was to demonstrate the viability of optimizing launch vehicles using a genetic algorithm (GA) along with an objective function containing detailed preliminary design level models. The three goals of the design optimization process were to match the desired orbital altitude and orbital velocity

values along with minimizing the total vehicle mass and also vehicle cost. Both model validation and design optimizations using a GA have been performed for a wide variety of space launch vehicle configurations. The results show the feasibility of this approach in the improvement of launch vehicle design. The best example is the four-stage solid propellant launch vehicle. The validated model closely matched the real world example launch vehicle. The subsequent design optimization improved on the real world example resulting in a significant mass savings. Thus, through the validation of the system models and the resulting design optimizations, the stated purpose of this study has been accomplished.

7.0 RECOMMENDED IMPROVEMENTS

The preliminary design level results generated in this study for the design of space launch vehicles are very useful in the continuous effort to improve space transportation systems. For future design optimization work, it is recommended that the following improvements be implemented.

7.1 Types of Solid and Liquid Propellants

As mentioned in Chapter 6, the choice of propellants available in the optimization process can greatly affect the results. Expanding the different types of propellants available for the genetic algorithm (GA) to choose or allowing the GA to design the propellants directly could improve the performance of the launch vehicles. Specifically, more energetic propellants would increase the I_{sp} and characteristic exhaust velocity (c^*) which should lower the overall weight of the propellants.

For the solid propellants, two additional types of propellants (DB/AP-HMX/Al and the energetic Star 37) were added to the existing list of available solid propellant types. As it turned out, the GA ended up choosing these propellants in the design optimizations that were run. On the liquid propellant side, the choices were restricted to only a few types of storable propellant combinations (LOX/Kerosene, LOX/Hydrazine, etc.) Allowing the GA to choose one of the most common propellant combinations, LOX/LH₂, should greatly enhance the liquid propellant launch vehicle results.

7.2 Aerodynamics Model

The aerodynamics model used in this study, AeroDesign, is configured to model only certain aerodynamic shapes. AeroDesign can only analyze conical and ogive shaped nosecones and cylindrical shaped center bodies. For the most part, this is not a problem since many rocket and missile designs employ these shapes. However, for more complex vehicle designs, AeroDesign needs to be altered in order to generate the aerodynamic characteristics of different shaped vehicles.

An improvement on the modeling for variable diameter vehicles should be done. A very basic estimate for the increased drag associated with variable diameter shapes was used in this study. This estimate was probably on the high side since most launch vehicles have skirts and interstages that allow for a smooth geometric transition between stages of differing diameters. Also, AeroDesign needs to be modified in order to analyze the aerodynamic characteristics of strap-on boosters common in many modern launch vehicle designs.

7.3 Six-Degree-of Freedom (6DOF) Flight Dynamics Simulator

The 6DOF flight dynamics simulator used in this study analyzed a basic ballistic flight trajectory. Future work should investigate using the autopilot and pronav applications in the 6DOF flight dynamics simulator to allow for greater accuracy in attaining the desired orbital altitude and orbital velocity. For this preliminary study, the use of the ballistic trajectory provided the required analysis for the flight of the vehicle. However, an autopilot and inertial navigation system would greatly enhance the flight trajectory with the subsequent benefit of optimizing the amount of payload to orbit. These capabilities are currently available in the 6DOF flight dynamics simulator. They

should be implemented in order to investigate another aspect of the design of space launch vehicles: the optimization of launch vehicle flight trajectory.

For this study, the use of a coast time between stages and an orbit insertion burn were modeled in the four-stage solid propellant launch vehicle. This type of modeling needs to be extended to all the launch vehicle types. Like the autopilot and pronav applications, coast times and an orbit insertion burn would greatly increase the accuracy of the launch vehicle in attaining the desired orbit.

7.4 Cost Model

The *TRANSCost 7.1* cost model used in this study provided excellent insight into the calculation of cost per launch values for optimized space launch vehicles. However, the model could be improved to more accurately reflect insurance costs as well as ground and flight operations costs.

7.5 Payload Masses and Orbits

Finally, performing design optimizations using a wider variety of payload masses would provide even more insight to launch vehicle design. A majority of the payloads used in this study weighed 1,000 pounds so that vehicle comparisons could be made. Also, this payload class is what the USAF is looking for when it comes to responsive space launch vehicles. However, the USAF, along with civil agencies and commercial companies, launch much larger payloads into orbit. The launch vehicles that carry these types of payloads need to be analyzed as well.

Also, all of the launch vehicles in this study carried their payloads to low-Earth, circular orbits. Future work should look at launches to semi-synchronous orbit as well as to geosynchronous transfer orbit.

Finally, the two primary United States launch sites, Vandenberg AFB, CA and Cape Canaveral AFS, FL were the only two launch sites considered in this study. While these two sites are the primary launch sites for the USAF, other worldwide launch sites are used for space missions. Alternative launch sites such as Wallops Island, VA or Kourou, French Guiana should be considered for future work.

REFERENCES

1. Chilton, K.P., “Assured Access to Space in a Competitive World”, *High Frontier: The Journal for Space and Missile Professionals*, Vol. 3, No. 1, 2006, pp. 2-3.
2. System Description: Force Application and Launch from CONUS (FALCON), <http://www.globalsecurity.org/space/systems/falcon.htm>.
3. Foulds, L.R., Optimization Techniques: An Introduction, Springer-Verlag, New York, NY, 1981.
4. Siddal, J.N., Optimal Engineering Design: Principles and Applications, Merrell Dekker Inc., New York, NY, 1982.
5. Gabasov, R.F. and Kirillova, F.M., Methods of Optimization, Optimization Software Inc., New York, NY, 1988.
6. Fisher, R.A., The Design of Experiments: 8th Edition, Hafner Publishing Company, New York, NY, 1971.
7. Weber, D.C. and Skillings, J.H., A First Course in the Design of Experiments: A Linear Models Approach, CRC Press, Boca Raton, FL, 2000.
8. Rodriguez, D.L., “Response Surface Based Optimization with a Cartesian CFD Method”, AIAA Paper 2003-0465, Presented at the 41st AIAA Aerospace Sciences Meeting, Reno, NV, January 2003.
9. Mitchell, M., An Introduction to Genetic Algorithms, MIT Press, Cambridge, MA, 1998.

10. Coley, D.A., An Introduction to Genetic Algorithms for Scientists and Engineers, World Scientific Publishing Co., Singapore, 1999.
11. Billheimer, J.S., “Optimization and Design Simulation in Solid Rocket Design”, AIAA Paper 68-488, Presented at the 3rd AIAA Solid Propulsion Conference, June 1968.
12. Woltosz, W.S., “The Application of Numerical Optimization Techniques to Solid-Propellant Rocket Motor Design”, Masters Thesis, Auburn University, March 1977.
13. Foster, W.A., Jr., and Sforzini, R.H., “Optimization of Solid Rocket Motor Igniter Performance Requirements”, AIAA Paper 78-1016, Presented at the 14th AIAA/SAE Joint Propulsion Conference, Las Vegas, NV, July 1978.
14. Sforzini, R.H., “An Automated Approach to Design of Solid Rockets Utilizing a Special Internal Ballistics Model”, AIAA Paper 80-1135, Presented at the 16th AIAA/SAE/ASME Joint Propulsion Conference, July 1980.
15. Washington, W.D., “Missile Aerodynamic Design Program”, 1980, 1990.
16. Anderson, M.B., “Design of a Missile Interceptor Using a Genetic Algorithm”, Doctoral Dissertation, Auburn University, 1998.
17. Etkin, Bernard, Dynamics of Atmospheric Flight, John Wiley & Sons Inc., New York, NY, 1972.
18. Burkhalter, J.E., Jenkins, R.M., and Hartfield, R.J., “Genetic Algorithms for Missile Analysis – Final Report”, Submitted to Missile and Space Intelligence Center, Redstone Arsenal, AL, 35898, February 2003.
19. Hartfield, R.J., Burkhalter, J.E., Jenkins, R.M., and Metts, J.G., “Genetic Algorithm Upgrade – Final Report”, Submitted to Missile and Space Intelligence Center, Redstone Arsenal, AL, 35898, June 2005, Reference Contract No. HHM402-04-P-0061.

20. Metts, J.G., "Determination of Key Parameters for Reverse Engineering Solid Rocket Powered Missiles", Masters Thesis, Auburn University, 2006.
21. Riddle, D.B., "Design Tool Development for Liquid Propellant Missile Systems", Masters Thesis, Auburn University, 2007.
22. Hartfield, R.J., Jenkins, R.M., and Burkhalter, J.E., "Ramjet Powered Missile Design Using a Genetic Algorithm," AIAA Paper 2004-0451, Presented at the 42nd AIAA Aerospace Sciences Meeting, Reno, NV, January 2004.
23. Budianto, J., and Olds, J., "Design and Deployment of a Satellite Constellation Using Collaborative Optimization," *Journal of Spacecraft and Rockets*, Vol. 41, No. 6, 2004, pp. 956-963.
24. Lian, Y., and Liou, M., "Multi-Objective Optimization of Transonic Compressor Blade Using Evolutionary Algorithm," *Journal of Propulsion and Power*, Vol. 21, No. 6, 2005, pp. 979-987.
25. Brown, N., and Olds, J., "Evaluation of Multidisciplinary Optimization (MDO) Technique Applied to a Reusable Launch Vehicle," AIAA Paper 2005-707, Presented at the 43rd AIAA Aerospace Sciences Meeting, Reno, NV, January 2005.
26. Tsuchiya, T., and Mori, T., "Orbital Design of Two-Stage-to-Orbit Space Planes with Airbreathing Engines," *Journal of Spacecraft and Rockets*, Vol. 42, No. 1, 2005, pp. 90-97.
27. Casalino, L., and Pastrone, D., "Optimal Design and Control of Hybrid Rockets for Access to Space," AIAA Paper 2005-3547, Presented at the 41st AIAA/ASME/SAE/ASEE Joint Propulsion Conference, Tucson, AZ, July 2005.

28. Anderson, M.B., Burkhalter, J.E., and Jenkins, R.M., "Design of an Air to Air Interceptor Using Genetic Algorithms", AIAA Paper 99-4081, Presented at the AIAA Guidance, Navigation and Control Conference, Portland, OR, August 1999.
29. Anderson, M.B., Burkhalter, J.E., and Jenkins, R.M., "Intelligent Systems Approach to Designing an Interceptor to Defeat Highly Maneuverable Targets", AIAA Paper 2001-1123, Presented at the 39th AIAA Aerospace Sciences Meeting, Reno, NV, January 2001.
30. Chernyavsky, B., Stepanov, V., Rasheed, K., Blaize, M., and Knight, D., "3-D Hypersonic Inlet Optimization Using a Genetic Algorithm", AIAA Paper 98-3582, Presented at the 34th AIAA/ASME/SAE/ASEE Joint Propulsion Conference, Cleveland, OH, July 1998.
31. Shelton, J., Frederick, R., Wilhite, A., "Launch Vehicle Propulsion Design with Multiple Selection Criteria," AIAA Paper 2005-3851, Presented at the 41st AIAA/ASME/SAE/ASEE Joint Propulsion Conference, Tucson, AZ, July 2005.
32. Portz, R., "Launch Vehicle Design Features for Minimum Cost," AIAA Paper 2004-3562, Presented at the 40th AIAA/ASME/SAE/ASEE Joint Propulsion Conference, Fort Lauderdale, FL, July 2004.
33. Braun, R.D., Moore, A.A., and Kroo, I.M., "Collaborative Approach to Launch Vehicle Design," *Journal of Spacecraft and Rockets*, Vol. 34, No. 4, 1997, pp. 478-486.
34. Wollam, J., Kramer, S., and Campbell, S., "Reverse Engineering of Foreign Missiles via Genetic Algorithm," AIAA Paper 2000-0685, Presented at the 38th AIAA Aerospace Sciences Meeting, Reno, NV, January 2000.

35. Anderson, M.B., Burkhalter, J.E., and Jenkins, R.M., "Multi-Disciplinary Intelligent Systems Approach to Solid Rocket Motor Design, Part I: Single and Dual Goal Optimization," AIAA Paper 2001-3493, Presented at the 37th AIAA/ASME/SAE/ASEE Joint Propulsion Conference, Salt Lake City, UT, July 2001.
36. Anderson, M.B., Burkhalter, J.E., and Jenkins, R.M., "Multi-Disciplinary Intelligent Systems Approach to Solid Rocket Motor Design, Part II: Multiple Goal Optimization," AIAA Paper 2001-3494, Presented at the 37th AIAA/ASME/SAE/ASEE Joint Propulsion Conference, Salt Lake City, UT, July 2001.
37. Briggs, G.P., Ray, T., and Milthorpe, J.F., "Evolutionary Algorithm use in Optimization of a Launch Vehicle Stack Model," AIAA Paper 2007-364, Presented at the 45th AIAA Aerospace Sciences Meeting and Exhibit, Reno, NV, January 2007.
38. Wertz, J.R., "Responsive Launch Vehicle Cost Model," AIAA Paper RS2-2004-2004, Presented at the 2nd AIAA Responsive Space Conference, Los Angeles, CA, April 2004.
39. Unal, R., Braun, R.D., Moore, A.A., and Lepsch, R.A., "Design Optimization for Cost Using Genetic Algorithms," *Proceedings of the 17th Annual Conference of the International Society of Parametric Analysts*, May 1995, pp. 183-191.
40. Olds, J.R. and Lee, H., "Application of a New Economic Analysis Tool to a Two-Stage-to-Orbit RBCC Launch Vehicle," AIAA Paper 1996-4092, Presented at the 6th AIAA/NASA/ISSMO Symposium on Multidisciplinary Analysis and Optimization, Bellevue, WA, September 1996.
41. Koelle, D.E., *Handbook of Cost Engineering for Space Transportation Systems, Revision 1, with TRANSCost 7.1*, TransCostSystems, Ottobrunn, Germany, 2003.

42. Wertz, J.R., "Economic Model of Reusable vs. Expendable Launch Vehicles", Presented at the IAF Congress, Rio de Janeiro, Brazil, October 2000.
43. Anderson, M.B., "Users Manual for IMPROVE[®] Version 2.8: An Optimization Software Package Based on Genetic Algorithms", Sverdrup Technology Inc. / TEAS Group, Eglin AFB, FL, March 6, 2001.
44. Burkhalter, J.E., "Rocket Propulsion II Course Notes", Auburn University, Auburn, AL, 1985.
45. Sforzini, R.H., "Notes on Solid-Propellant Rocket Motors Including Jet Propulsion Fundamentals", Auburn University Engineering Extension Service, 1983.
46. Gage, P., and Kroo, I., "A Role of Genetic Algorithms in a Preliminary Design Environment," AIAA Paper 1993-3933, Presented at the AIAA Aircraft Design, Systems, and Operations Meeting, Monterey, CA, August 1993.
47. Cosner, R.R., Oberkampf, W.L., Rumsey, C.L., Rahaim, C.L., Shih, T.P., "AIAA Committee on Standards for Computational Fluid Dynamics: Status and Plans", AIAA Paper 2006-889, Presented at the 44th AIAA Aerospace Sciences Meeting and Exhibit, Reno, NV, January 2006.
48. Roy, C.J., "Introduction to Computational Fluid Dynamics Course Notes", Auburn University, Auburn, AL, 2006.
49. Riddle, D.B., Hartfield, R.J., Burkhalter, J.E., Jenkins, R.J., "Genetic Algorithm Optimization of Liquid Propellant Missile Systems," AIAA Paper 2007-362, Presented at the 45th AIAA Aerospace Sciences Meeting and Exhibit, Reno, NV, January 2007.
50. Humble, R.W., Henry, G.N., and Larson, W.J., Space Propulsion Analysis and Design, The McGraw-Hill Companies, Inc., New York, NY, 1995.

51. U.S. Air Force Fact Sheet, LGM-30G Minuteman III ICBM, Air Force Space Command, November 2006.
52. System Description: Weapons of Mass Destruction, LGM-30 Minuteman III, <http://www.globalsecurity.org>.
53. Minuteman ICBM History Website, Minuteman ICBM Diagrams, Minuteman III – Ballistic Flight Profile, http://www.geocities.com/minuteman_missile/index.html.
54. Minotaur I User's Guide, Release 2.1, Orbital Sciences Corporation, January 2006.
55. System Description: Orbital Sciences Corporation, Space Launch Systems, Minotaur Space Launch Vehicle, <http://www.orbital.com/SpaceLaunch/Minotaur/index.html>.
56. U.S. Air Force Fact Sheet, Titan II Space Launch Vehicle, Air Force Space Command, March 2001.
57. System Description: Space, Titan II SLV, <http://www.globalsecurity.org>.
58. AirLaunch LLC Fact Sheet, QuickReach™ Launch Vehicle, November 2006.
59. System Description: Directory of U.S. Military Rockets and Missiles, AirLaunch QuickReach, <http://designation-systems.net/dusrm>.
60. Sutton, G.P., Rocket Propulsion Elements: An Introduction to the Engineering of Rockets, 6th Edition, John Wiley & Sons, Inc., New York, NY, 1992.
61. Sellers, J.J., Astore, W.J., Giffen, R.B., and Larson, W.J., Understanding Space: An Introduction to Astronautics, 3rd Edition, McGraw-Hill Primis Custom Publishing, New York, NY, 2003.
62. System Description: Zenit Rocket, http://en.wikipedia.org/wiki/Zenit_rocket.
63. NASA Exploration Systems Architecture Study (ESAS) – Final Report, November 2005, pp. 669-710.

APPENDIX: Mass Table Example for Three-Stage Solid Propellant Launch Vehicle

Part Name	mass	xcg	ixx	iyy	izz
blunt nose	5.16	3.47	421.7	354.3	354.3
ogive section	98.66	47.99	74196.5	170582.7	170582.7
payload	1000.00	39.67	0.0	1573340.4	1573340.4
electronics	100.00	91.33	0.0	834129.9	834129.9
curved bulk 3	31.60	106.86	11200.8	366521.5	366521.5
ignitor 3	15.00	106.86	0.0	171275.5	171275.5
press vessel 3	318.25	174.35	220358.8	10318916.4	10318916.4
liner 3	87.55	174.35	60406.1	2838684.6	2838684.6
insulation 3	461.79	177.87	318607.7	15545957.4	15545957.4
nozzle 3	132.62	275.32	458636.9	9954230.1	9954230.1
grain 3	12754.48	175.22	5411860.2	412149855.0	412149855.0
curved bulk 2	99.04	305.65	51602.5	9278345.8	9278345.8
ignitor 2	26.00	305.64	0.0	2428887.2	2428887.2
press vessel 2	1056.52	392.56	1075261.6	166281361.0	166281361.0
liner 2	136.12	392.56	137662.8	21422199.8	21422199.8
insulation 2	717.93	396.84	726092.7	115412630.9	115412630.9
nozzle 2	350.34	510.18	5307228.4	91819317.4	91819317.4
grain 2	18965.35	393.62	13556946.2	2989514231.7	2989514231.7
curved bulk 1	125.14	537.55	82393.7	36203426.3	36203426.3
ignitor 1	26.00	537.55	0.0	7512900.0	7512900.0
press vessel 1	2233.91	704.27	2872844.1	1131358075.5	1131358075.5
liner 1	287.90	704.27	368185.4	145806550.1	145806550.1
insulation 1	1518.52	709.08	1941968.7	779359905.1	779359905.1
nozzle 1	419.34	905.86	9145618.0	343356082.9	343356082.9
grain 1	48939.05	705.46	44013937.8	24812033772.8	24812033772.8